

**Effects of the Desorption and Dissolution of Polycyclic  
Aromatic Hydrocarbons on Phytoremediation at a Creosote-  
Contaminated Site**

Helen A. Smartt

Thesis submitted to the faculty of Virginia Polytechnic Institute and State University in  
partial fulfillment of the requirements for the degree of

**MASTER OF SCIENCE**

**In**

**CIVIL ENGINEERING**

John T. Novak, Co-Chair  
Mark A. Widdowson, Co-Chair  
Duane F. Berry

October 14th, 2002

Blacksburg, Virginia

# **Effects of the Desorption and Dissolution of Polycyclic Aromatic Hydrocarbons on Phytoremediation at a Creosote-Contaminated Site**

by

Helen A. Smartt

Committee Co-Chairmen: John T. Novak, Mark A. Widdowson  
Civil Engineering w/ Geoenvironmental Concentration

## **ABSTRACT**

Creosote, containing many high molecular weight hydrophobic polycyclic aromatic hydrocarbons (PAH's), is present in the subsurface environment at the Oneida Tie-Yard in Oneida, Tennessee. Phytoremediation using hybrid poplar trees was chosen as the remedial technology on-site. Since monitoring began, the contaminant plume has been shrinking consistently and evidence has shown that remediation is taking place. However, remediation may be rate-limited by the desorption and dissolution kinetics of the PAH's on-site.

The objectives of this research are to: (1) estimate the desorption and dissolution rates of 10 PAH's found in the subsurface and (2) estimate the amount of each PAH and total mass of contaminant that is irreversibly sorbed to the soil. Three laboratory desorption and dissolution experiments were performed using contaminated soil samples from the Oneida Tie-Yard site. The first experiment was a batch desorption equilibrium experiment, the second was a batch desorption kinetics experiment, and the third was a soil column dissolution kinetics experiment. The target compounds in this study were: naphthalene, acenaphthylene, acenaphthene, fluorene, phenanthrene, anthracene, fluoranthene, pyrene, chrysene, and benzo(b)fluoranthene.

The resulting data for the desorption equilibrium experiment revealed that rates of equilibrium were truly not instantaneous in the systems studied. However, because approximately 76% of PAH's desorbed by the first sampling event (3 days), an equilibrium isotherm was considered appropriate. Results showed that there is a sorbed reversible concentration that readily desorbs to the aqueous phase for each PAH. Additionally, it was determined that the percent removal of sorbed PAH's decreases with increasing molecular weight. Desorption curves based on experimental data were found to exhibit linear behavior over large variations in aqueous concentration, but showed exponential behavior as concentrations approached zero. Freundlich sorption equilibrium isotherms for the 10 monitored PAH's on-site were generally found to have N coefficient values over 1, especially over large variations in solution phase concentration, indicating a non-uniform sorbent.

Dissolution of resistant PAH's under field-like conditions was determined to occur over long periods of time. Dissolution rates calculated from experimental data were shown to generally decrease with increasing molecular weight. Overall, desorption and dissolution kinetics of PAH's were shown to be rate-limiting factors to remediation at the Oneida Tie-Yard.

## ACKNOWLEDGEMENTS

I would like to thank my co-advisors, Dr. Mark Widdowson and Dr. John Novak, for their guidance, involvement, and encouragement throughout my time in the graduate program. I would also like to thank Dr. Duane Berry for his feedback on my thesis and willingness to serve on my committee.

In addition, I would like to thank Jody Smiley and Julie Petruska for their invaluable help with analytical methods and creative ideas for laboratory work. Thanks also go to Betty Wingate and Merry-Gayle Moeller for their help in smoothly running the essentials of the environmental and hydrosystems departments.

I would like to extend a special thanks to Sandra Robinson for training me in laboratory procedures and helping me to make an easy transfer onto the Oneida project. Thanks to Rikke Andersen for all her hard work in taking over the Oneida background analysis and her willingness to help in contributing to my research and cleaning laboratory equipment. In addition, thanks to Mark Pitterle, Heather Rectanus, and Meg Cooney for their help in taking field samples.

Thank you to my family, especially my parents Doug and Carole Smartt, for their constant love, encouragement, and patience. I would also like to thank my fiancé, Brendan Lockard, for joining me in graduate school and steadfastly supporting me throughout all of its ups and downs. Finally, I would like to thank God for helping me to complete one of the most challenging yet rewarding and valuable roads that I have ever been down.

# TABLE OF CONTENTS

ABSTRACT .....	ii
ACKNOWLEDGEMENTS .....	iii
TABLE OF CONTENTS .....	iv
LIST OF FIGURES .....	vi
LIST OF TABLES .....	ix
1. INTRODUCTION .....	1
2. LITERATURE REVIEW .....	5
2.1 Characteristics of Chemicals of Concern .....	5
2.1.1 Creosote.....	5
2.1.2 Monitored Polycyclic Aromatic Hydrocarbons .....	7
2.2 Remediation Techniques .....	10
2.3 Phytoremediation .....	14
2.3.1 Contaminant Removal Mechanisms .....	15
2.3.2 Phytodegradation.....	16
2.3.3 Hybrid Poplar Tree Phytoremediation .....	19
2.4 Principles of Adsorption .....	20
2.4.1 Partitioning Coefficients .....	23
2.4.2 Linear Sorption.....	24
2.4.3 Non-Linear Sorption .....	25
2.4.4 Irreversible Sorption.....	28
2.4.5 Non-Equilibrium Sorption .....	28
2.4.6 Cosolvency .....	29
2.4.7 Competitive Sorption .....	30
2.4.8 Mass-Transfer Limitations & Bioavailability .....	31
2.4.9 Effects of Aged Contaminants & Soil Properties.....	32
3. STUDY AREA & SAMPLING-SITE DESCRIPTION .....	35
3.1 Introduction .....	35
3.2 Site History.....	35
3.3 Remediation Plan .....	37

3.4 Rainfall & Uptake Data.....	39
3.5 Groundwater Characteristics .....	40
3.6 Soil Characteristics.....	46
3.7 Site Desorption & Dissolution Characteristics.....	51
<b>4. MATERIALS &amp; METHODS .....</b>	<b>55</b>
4.1 Experimental Design Approach .....	55
4.2 Batch Experiment Setup.....	55
4.3 Desorption Equilibrium Experiment.....	56
4.4 Desorption Kinetics Experiment .....	59
4.5 Dissolution Kinetics Experiment .....	59
4.6 Field Procedures .....	64
4.7 Laboratory Procedures .....	64
4.7.1 Water Extraction Procedure .....	65
4.7.2 Soil Extraction Procedure.....	66
4.8 Analytical Methods .....	68
4.8.1 Gas Chromatography.....	68
4.8.2 Mass Spectrometry.....	69
4.9 Statistical Analysis & Calculations.....	69
<b>5. RESULTS &amp; DISCUSSION.....</b>	<b>71</b>
5.1 Introduction.....	71
5.2 Desorption Equilibrium Experiment Results .....	71
5.2 Desorption Kinetics Experiment Results .....	77
5.3 Dissolution Kinetics Experiment Results.....	105
<b>6. CONCLUSIONS .....</b>	<b>110</b>
<b>7. LITERATURE CITED .....</b>	<b>112</b>
<b>APPENDIX A – DESORPTION EQUILIBRIUM EXPERIMENT</b>	<b>118</b>
<b>APPENDIX B – DESORPTION KINETICS EXPERIMENT</b>	<b>154</b>
<b>APPENDIX C – DISSOLUTION KINETICS EXPERIMENT</b>	<b>230</b>
<b>VITA</b>	<b>253</b>

## LIST OF FIGURES

Figure 2.1 Schematic of chemical and physical reactions in soil contaminated with non-aqueous phase liquid .....	22
Figure 2.2 Typical equilibrium isotherms.....	27
Figure 2.3 Freundlich sorption-desorption isotherms displaying hysteresis .....	31
Figure 3.1 Oneida Tie-Yard site layout .....	36
Figure 3.2 Hybrid poplar tree layout.....	39
Figure 3.3 Average total PAH concentrations ( $\mu\text{g/L}$ ) in groundwater, 3 to 8 feet above bedrock .....	43
Figure 3.4 Average total PAH concentrations in groundwater, 0 to 2.5 feet above bedrock .....	44
Figure 3.5 PAH concentration in groundwater changes with time and depth at MLS-7 & MLS-12 .....	45
Figure 3.6 Cross section of soil transect 2 .....	47
Figure 3.7 Multi-level sampler & soil boring locations at the Oneida Tie-Yard site .....	48
Figure 3.8 Soil concentration (mg/kg) depth profile for fluoranthene along transect 2 .....	50
Figure 3.9 Percent high molecular weight polycyclic aromatic hydrocarbons in groundwater with time at MLS-7, 3.27 feet above bedrock.....	52
Figure 3.10 Ratios of monitored polycyclic aromatic hydrocarbons to chrysene in soil at SB-10, 3 feet above bedrock .....	54
Figure 4.1 Depth profile for study area and sampling site soil boring locations .....	57
Figure 4.2 Schematic of batch experiment.....	58
Figure 4.3 Batch experiment example .....	58
Figure 4.4 Batch experiment storage location .....	58
Figure 4.5 Soil column side view .....	61
Figure 4.6 Schematic of soil column .....	61
Figure 4.7 Phase A & phase B soil columns.....	61
Figure 4.8 Soil column storage location .....	62
Figure 4.9 Soil column drainage technique .....	62
Figure 5.1 Average fluorene aqueous concentration versus time at SB-10, 6 feet below land surface .....	72

Figure 5.2 Fluoranthene desorption Freundlich isotherm based on soil samples from all SB locations.....	76
Figure 5.3 Reversible sorbed naphthalene concentration verses the number of fluid exchanges at SB-10, 7 feet below land surface .....	83
Figure 5.4 Reversible sorbed acenaphthylene concentration verses the number of fluid exchanges at SB-10, 7 feet below land surface .....	83
Figure 5.5 Reversible sorbed acenaphthene concentration verses the number of fluid exchanges at SB-10, 7 feet below land surface .....	84
Figure 5.6 Reversible sorbed fluorene concentration verses the number of fluid exchanges at SB-10, 7 feet below land surface.....	84
Figure 5.7 Reversible sorbed phenanthrene concentration verses the number of fluid exchanges at SB-10, 7 feet below land surface .....	85
Figure 5.8 Reversible sorbed anthracene concentration verses the number of fluid exchanges at SB-10, 7 feet below land surface .....	85
Figure 5.9 Reversible sorbed fluoranthene concentration verses the number of fluid exchanges at SB-10, 7 feet below land surface .....	86
Figure 5.10 Reversible sorbed pyrene concentration verses the number of fluid exchanges at SB-10, 7 feet below land surface.....	86
Figure 5.11 Reversible sorbed chrysene concentration verses the number of fluid exchanges at SB-10, 7 feet below land surface .....	87
Figure 5.12 Reversible sorbed benzo(b)fluoranthene concentration verses the number of fluid exchanges at SB-10, 7 feet below land surface .....	87
Figure 5.13 Reversible sorbed total polycyclic aromatic hydrocarbon concentration verses the number of fluid exchanges at SB-10, 7 feet below land surface.....	88
Figure 5.14 Aqueous concentration of naphthalene and 3-ring PAH's versus the number of fluid exchanges at SB-10, 7 feet below land surface .....	88
Figure 5.15 Aqueous concentration of naphthalene and 4 to 5-ring PAH's versus the number of fluid exchanges at SB-10, 7 feet below land surface.....	89
Figure 5.16 Naphthalene Freundlich isotherm for SB-10,7 feet below land surface.....	92
Figure 5.17 Acenaphthylene Freundlich isotherm for SB-10,7 feet below land surface..	92
Figure 5.18 Acenaphthene Freundlich isotherm for SB-10, 7 feet below land surface....	93
Figure 5.19 Fluorene Freundlich isotherm for SB-10, 7 feet below land surface.....	93
Figure 5.20 Phenanthrene Freundlich isotherm for SB-10, 7 feet below land surface.....	94
Figure 5.21 Anthracene Freundlich isotherm for SB-10, 7 feet below land surface .....	94

Figure 5.22 Fluoranthene Freundlich isotherm for SB-10, 7 feet below land surface.....	95
Figure 5.23 Pyrene Freundlich isotherm for SB-10, 7 feet below land surface.....	95
Figure 5.24 Chrysene Freundlich isotherm for SB-10, 7 feet below land surface.....	96
Figure 5.25 Benzo(b)fluoranthene Freundlich isotherm for SB-10, 7 feet below land surface .....	96
Figure 5.26 Total polycyclic aromatic hydrocarbon Freundlich isotherm for SB-10, 7 feet below land surface.....	97
Figure 5.27 Aqueous concentration versus sampling time for all phase A soil columns	107
Figure 5.28 Aqueous concentration versus sampling time for all phase B soil columns	107

## LIST OF TABLES

Table 2.1 Percent monitored polycyclic aromatic hydrocarbons in creosote .....	6
Table 2.2 Chemical characteristics of monitored polycyclic aromatic hydrocarbon constituents.....	8
Table 4.1 Dissolution kinetics sampling time line.....	63
Table 5.1 Desorption equilibrium experiment sampling event - 3 days .....	73
Table 5.2 Summary of Freundlich desorption parameters for desorption equilibrium experiment.....	76
Table 5.3 Summary of desorption kinetics experiment for naphthalene and acenaphthylene at SB-10, 7 feet below land surface.....	79
Table 5.4 Summary of desorption kinetics experiment for acenaphthene and fluorene at SB-10, 7 feet below land surface .....	79
Table 5.5 Summary of desorption kinetics experiment for phenanthrene and anthracene at SB-10, 7 feet below land surface .....	80
Table 5.6 Summary of desorption kinetics experiment for fluoranthene and pyrene at SB- 10, 7 feet below land surface.....	80
Table 5.7 Summary of desorption kinetics experiment for chrysene and benzo(b)fluoranthene at SB-10, 7 feet below land surface .....	81
Table 5.8 Summary of desorption kinetics experiment for total polycyclic aromatic hydrocarbons at SB-10, 7 feet below land surface.....	81
Table 5.9 Summary of Freundlich and rate parameters for desorption kinetics experiment at SB-10, 7 feet below land surface.....	90
Table 5.10 Reversible and irreversible sorption as determined by desorption kinetics experiment at SB-10, 7 feet below land surface.....	98
Table 5.11 Desorption rate constants by sample location as determined by desorption kinetics experiment .....	100
Table 5.12 Freundlich constant, $K_f$ , by sample location as determined by desorption kinetics experiment .....	101
Table 5.13 Freundlich coefficient, $N$ , by sample location as determined by desorption kinetics experiment .....	102
Table 5.14 Reversible sorbed concentration as a percent of the total polycyclic aromatic hydrocarbons as determined by desorption kinetics experiment .....	104
Table 5.15 Dissolution rates for soil columns sampled every 12 days.....	109

# 1. INTRODUCTION

There is concern in the United States about the increasing number of industrial sites contaminated with polycyclic aromatic hydrocarbons (PAH's). Wood treatment facilities are prime examples of such sites due to the use of chemicals containing PAH's during wood treatment operations. Creosote is used to treat wood in order to resist degradation and was commonly used in the railroad industry. Creosote is a complex mixture composed of 200 or more components of which approximately 85% are PAH's, 10% are phenolic compounds, and 5% are N-, S-, and O-heterocyclic compounds (Carriere and Mesania 1995; Mueller et al. 1989). Creosote oils are petroleum byproducts, produced by the destructive distillation of coal-tar. Being a dense non-aqueous phase liquid (DNAPL), a creosote plume will sink to the bedrock and continuously travel away from the source, contaminating groundwater as it moves through the soil.

PAH's in creosote are known carcinogens and mutagens. Consequently, the United States Environmental Protection Agency (US EPA) has classified 17 PAH's as Priority Pollutants (Peters et al. 1999; Brown et al. 1999). Biodegradation, direct plant uptake, irreversible sorption, leaching, photodegradation, and volatilization are some of the key degradation processes affecting the fate of PAH compounds in the subsurface (Brubaker and Stroo 1992; Mueller et al. 1989; Reilly et al. 1996). Some common remedial techniques used in the past to eliminate PAH contamination include the following: excavation and off-site disposal or incineration, containment, pump-and-treat, thermal desorption, vapor extraction, bioremediation, and natural attenuation (Luthy et al. 1994). However, these methods depend to a large extent on the mass transfer of contaminants from the solid to the aqueous phase. By nature, creosote is composed of many high molecular weight hydrophobic PAH's so the choice of a remediation technique presents a difficult challenge.

The study area and sampling-site for this research is a railway tie yard, located in Oneida, Tennessee, which was formerly used to treat railroad ties. When the site was active, creosote was discharged to the soil and groundwater below the land surface through various site operations. As a result, the site is highly contaminated with waste creosote.

In 1995, ARCADIS Geraghty & Miller, a consulting engineering firm, was hired to study the site and determine an appropriate method of remediation. In order to prevent creosote from traveling off-site and into a nearby stream, a trench was installed in 1991 to collect groundwater and send contaminated wastewater through an on-site oil/water separator (ARCADIS Geraghty & Miller 2001). ARCADIS Geraghty & Miller contracted with Ecolotree to plant approximately 1000 hybrid poplar trees on the site in 1997 to promote an intrinsic biological cleanup process called phytoremediation (ARCADIS Geraghty & Miller 2001).

Phytoremediation is a process whereby plants are used to promote degradation of contaminants through 2 methods: direct and indirect phytoremediation. Direct phytoremediation is the uptake of contaminants through tree leaves and roots, followed by plant metabolism, and either incorporation of the contaminant into the plant structure or volatilization into the atmosphere. Indirect phytoremediation, otherwise known as rhizosphere degradation, is a method where microbial populations in the root structure of a plant degrade contaminants. In particular, hybrid poplar trees were chosen for this site based upon their evapotranspiration potential, growth rate, depth and distribution of roots, biomass yield and degradative enzymes produced, and their ability to bioaccumulate contaminants (Al-Yousfi et al. 2000). Since they were planted, the tree roots have penetrated the groundwater table and reached the contaminated creosote plume. The increased bacterial populations around the roots of these trees are believed to degrade many of the contaminants in creosote.

The goals of this project are to demonstrate that phytoremediation is a successful technology and to assess its potential for use at similar sites. In order to obtain a more accurate representation of the contaminated plume and soil and groundwater parameters, extensive sampling is conducted over the entire site. Over 20 multi-level samplers (MLS's), with ports located every foot above bedrock, were installed on-site so that groundwater could be sampled. In addition to monitoring wells, the site contains piezometers and pressure transducers to measure the effect of the trees on groundwater flow patterns. Ten PAH's are monitored for bi-annually though hydrocarbon samples tested at a Virginia Tech laboratory. Field tests are conducted to measure dissolved oxygen, nitrate, iron, and sulfate. Each of these tests helps to estimate the overall effect

of the poplar trees on the natural remediation process and to assess whether degradation is occurring fast enough so that the risk to the public and the environment is minimized.

Since monitoring began, the contaminant plume at the Oneida Tie-Yard has been consistently shrinking. However, it cannot be determined when the site will be considered remediated. Only aqueous phase contaminants are thought to be bioavailable since a substance must be dissolved in order to be transported across the cell membrane of a microorganism (Zhang et al. 1998). In addition, direct uptake during phytoremediation depends largely on whether contaminants are in the dissolved phase. Therefore, it is necessary for PAH's to desorb from the soil and enter the aqueous phase for bioremediation and/or phytoremediation to take place. While low molecular weight PAH's (1 to 2 rings) can be directly taken up by the roots of plants and/or bioremediated, many of the high molecular weight PAH's (3 or more rings) have a strong tendency to sorb onto subsurface particles rendering them less susceptible to phytoremediation and bioremediation (Brubaker and Stroo 1992). Consequently, remediation at the Oneida Tie-Yard site may be rate limited by the desorption and dissolution kinetics of the PAH's on-site.

Although there is a considerable amount of research on desorption and dissolution rates at PAH contaminated sites, the rate of desorption and the extent of bioavailability are site specific and not readily predictable. Therefore, the objectives of this research are to: (1) estimate the desorption and dissolution rates of 10 PAH's found in the subsurface of the Oneida Tie-Yard and (2) estimate the amount of each PAH and total mass of contaminant that is irreversibly sorbed to the soil. In order to meet the goals of this research, 3 desorption experiments were performed using contaminated soil samples collected in July 2001 and February 2002 from the Oneida Tie-Yard site. The target compounds in this study were: naphthalene, acenaphthylene, acenaphthene, fluorene, phenanthrene, anthracene, fluoranthene, pyrene, chrysene, and benzo(b)fluoranthene. These PAH's are prevalent in creosote and represent a range of chemical characteristics and solubilities.

The first experiment was a batch test to determine the isotherms and the maximum equilibrium desorption and dissolution capacity for 10 monitored PAH's. This trial was setup in twenty-four 250 mL amber jars containing approximately 40 grams of soil and

distilled water. Samples were agitated daily by hand over a 77 day period. The second batch experiment used the same setup as the first, but incorporated a draw and fill method whereby distilled water was added after every 3 day sampling event. The purpose of this experiment was to determine the amount of contaminant mass irreversibly sorbed to the soil and also to establish the rates of desorption and dissolution for each monitored PAH. The final experiment was a soil column trial in which contaminated soil was overlain by medium grade sand and filled with distilled water in a portion of capped clear polyvinyl chloride (PVC) pipe. Gravity drained water samples were taken at the soil/sand interface over 3 day, 6 day, and 12 day time periods. The purpose of this experiment was also to determine the rates of desorption and dissolution for each monitored PAH.

Chapter 2 provides a literature review of background information for the aforementioned research. Chapter 3 presents a brief history of the Oneida Tie-Yard and a summary of the recent soil and groundwater contamination trends on-site. Chapter 4 is an overview of the materials, sampling procedures, and analytical methods used in each of the 3 experiments. Chapter 5 includes information obtained through the aforementioned laboratory experiments and a discussion of how the data obtained from these experiments can be applied to the site and used to estimate the sorptive properties of PAH's. Chapter 6 is a summary of the most important inferences of this study.

## 2. LITERATURE REVIEW

### 2.1 Characteristics of Chemicals of Concern

#### 2.1.1 Creosote

Creosote has been used as a wood preservative and pesticide in the United States for over 150 years (Carriere and Mesania 1995). Typically, it is used to protect wood products such as telephone poles, railroad ties, and marine pier pilings. Due to discoveries regarding the toxicity of creosote, its use has been highly regulated by the US EPA. Despite tight sanctions, there are approximately 700 wood-preserving sites in the United States where creosote is used presently or was used in the past (Hale and Aneiro 1997; Mueller et al. 1989). Creosote's wood preservative and pest control properties are outstanding and when properly used this compound is not a threat to ecological or human health. However, mistreatment, accidental spills, and inappropriate disposal of creosote can result in risks to human health and the environment. Accidental spills are quite common at wood-treater facilities during pressure treatment of wood products, leakage from holding tanks and unlined ponds, and even dripping from treated lumber.

Creosote is a brown to black oil generated during the distillation of coal-tar, which is derived from bituminous coal. Fifty percent of the pitch, or heavy substance remaining after the creation of creosote, is made up of constituents with 7 or more aromatic rings (Hale and Aneiro 1997). Creosote is a complex mixture composed of 200 or more components of which approximately 85% are PAH's, 10% are phenolic compounds, and 5% are N-, S-, and O-heterocyclic compounds (Carriere and Mesania 1995; Mueller et al. 1989). Of the many chemicals in creosote, only a few exist in quantities of greater than 1%; therefore, a small portion of compounds represent between 40-45% of any creosote composition (Mueller et al. 1989). The major components of creosote, as shown in Table 2.1, are multiple ring PAH's with varied chemical and physical properties.

Due to the complexity of creosote, each of its components will fractionate as a function of physical and chemical properties making fate and concentration evaluation difficult. Depending on the nature of the subsurface and the composition of the compound, contaminants may stay in the NAPL form, dissolve into the aqueous phase, sorb onto soil or colloidal material, volatilize into the atmosphere, be degraded by microbes, or drawn in by plants. In most cases, the contact of clean groundwater with

creosote causes desorption and dissolution of creosote constituents ultimately resulting in the generation of a PAH contaminated groundwater plume.

The density of creosote is greater than that of water thus creosote forms a dense non-aqueous phase liquid. DNAPL's migrate downward through the saturated zone until reaching a low permeability layer, usually bedrock. The movement of light NAPL's, which are less dense than water, is mainly controlled by groundwater. On the other hand, DNAPL movement is influenced by the geologic gradient of the confining layers as well as the hydraulic gradient (Mueller et al. 1989). In some instances, creosote can move in an opposite direction to groundwater flow. The difficulty in monitoring its movement, coupled with creosote's recalcitrance and limited bioavailability, make amelioration of creosote-contaminated sites a formidable challenge.

**Table 2.1 Percent monitored polycyclic aromatic hydrocarbons in creosote**

<b>Polycyclic Aromatic Hydrocarbon</b>	<b>Relative Percentage by Weight</b>
Naphthalene	13
Phenanthrene	13
Anthracene	13
Fluorene	8
Acenaphthene	4
Fluoranthene	4
Chrysene	2
Pyrene	2
Acenaphthylene	<1
Benzo(b)fluoranthene	<1
<b>Total Monitored PAH's</b>	<b>59</b>
<b>Other PAH's</b>	<b>41</b>
<b>Total</b>	<b>100</b>

(Fetterolf 1998; Mueller et al. 1999; Robinson 2001)

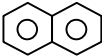
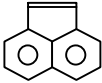
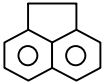
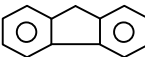
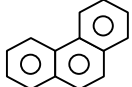
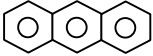
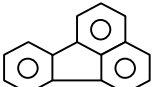
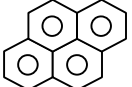
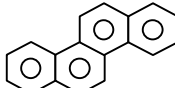
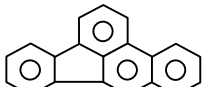
### 2.1.2 Monitored Polycyclic Aromatic Hydrocarbons

The majority of PAH's are formed during combustion when organic substances, such as coal, are exposed to temperatures higher than 500°C (Carriere and Mesania 1995). PAH's in nature are created by plant or microbial synthesis, forest and prairie fires, and volcanoes. On the other hand, man-made sources of PAH's typically result from fossil fuel burning or in the case of this research, wood-treatment (Edwards 1983). However, the quantity of PAH's formed in nature are insignificant compared to those from man-made sources.

As defined by their name, polycyclic aromatic hydrocarbons are chemicals composed of multiple aromatic rings in linear, angular, or cluster arrangements made up of only hydrogen and carbon atoms (Edwards 1983; Reilly et al. 1996). PAH's are non-polar, hydrophobic, neutral compounds distinguished by their low water solubility and large octanol-water partition coefficient ( $\log K_{ow}$ ). In general, the solubility of a PAH in water decreases with the more ring structures contained in that PAH or as its molecular weight increases. Furthermore, the ring structure of a PAH is also directly related to its dissolution rate (Link 2000). Common properties of the PAH's being tested in this research are summarized in Table 2.2. These 2 to 5-ring compounds were chosen in order to provide a representative sample of the constituents in creosote.

Many creosote applicators have recognized the toxic effects of PAH's on wood destroying pests. Likewise, PAH's are a known group of environmental contaminants, many of which are toxic, mutagenic, and some carcinogenic. The majority of familiar PAH's are harmless themselves but their intermediate products, formed during decay, are known carcinogens and mutagens (Edwards 1983; Jones et al. 1989). Therefore, remediation of PAH's is important to protecting the public health and environment. The US EPA has classified 17 PAH's as Priority Pollutants (Brown et al. 1999; Peters et al. 1999). Seven of the listed compounds are identified as probable human carcinogens and the others are not classifiable as of yet (Peters et al. 1999).

**Table 2.2 Chemical characteristics of monitored polycyclic aromatic hydrocarbon constituents**

Polycyclic Aromatic Hydrocarbon	Chemical Formula	Molecular Weight	Water Solubility 25°C (mg/L)	Log K <sub>OW</sub>	Log K <sub>OC</sub>	Vapor Pressure 20°C (Torr)	*Biodegradation Rate (day <sup>-1</sup> )	Chemical Structure
Naphthalene	C <sub>10</sub> H <sub>8</sub>	128	31	3.37	2.97	0.0492	0.337	
Acenaphthylene	C <sub>12</sub> H <sub>8</sub>	152	3.9	4.07	4.10	10 <sup>-3</sup> – 10 <sup>-2</sup>	0.02	
Acenaphthene	C <sub>12</sub> H <sub>10</sub>	154	3.8	4.33	3.66	10 <sup>-3</sup> – 10 <sup>-2</sup>	0.01	
Fluorene	C <sub>13</sub> H <sub>10</sub>	166	1.9	4.18	3.86	10 <sup>-3</sup> – 10 <sup>-2</sup>	0.015	
Phenanthrene	C <sub>14</sub> H <sub>10</sub>	178	1.1	4.46	4.15	6.8 x 10 <sup>-4</sup>	0.0447	
Anthracene	C <sub>14</sub> H <sub>10</sub>	178	0.05	4.45	4.15	1.95 x 10 <sup>-4</sup>	0.0052	
Fluoranthene	C <sub>16</sub> H <sub>10</sub>	202	0.26	4.90	4.58	10 <sup>-6</sup> – 10 <sup>-4</sup>	0.0018	
Pyrene	C <sub>16</sub> H <sub>10</sub>	202	0.13	4.88	4.58	6.85 x 10 <sup>-7</sup>	0.0027	
Chrysene	C <sub>18</sub> H <sub>12</sub>	228	0.002	5.61	5.30	10 <sup>-11</sup> – 10 <sup>-6</sup>	0.0019	
Benzo(b)fluoranthene	C <sub>20</sub> H <sub>12</sub>	252	0.0015	6.04	5.74	10 <sup>-11</sup> – 10 <sup>-6</sup>	0.0024	

\*Based on data from one source – Peters et al. 1999

(Callahan et al. 1979; Mackay et al. 1992; Montgomery 2000; Peters et al. 1999)

The human health risk posed by a PAH is determined not only by the toxicity of the PAH but also the potential for human exposure to the PAH. Low molecular weight PAH's have high solubilities and thus contribute to the health risk due to their potential for high doses in groundwater. On the other hand, high molecular weight PAH's are known to be more carcinogenic and contribute to the health risk because of their high toxicities (Peters et al. 1999). In addition to the human health risk, PAH's can accumulate in aquatic organisms affecting the marine community (Fetterolf 1998). Microorganisms are also prone to the toxic effects of PAH's, which can reduce degradation rates considerably.

In addition to their toxicity, PAH's pose an environmental threat due to their low volatility, resistance to microbial decay, and strong tendency to sorb to soil and organic matter. Biodegradation, direct plant uptake, irreversible sorption, leaching, photodegradation, and volatilization are some of the key degradation processes affecting the fate of PAH compounds in the subsurface (Brubaker and Stroo 1992; Mueller et al. 1989; Reilly et al. 1996). PAH's are not affected by hydrolysis because they do not contain groups amenable to this degradation pathway. Oxidation is also ineffective because it is an extremely slow process in PAH's (Callahan et al. 1979). While some dissolved portions of PAH's can undergo photodegradation, or decay through exposure to ultraviolet light, this degradation mechanism is not significant in the subsurface. Additionally, leaching is irrelevant in most PAH's due to their low solubility in groundwater and high affinity for sorption (Reilly et al. 1996). Only the low molecular weight PAH's have a high enough vapor pressure to be considered volatile; therefore, volatilization is also an improbable mechanism of degradation (Reilly et al. 1996).

Low molecular weight PAH's, such as naphthalene, are susceptible to direct uptake by plants and also bioremediation. However, for high molecular weight PAH's, as monitored in this study, adsorption to soil or organic matter is the most dominant subsurface fate. For the highest molecular weight PAH's, irreversible sorption is a possible pathway. The hydrophobic nature of high molecular weight PAH's makes bioremediation and direct uptake difficult because these water-based remedial methods depend to a large extent on a mass transfer of PAH's from the soil to the aqueous phase.

According to Callahan et al. (1979), PAH's with 3 rings or less (naphthalene, acenaphthylene, acenaphthene, fluorene, anthracene, phenanthrene) will adsorb strongly

to suspended sediments in the groundwater or to soil. Although, these low molecular weight compounds do not have high octanol-water partition coefficients, they should be strongly adsorbed to colloids and organic matter. The aforementioned 2 to 3-ring PAH compounds are susceptible to biodegradation in the subsurface. Naphthalene, a 2-ring compound, has the lowest octanol-water partition coefficient of this study and will not sorb as strongly as the high molecular weight PAH's; consequently, volatilization and adsorption are both possible degradative pathways for this compound. The higher molecular weight PAH's (fluoranthene, chrysene, pyrene, benzo(b)fluoranthene) will most likely accumulate in the sediment, because of their high affinity for adsorption, where they will undergo some biodegradation (Callahan et al. 1979).

## **2.2 Remediation Techniques**

In general, subsurface contaminants such as creosote exist as very complex mixtures made up of a number of different compounds. Each component has a different subsurface fate depending upon the physical, chemical, and toxicological properties of that compound thus making hazardous waste site management extremely complicated. A number of remedial techniques have been used in the past to eliminate PAH contamination including in-situ and ex-situ processes such as the following: excavation and off-site disposal or incineration, containment, pump-and-treat, thermal desorption, vapor extraction, bioremediation, and natural attenuation (Luthy et al. 1994). In most cases, in-situ techniques are generally less expensive than ex-situ methods. Nonetheless, the cost to clean up a hazardous waste site can be substantial, many times reaching prices in the billions (Reuther 1999).

Remediation goals are often determined in terms of lumped parameters, such as total polycyclic aromatic hydrocarbons (TPAH), due to the difficulties in characterizing the individual PAH's within creosote. While this method may simplify the choice of a remedial technology, it makes the erroneous assumption that the composition of NAPL will not change with time. If temporal changes in the composition of creosote are ignored, remediation activities may not reduce contamination and risk as expected. In order for a remediation scheme to have the highest potential to reduce risk, while at the same time decreasing pollutant concentrations, NAPL compositional changes must be accounted for over time (Brown et al. 1999; Luthy et al. 1994; Peters et al. 1999).

Generally, the physical and chemical properties of PAH's such as solubility, vapor pressure, and biodegradation rate are more recalcitrant with increasing molecular weight (Brown et al. 1999). For example, naphthalene has a molecular weight of 128 amu and a solubility of approximately 31 mg/L thus making this compound readily bioavailable. On the other hand, chrysene has a molecular weight of 228 amu and a solubility of only 0.002 mg/L thereby making this compound fairly recalcitrant. In the early stages of NAPL contamination, compounds with low molecular weight like naphthalene have a greater potential to contribute to risk and aqueous contamination. As remediation progresses, there may be a considerable reduction in concentration of lower molecular weight PAH's and a shift in dominant risk to the heavier weight compounds (Peters et al. 1999). In some cases, however, the higher molecular weight PAH's do not pose a great risk because they have limited mobility (Brown et al. 1999). In order to avoid under or over estimation of the true PAH concentrations and risks associated with a NAPL, remediation goals must take compositional changes into account. Normally, the remediation technologies that reduce risk the most drastically are those that decrease the concentration of carcinogenic and mutagenic compounds (Peters et al. 1999).

Two treatment techniques commonly used for organic contamination are isolation and removal of source material, or "hot spots". Stabilization is a method that does not reduce the quantity of contaminants at a site, but alters the soil chemistry using additives to keep contaminants from moving off-site (Cunningham et al. 1995). The removal of source material by excavation and off-site disposal or incineration is a frequently used remediation technique when PAH's are involved. While this method removes contaminated material from the area of concern, drastically reducing pollutant concentrations, it is an extremely expensive alternative and leaves large holes in the earth that must be refilled with clean soil. In some cases, excavated free product can be recycled as a raw material in the production of asphalt and other petroleum byproducts (Luthy et al. 1994). If a landfill is the choice for off-site disposal, the contaminated dirt takes up valuable space where other contaminants could be placed (Reuther 1999).

In cases involving volatile organic contamination, in-situ, or on-site, remediation treatments such as thermal desorption and soil vapor extraction are applicable. Thermal desorption involves heating contaminated soil to 300 - 400 °C while clean air is blown into the soil. Contaminants such as PAH's then desorb from soil particles into the clean

air. Further treatment may be required for the resulting contaminated air stream. Soil vapor extraction is a technique that introduces air into the subsurface in order to promote volatilization of organic compounds. In the case of this research, most of the monitored PAH's have extremely high molecular weights and are not very volatile; therefore, techniques aimed at volatilization will not be effective (Luthy et al. 1994).

Water based technologies such as pump-and-treat are also used regularly at sites contaminated with organics. Groundwater pump-and-treat systems usually consist of recovery wells followed by ex-situ treatment such as oil/water separation, air stripping, or carbon adsorption. In some cases, extraction wells are also used to manage off-site migration of contaminants. Pump-and-treat depends to a large extent on the mass transfer of contaminants from the solid to the aqueous phase. Consequently, remediation at some sites may be limited by the rate of desorption and dissolution of the PAH's on-site. According to Brubaker and Stroo (1992), there is almost no reduction in concentration of 3, 4, and 5-ring PAH's by pump-and-treat processes alone. By nature, creosote is composed of many high molecular weight hydrophobic PAH's so the choice of pump-and-treat as a remediation technique for this research presents a difficult challenge.

Bioremediation, another means of site restoration, utilizes the ability of microorganisms to degrade contaminated materials in the subsurface. The rate of biodegradation of a compound depends on a number of factors including both soil and contaminant characteristics. Generally, the rate of biodegradation is the greatest when a microbial population has had time to acclimate to a particular compound such as a PAH (Callahan et al 1979). As a result, bioremediation may take many years to go into effect. In addition, in some cases, bioremediation of PAH contaminants can lead to enhanced environmental mobility which may further complicate remediation (Hale and Aneiro 1997).

Only aqueous phase contaminants are thought to be bioavailable since a substance must be dissolved in order to be transported across the cell membrane of a microorganism (Zhang et al. 1998). In general, the number of rings in a PAH is inversely related to the ease with which microbes can degrade that compound (Brown et al. 1999; Callahan et al. 1979; Reilly et al. 1996). Research has demonstrated that microorganisms can metabolize some PAH compounds with less than 4 rings (Callahan et al. 1979). Four and 5-ring PAH's are most likely cometabolized by microorganisms with lower molecular

weight compounds that are more readily degradable. Of the monitored PAH's included in this research, naphthalene, which is a 2-ring compound, is probably the most easily biodegraded.

In order to enhance contaminant solubility and biodegradation, synthetic and biological solvents and surfactants can be added to contaminated soil and groundwater. This technique improves contaminant recovery by reducing interfacial surface tension between soil and hydrophobic compounds either sorbed on soil or present in the NAPL phase. By adding surfactants to a soil/water system, contaminant solubility and dissolution are increased making compounds more readily remediated by pump-and-treat technologies and more bioavailable for degradation by microorganisms. Lab and field-scale research has shown that surfactant addition can enhance bioremediation of PAH's in soils and accelerate the partitioning of the contaminants from soil particles to groundwater (Carriere and Mesania 1995, Grasso et al. 2001; Mueller et al. 1989; Yeom et al. 1995; Yeom et al. 1996). In one study completed in 1995 on the effect of surfactants on PAH's, low molecular weight compounds experienced a greater increase in solubility within a 24 hour period (Carriere and Mesania 1995). However, given time, more hydrophobic compounds generally experience a greater increase overall in solubility in the presence of solvents than less hydrophobic pollutants (Link 2000; Luthy et al. 1994). Most often, solvents and surfactants are used in conjunction with pumping wells in order to control movement of the mobilized NAPL. This remedial technique should only be used at sites where the outward and downward migration of both NAPL and solvent or surfactant can be controlled with certainty.

Although there are a number of remediation technologies available for the treatment of organics, due to limitations of individual methods, comprehensive remediation of many sites may not be possible. In fact, most regulatory agencies recognize that complete groundwater and soil restoration may be infeasible at sites contaminated with NAPL's (Luthy et al. 1994). For this reason, treatment trains, or a combination of control and treatment technologies are often used when no single operation is adequate (U.S. EPA 1995; Schnoor et al. 1995). A sequence of remedial actions can include pretreatment and/or post-treatment activities in addition to treatment technologies targeted at achieving specific site clean up objectives.

### **2.3 Phytoremediation**

Phytoremediation, or the use of plants to degrade soil and groundwater contaminants, is the in-situ remediation strategy on which this research is based. This approach takes advantage of the ability of vegetation to degrade compounds from the environment through volatilization, extraction, stabilization, oxidation, and degradation (Reuther 1999; Salt et al. 1998; Schnoor et al. 1995). Phytoremediation can also be used as a method to control runoff. Vegetation has been used for many years to clean wastewater of inorganic and organic pollutants, but until recent decades the use of plants to remediate soils had not been explored (Matso 1995; Salt et al. 1998).

The use of vegetation for remediation is an attractive alternative because it is a relatively inexpensive, environmentally compatible, and non-intrusive technique. In most cases, phytoremediation is much cheaper than other available treatment technologies for contaminated soil and groundwater. This method is a self-sustaining process that normally requires little management. One of the greatest advantages of phytoremediation is its political correctness and aesthetic value. In general, the public will accept a treatment technology that makes the environment more pleasing visually.

The use of phytoremediation depends largely on the type of contaminant present as well as the type of plant employed for treatment. If pollutants are too water soluble and mobile, then they may leach outside the root zone, with minimal uptake, and travel off-site (Al-Yousfi et al. 2000; Cunningham et al. 1995). On the other hand, if pollutants are bound too tightly to the soil, they may not be available for uptake or biodegradation. Most plants have the capacity to degrade mixed wastes including toxic heavy metals and organic pollutants. In general, plants can be exposed to higher concentrations of hazardous waste than the majority of microorganisms (Schnoor et al. 1995). Phytoremediation has been used to treat herbicides, pesticides, and munitions wastes like trinitrotoluene (TNT), polychlorinated phenols (PCB), and trichloroethylene (TCE) (Cunningham et al. 1995; Matso 1995; Salt et al. 1998).

A number of environmental factors must be present in order for phytoremediation to be successful in reducing contaminant levels. Because plants are living organisms, their roots require certain fundamental resources such as an adequate supply of oxygen, water, and nutrients. In addition, the soil texture, pH, salinity, and pollutant levels must not be

toxic to the chosen plant (Al-Yousfi et al. 2000; Cunningham et al. 1995).

Phytoremediation is generally most effective in cases with large surface areas of relatively immobile contamination less than 5 meters in depth (Cunningham et al. 1995; Schnoor et al. 1995).

Because phytoremediation is a developing method and associated risks are not yet well defined, this technology is not widely accepted by members of the regulatory community and, therefore, is not commonly used. One case brought up against phytoremediation by regulators is that the process may be rate-limited by the desorption and dissolution kinetics of the contaminants on-site requiring a longer time for complete restoration as compared with other methods (Cunningham et al. 1995; Schnoor et al. 1995). Another important consideration when using phytoremediation is that there is a possibility that the metabolic endproducts of plant and biodegradation may be more toxic than the original contaminants (Salt et al. 1998). Although phytoremediation is not necessarily the best treatment in all situations, it has proven effective in a number of demonstration pilot and full-scale studies. As of now, phytoremediation is often seen as the final “polishing step” after other remedial methods are used to treat hot spots.

### **2.3.1 Contaminant Removal Mechanisms**

Phytoremediation is divided into the following subsections: phytodegradation, phytoextraction, rhizofiltration, phytostabilization, and phytovolatilization. For sites contaminated with metals that are not easily biodegraded such as cadmium, nickel, and zinc, plants are used to extract pollutants from the subsurface. Phytoextraction is the use of plants with a high tolerance for toxic metals to remove metals from the soil through their roots and concentrate them in parts that can be harvested. During phytoextraction, plants do not degrade contaminants but simply absorb and store them. Metals concentrations in certain plants may be up to fifty times that of the surrounding contaminated soil (Reuther 1999). Rhizofiltration is the use of plant roots to adsorb or absorb pollutants from surface and groundwater. This technique, similar to phytoextraction, is often used for metals degradation. In some cases, synthetic and biological solvents and surfactants can be added to contaminated soil to make pollutants more soluble thus enhancing phytoextraction and rhizofiltration (Salt et al. 1998).

However, once soluble, metals and organics may be mobilized by rains and washed off-site.

Phytostabilization is a technique where plants are used to either precipitate or entrap pollutants in the soil matrix or plant tissue rendering them less bioavailable. Although this process does not remove contaminants from the soil and decreases the availability of compounds for bioremediation, phytostabilization reduces the chance of leaching and greatly reduces the ecological and public health risk. Plants bind contaminants through altering the groundwater flux, adsorbing pollutants to their roots, and impeding erosion due to wind and rainfall. Some specific plants can also bind pollutants through the initiation of redox reactions or precipitation of dissolved contaminants (Cunningham et al. 1995). In some cases, soil amendments added to the soil such as alkalizing agents, phosphates, mineral oxides, organic matter, and biosolids can also increase sequestration (Matso 1995).

Phytovolatilization is the use of plants to specifically volatilize contaminants from the soil and release them as a vapor into the air. This process occurs when certain volatile organic and some metallic contaminants are exposed to specific types of plants. The method was developed at PhytoWorks in Gladwayne, Pennsylvania for use in particular on mercury to avoid the problems associated with toxic accumulation in plants (Reuther 1999). However, there is a concern that some pollutants such as mercury could be released into the air and precipitate off-site when exposed to rainfall (Reuther 1999).

### **2.3.2 Phytodegradation**

Phytodegradation is the use of plants and microorganisms in the root area to degrade organic contaminants. Although the plant/chemical interaction during phytodegradation is not fully understood, it is known that the contaminant is destroyed or degraded in 2 ways: direct and indirect phytoremediation. Direct phytoremediation is the actual uptake of contaminants through tree roots and shoots, followed by plant metabolism, and either incorporation of the contaminant into the plant structure or volatilization into the atmosphere (Schnoor et al. 1995; Salt et al. 1998). Indirect phytoremediation, otherwise known as rhizosphere degradation, is a method where microbial populations in the root structure of a plant degrade contaminants (Schnoor et al. 1995; Salt et al. 1998).

Controlled experiments have shown that plants can directly draw in PAH's by both leaves and roots but, following uptake, little is known about their fate within a plant (Edwards 1983). PAH's may be translocated to other plant tissues where they are either volatilized into the atmosphere, completely or partially degraded, or stored unchanged (Salt et al. 1998). In some cases where high concentration of organics exist in the soil, absorption might exceed metabolism within a plant causing accumulation of contaminants within plant tissues (Edwards 1983). Certain plant parts may contain higher concentrations of PAH contaminants than others. Most often, the concentration of PAH's are greater on plant surfaces than internal tissues and higher in parts above ground than those below ground (Edwards 1983). However, some research indicates that adsorption onto roots may be significant for higher molecular weight PAH's (Reilly et al. 1996).

A number of processes play a role in the uptake of contaminants by plants. Some considerations when choosing a particular type of plant for phytodegradation are the physical state of the organic contaminant and that different plants partition organics in different ways between roots and shoots (Edwards 1983; Salt et al. 1998). Uptake and distribution are dependent on chemical properties such as PAH concentration, solubility, phase, molecular weight, vapor pressure, and octanol-water partition coefficient (Edwards 1983; Paterson et al. 1994). Although plants can take up chemicals from the vapor, liquid, and solid phases, for the most part, uptake occurs by way of the liquid phase. Therefore, hydrophobic chemicals that are bound strongly to the soil and roots ( $\log K_{ow} > 3.0$ ) will be less likely to be drawn in by plants, while contaminants with octanol-water partition coefficients ranging from 0.5 to 3.0 are likely to be taken up (Schnoor et al. 1995; Salt et al. 1998). In addition to the chemical characteristics of target compounds, uptake rates are also dependent upon plant physiology, such as transpiration rates, and atmospheric properties. Soil conditions such as organic content, water content, pH, and temperature all affect the uptake of contaminants by plants (Paterson et al. 1994; Salt et al. 1998).

Indirect phytoremediation works on the principle that certain microbial populations and plant enzymes are capable of degrading contaminants from subsurface soils and groundwater near plant roots, or the rhizosphere (Schnoor et al. 1995; Salt et al. 1998). Environmental properties in the soil such as organic carbon, pH, and microbiological

activity are significantly different in the rhizosphere than in soil with no vegetation present. Plants supply oxygen to the root zone, which stimulates aerobic degradation of contaminants that may not occur in unvegetated areas (Schnoor et al. 1995). In addition, plants release root exudates and decomposing root materials into the soil that are high in carbon, which in turn serves as a substrate for the growth of microbes. Some plants even release enzymes into the soil that are capable themselves of degrading organic contaminants. Exudates are typically sugars, alcohols, and acids, but their chemical composition as well as the rate at which these compounds are released can differ between plant species (Schnoor et al. 1995; Salt et al. 1998).

The overall effect of indirect phytoremediation is an enhancement of microbial activity in the rhizosphere of up to 100 times that found in surrounding unvegetated soil (Reilly et al. 1996). The root zone supports a variety of microorganisms such as fungi and bacteria that metabolize organic contaminants. The density of bacteria in the root zone can be as much as 4 orders of magnitude higher than in unplanted soil (Reuther 1999; Salt et al. 1998). A number of pollutants such as pesticides and PAH's can be completely metabolized by soil microorganisms but the rate of degradation is typically slow (Cunningham et al. 1995; Edwards 1983). Indirect phytoremediation has an advantage over many mechanical remediation schemes because plants have the ability to reach into micropores in the soil matrix that often contain trapped contaminants. However, in order to be successfully degraded by microorganisms, these contaminants must be bioavailable.

A thorough understanding of the pathways and endproducts of contaminants during phytoremediation can only be obtained through scientific research. A number of pilot and field-scale studies are currently being conducted to examine the phytoremediation potential for several plants and compounds. One investigation of anthracene and pyrene contaminants, placed in both vegetated and unvegetated soils, revealed that over time vegetated soils contained approximately 30 to 44% lower concentrations of these compounds than unvegetated soils (Reilly et al. 1996). Increased degradation of anthracene and pyrene was attributed to enhanced biodegradation due to elevated levels of microorganisms around plant roots. The results of this investigation verify that phytoremediation may be effective for other 3 and 4-ring PAH's. Other studies suggest that the octanol-water partition coefficient can be used to estimate the fate of organic

contaminants in phytoremediation. One investigation, conducted by Burken and Schnoor (1998), showed that the log  $K_{ow}$  can be used to roughly estimate the fate of trichloroethylene (TCE) in phytoremediation by hybrid poplar trees. Based upon the log  $K_{ow}$ , hybrid poplars have the capability to transpire TCE from their leaves to the atmosphere or transform TCE to aerobic metabolites in leaf tissue (Burken and Schnoor 1998; Matso 1995). The results of the aforementioned studies, as well as others, can be used to select specific plants to use in the phytoremediation of particular compounds.

### **2.3.3 Hybrid Poplar Tree Phytoremediation**

The characteristics of each cleanup site are inherently unique; therefore, specific types of plants are applicable in different situations. For the site described in this research, hybrid poplar trees were chosen based upon several distinct advantages such as their growth rate, depth and distribution of roots, evapotranspiration potential, and ability to contain and degrade organic contaminants.

Hybrid poplar trees are grown easily from cuttings and can grow more than 3 meters per year (Al-Yousfi et al. 2000; Schnoor et al. 1995). This tree species takes approximately 5 years to fully mature and can live as long as 25 to 50 years (Al-Yousfi et al. 2000; Schnoor et al. 1995). Because of the time requirement for root development, the short-term remedial effects of hybrid poplar trees are hardly recognizable. However, in the long run, the poplar trees eventually reach their full potential and reduce organic contamination in the deeper zones. While many plant roots can only extend through the top few feet of soil, poplar tree roots can reach depths of 20 feet or more (Matso 1995; Reuther 1999). In addition to reaching contaminants, poplar tree roots are also valuable for stabilizing the soil thereby reducing the risk of windblown human exposure to pollutants (Schnoor et al. 1995).

Poplar trees can transpire relatively large volumes of water, which reverses the downward migration of pollutants and prevents contaminants from moving off-site. When fully grown, hybrid poplars can uptake and transpire over 50 gallons of water per tree per day which makes them useful for hydraulic control (Matso 1995). In some cases, poplar trees have even been found to transpire up to 350 gallons of water per day (Matso 1995). Using conventional pump and treat methods, the installation of wells is extremely expensive and material transport to a well can take long periods of time. However,

hybrid poplar trees can serve as inexpensive miniature extraction wells, or “straws”, that can be planted in close proximity so contaminants do not have to be relocated (Al-Yousfi et al. 2000; Matso 1995).

Due to their high tolerance for organics, poplar trees are being considered for the remediation of many sites contaminated with organic chemicals. As previously mentioned, hybrid poplar trees have the ability to uptake and transpire volatile organic compounds such as TCE (Burken and Schnoor 1998; Matso 1995). In addition, it has been determined that the roots of hybrid poplar trees can harbor microbial communities capable of breaking down organics (Robinson 2001). Although hybrid poplars are tolerant of organic pollutants, metals, salts, and ammonia in high quantities can be toxic to this plant species (Schnoor et al. 1995).

## **2.4 Principles of Adsorption**

Because creosote NAPL is a complex matrix of contaminants, each of its components will fractionate into the air, water, or soil as a function of physical and chemical properties. As shown in Figure 2.1, a contaminant may undergo dissolution, diffusion, sorption, or biodegradation. Sorption processes included adsorption, absorption, and desorption. Adsorption is surface accumulation, absorption is penetration of the solid by contaminant, and desorption is the transfer of solid contaminants to the aqueous phase (Fetter 1993).

Partitioning depends largely on the chemical characteristics of a compound such as molecular weight, solubility, and octanol-water partition coefficient. Soil and biological properties of the physical environment also play a role in the behavior of a contaminant. For the most part, all creosote constituents will be represented at some concentration in the aqueous phase, but the ultimate fate of many compounds in creosote is irreversible sorption. With time, a portion of constituents that are sorbed to the soil or reside in the NAPL phase may desorb and dissolve into the surrounding soil pore water and groundwater. In the case of bioremediation, desorption and dissolution are critical to the degradability of PAH pollutants.

As a general rule, aqueous solubility decreases with increasing molecular weight. Low molecular weight PAH's are usually water soluble and thus are found in the aqueous phase. Conversely, high molecular weight PAH's with 4 or more rings are hydrophobic

and insoluble thus they tend to be strongly adsorbed to soil particles, sediments, or organic matter. Although high molecular weight compounds are not generally found in the aqueous phase, they are a threat even at low concentrations due to their carcinogenic and toxic effects (Peters et al 1999).

Over time, there is a significant possibility that NAPL composition will change as it is exposed to groundwater and soil pore water (Peters et al. 1999). When lower molecular weight compounds dissolve from the NAPL phase, the NAPL itself becomes enriched in high molecular weight compounds. The solubility of a compound depends to some extent on the amount of constituent in the NAPL phase (Peters et al. 1999). Given time, the low molecular weight compounds in a NAPL will dissolve, leaving behind high molecular weight compounds with normally low solubilities. Once these heavy compounds become the most soluble components in the NAPL, they have an increased driving force to dissolve and be present in the aqueous phase. In a study done by Peters et al. (1999) of PAH's such as benzo(b)fluoranthene, high molecular weight compounds were shown to increase in aqueous concentration over 30 years. Once the low molecular weight compounds are removed from creosote, the NAPL becomes denser, sometimes solidifying, and more difficult to remove from the subsurface. According to Rutherford et al. (1997), as low molecular weight PAH's leave the NAPL phase, the average molecular weight of creosote can increase up to 36%.

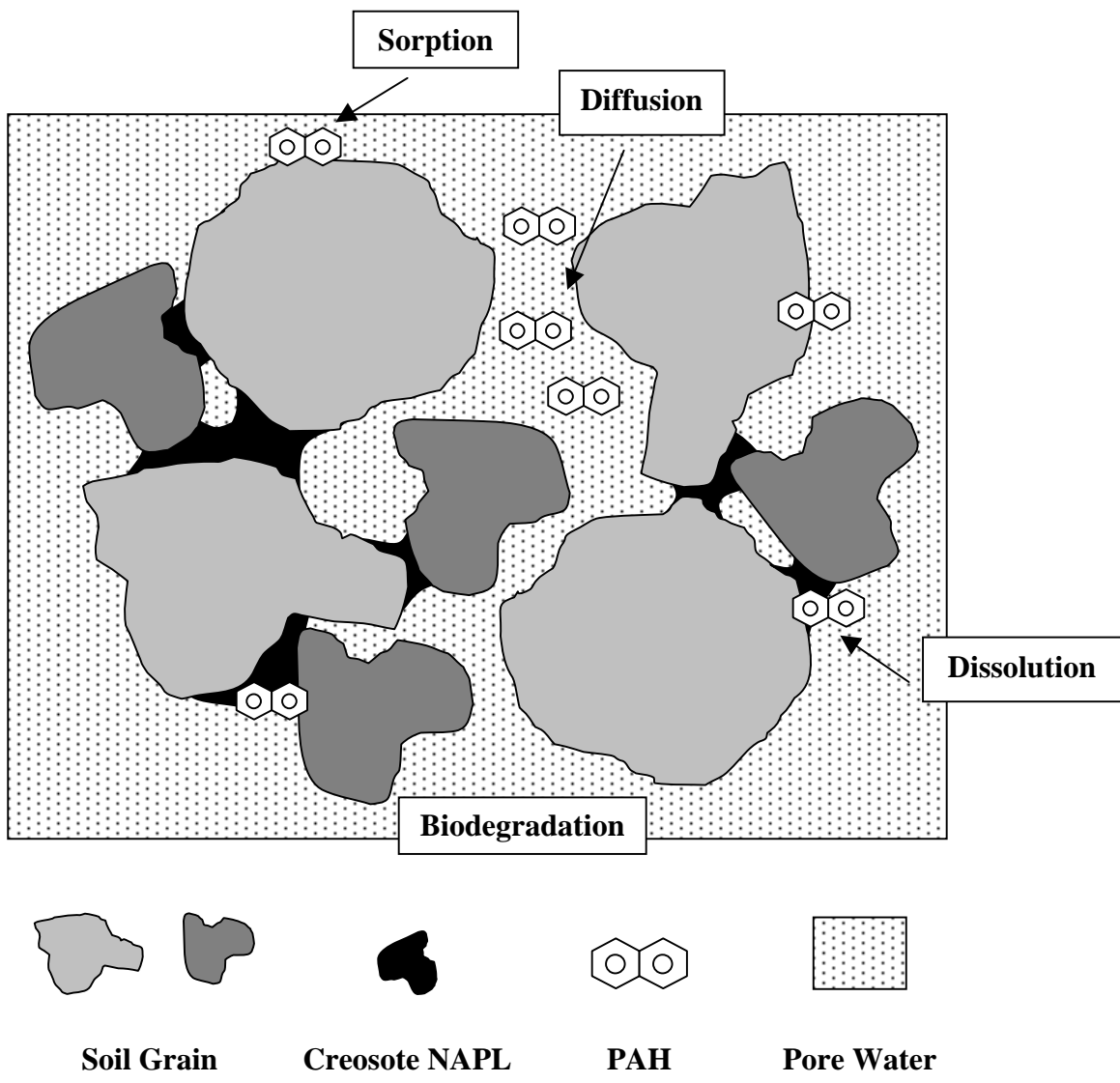


**Figure 2.1 Schematic of chemical and physical reactions in soil contaminated with non-aqueous phase liquid (Luthy et al. 1994)**

### 2.4.1 Partitioning Coefficients

The relative division of a chemical between the soluble and insoluble phases can be determined through a number of partitioning coefficients. The equilibrium constants,  $K_{ow}$  and  $K_{oc}$ , quantify the tendency of a constituent to sorb onto soil and organic matter. The octanol-water partition coefficient, or  $K_{ow}$ , defines the relative partitioning of a compound between water and liquid octanol.  $K_{ow}$  is calculated by dividing the concentration of a compound in octanol, which represents soil, by its aqueous phase concentration. This equilibrium constant is often used as a measure of hydrophobicity. The organic-carbon partition coefficient, or  $K_{oc}$ , defines the relative partitioning of a compound between water and organic carbon.  $K_{oc}$  is normally calculated using the  $K_{ow}$  as shown in Equation 2.1 and 2.2. Rao and Davidson (1980) estimate the  $K_{oc}$  for a number of pesticides as follows:

$$\mathbf{Log K_{oc} = 1.029 \times Log K_{ow} - 0.18} \quad \mathbf{(2.1)}$$

For a variety of organic compounds, Karickhoff (1983) suggests that the  $K_{oc}$  can be related to the  $K_{ow}$  through the following equation:

$$\mathbf{K_{oc} = 0.411 \times K_{ow}} \quad \mathbf{(2.2)}$$

The distribution coefficient, or  $K_d$ , measures the hydrophobicity of an organic chemical while taking into account the amount of soil organic matter. The  $K_d$  can be calculated by the following:

$$\mathbf{K_d = K_{oc} \times f_{oc}} \quad \mathbf{(2.3)}$$

where,

$f_{oc}$  = fraction of organic matter present in a soil

All 3 partition coefficients are helpful in establishing the subsurface fate of organics. In general, the higher the molecular weight and ring structure of a PAH, the higher hydrophobicity and the coefficients  $K_{ow}$  and  $K_{oc}$  (Link 2000). A higher value of both constants indicates a chemical's preference to be sorbed to the soil, sediment, or organic matter rather than be present in the aqueous phase.

#### 2.4.2 Linear Sorption

While partition coefficients are useful for making wide generalizations about the subsurface fate of compounds, they do not always predict accurately the processes of adsorption for complex mixtures such as creosote. Therefore, it is sometimes necessary to study the sorption processes of site-specific compounds individually (Mingelgrin and Gerstl 1983). The literature states that there are several types of sorption, which may be applicable to specific pollutants, such as the following: linear sorption, non-linear sorption, irreversible sorption, and non-equilibrium sorption (Brusseau 1993; Dzombak and Luthy 1984; Elzerman and Coates 1987; Miller and Weber, Jr. 1984; Travis and Etnier 1981; Weber, Jr. and Smith 1987; Weber, Jr. et al. 1991). An isotherm is a plot that relates the sorption distribution coefficient,  $K_d$ , with aqueous solubility for a particular compound. Linear sorption occurs when a compound is equally distributed between the sorbed and aqueous phases and is characterized by a linear isotherm such as the example in Figure 2.2. The slope of the linear sorption isotherm is described by the following equation:

$$C^* = K_d \times C \quad (2.4)$$

where,

$C^*$  = amount of solute sorbed to soil per dry unit weight of soil (mg/kg)

$C$  = equilibrium concentration of the solute in the aqueous phase (mg/L)

$K_d$  = linear distribution coefficient (L/kg)

In the case of linear sorption when  $K_d$  is greater than 1, contaminants move through an aquifer at a slower, but constant, rate in comparison to the groundwater (Link 2000). This delayed process is otherwise known as retardation. In the linear case, retardation can be estimated by the following:

$$R = 1 + \left( \frac{\rho_b \times K_d}{n} \right) \quad (2.5)$$

where,

$\rho_b$  = bulk density of soil (g/cm<sup>3</sup>)

n = porosity of soil (unitless)

There are some major drawbacks to using the linear sorption model. One limitation of this model (Equation 2.4) is that it restricts the amount of solute that can be sorbed to a soil once all the binding sites have been occupied; however, in reality, there may be more available binding sites to which contaminants can sorb increasing the upper limit to the sorbable quantity (Fetter 1993; Travis and Etnier 1981). Another limitation is that a series of extrapolated sorption data may be mistaken as a linear model when, in actuality, the series is curvilinear (Fetter 1993). However, the linear sorption model can be used when it is desired to describe sorption over a limited concentration range.

### 2.4.3 Non-Linear Sorption

Non-linear sorption is a distribution of solute between the sorbed and aqueous phases that can be characterized by a non-linear isotherm. Non-linearity occurs when the affinity of a compound for the soil decreases with increasing solute concentrations as sorption sites on the soil become filled. Several different isotherms have been proposed to describe non-linear sorption such as the Freundlich and Langmuir models but the appropriate choice is based on the conditions of the experiment.

The Langmuir sorption isotherm assumes that a soil grain has a finite number of sorption sites and when all these sites are filled, no more solute can sorb to the soil (Fetter 1993; Travis and Etnier 1981). The Langmuir isotherm is shown in Figure 2.2 and has the following form:

$$\frac{C^*}{C} = \left( \frac{1}{\alpha\beta} \right) + \left( \frac{C}{\beta} \right) \quad (2.6)$$

where,

$\alpha$  = binding energy absorption coefficient (L/mg)

$\beta$  = maximum amount of solute sorbed to soil (mg/kg)

In the Langmuir model, sorption data, when plotted as  $C^*$  versus  $C$ , plots curvilinear and reaches a maximum to which it becomes asymptotic (shown by the dashed line in Figure 2.2). If the same data is plotted as  $C^*/C$  versus  $C$ , the data will be linear. The inverse of the slope of the straight line is equivalent to  $\beta$ , while  $\alpha$  is equal to the slope of the line divided by its intercept. The Langmuir sorption isotherm can also be adapted to suit a 2-surface solid or soil.

While the Langmuir isotherm assumes that a soil has a fixed number of sorption sites, the Freundlich isotherm does not require this assumption of the system to which it is applied (Kohl and Rice 1999). Therefore, the Freundlich isotherm is applicable to more complicated sorption processes than the linear or Langmuir models. A plot of the Freundlich isotherm is represented in Figure 2.2 and has the following mathematical form:

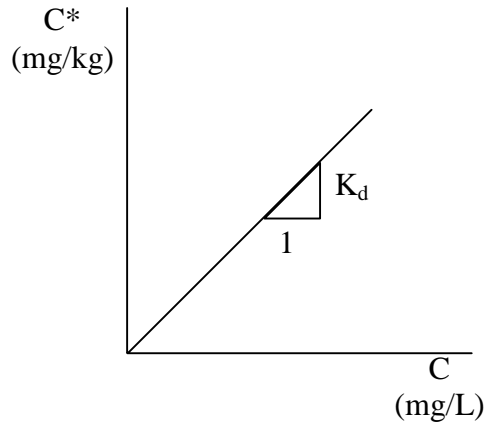
$$C^* = K_f \times C^N \quad (2.7)$$

where,

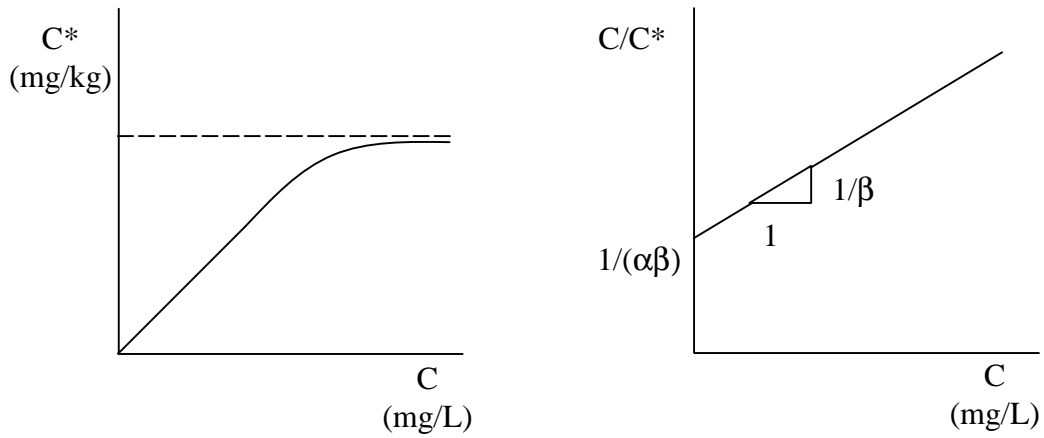
$N$  = empirical coefficient, distribution of adsorption sites (unitless)

$K_f$  = Freundlich distribution coefficient (L/kg)

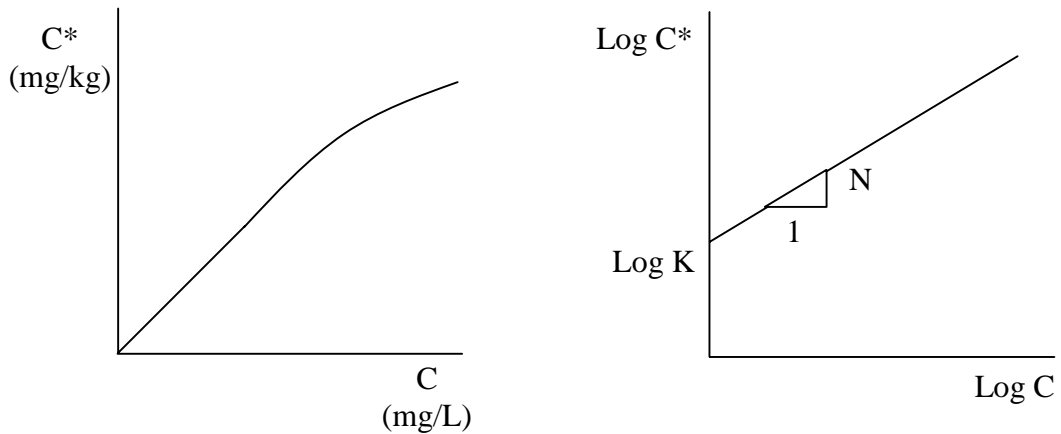
If the sorption data, when plotted as  $C^*$  versus  $C$ , is thought to fit to the Freundlich model, its shape will be curvilinear but will not reach a maximum like the Langmuir isotherm. If the same data is plotted as  $\log C^*$  versus  $\log C$ , the data will be linear. In this case, the slope of the straight line is equivalent to  $N$ , while  $K_d$  is equal to the intercept. If the value of  $N$  is 1, the Freundlich isotherm is equivalent to the linear isotherm. Variation from an  $N$  value of 1 denotes a non-uniform sorbent, or soil. When the value of  $N$  is greater than 1, the amount of solute sorbed increases with an increase in solute concentration. In this case, when compounds such as PAH's are present in high sorbed concentrations, the sorbed amount can act as another partitioning phase. PAH's in the aqueous phase can then partition into this new phase thereby increasing the sorbed quantity even further (Kohl and Rice 1999). In one investigation of the sorption of organic compounds in soil organic matter, conducted by Xing and Pignatello (1996), the decreasing value of  $N$ , less than 1, was correlated with an increase in sorption.



**Linear Isotherm**



**Langmuir Isotherm**



**Freundlich Isotherm**

$C^*$  = amount of solute sorbed to soil per dry unit weight of soil (mg/kg)  
 $C$  = equilibrium concentration of the solute in the aqueous phase (mg/L)

**Figure 2.2 Typical equilibrium isotherms  
 (Fetter 1993; Miller and Weber, Jr. 1984)**

The Freundlich sorption isotherm is often applied to organic compounds. Like the linear sorption isotherm, the Freundlich model does not limit the amount of solute that can be sorbed to a soil when realistically there should be an upper limit to the sorbable quantity (Fetter 1993).

#### **2.4.4 Irreversible Sorption**

Irreversible sorption occurs when contaminants are permanently sorbed to soil particles, sediments, or organic matter. Irreversible sorption can often be mistaken for slowly reversible sorption, which occurs when residual contaminants have diffused into remote voids in the soil matrix and gradually are released by molecular diffusion (Pignatello 1990; Pignatello and Xing 1996). In some cases, high molecular weight compounds that are subject to reversible sorption to the soil have a low potential for off-site migration and are thus viewed as less of a risk than reversibly sorbed pollutants. Desorption, or reversible sorption, can also occur in which a contaminant already in the sorbed phase dissolves into the surrounding groundwater or soil pore water. During the process of pump-and-treat remediation, a contaminant is likely to resorb and desorb over and over until it is finally drawn from the subsurface in the aqueous phase.

Park et al. (2001) conducted a series of dilution experiments on the degradation of naphthalene in soil and presented clear evidence of the existence of irreversible sorption. The results of this experiment showed the intercept for naphthalene desorption isotherms was significantly greater than the intercept for sorption isotherms, indicating a non-desorbable fraction of contaminant in the soil. A mass balance of naphthalene before and after the experiment further confirmed this evidence. Kan et al. (1998) presented similar results, confirming the occurrence of irreversible sorption for 7 different hydrocarbons to 4 different types of sediment. This investigation suggested that adsorption and desorption isotherms should be different and produced a combined adsorption/desorption isotherm for phenanthrene.

#### **2.4.5 Non-Equilibrium Sorption**

For simplicity, the partitioning of compounds between aqueous and sorbed phases is assumed to be instantaneous such as the case of the Freundlich and Langmuir isotherms.

However, this may not be the case for some contaminants such as organics that take longer to come into equilibrium. Therefore, non-equilibrium sorption can be assumed where the distribution of a compound is dependent upon time. The reversible linear kinetic sorption model is a common model that describes non-equilibrium sorption and is described as follows:

$$\frac{\partial C^*}{\partial t} = K_1 \times C - K_2 \times C^* \quad (2.8)$$

where,

$K_1$  = forward rate constant (time<sup>-1</sup>)

$K_2$  = backward rate constant (time<sup>-1</sup>)

This model is applicable when the rate of sorption is related to the sorbed concentration (Brusseau et al. 1991; Fetter 1993). As represented by the backward rate constant, this model assumes that sorption is a reversible reaction, or that desorption is possible.

#### 2.4.6 Cosolvency

Cosolvency refers to an enhancement in the concentration of a contaminant in the aqueous phase due to the presence of other aqueous phase compounds that act as solvents (Brusseau et al. 1991). When this process occurs compounds that are normally hydrophobic can dissolve and desorb causing their concentrations in groundwater to exceed the normal solubility limits. An example of this phenomenon is when high molecular weight compounds like benzo(b)fluoranthene exist at high concentrations in the aqueous phase. Benzo(b)fluoranthene is a 5-ring compound with a molecular weight of 252 amu and a low water solubility of 0.0015 mg/L. This constituent has a high affinity for sorption to soil and is likely to be present in the NAPL phase as well. When exposed to other solvent-like compounds already in the aqueous phase, such as naphthalene, benzo(b)fluoranthene can dissolve and desorb such that its aqueous concentration exceeds its limits of solubility in water. Cosolvency can be a beneficial reaction causing heavier sorbed compounds to become bioavailable and easier to remediate with pump-and-treat technologies. However, cosolvency can also cause larger

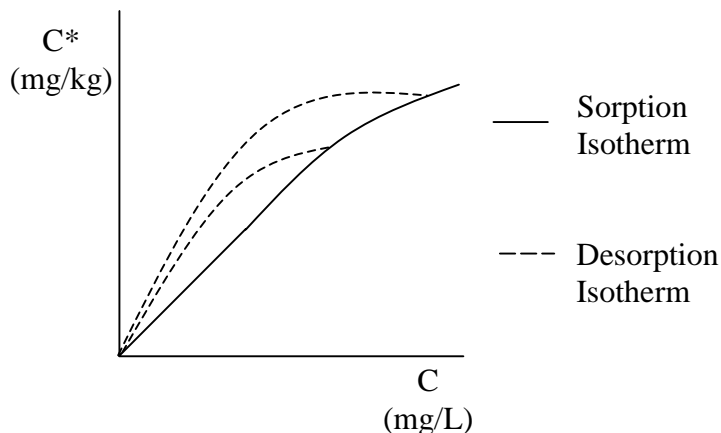
concentrations of high molecular weight cancer-causing compounds to be released in mobile groundwater and surface water; therefore, increasing the chance for transport off-site and the risk of human exposure.

#### **2.4.7 Competitive Sorption**

The interaction of humic organic matter in the soil with non-humic materials can change the sorptive properties of the soil (Kohl and Rice 1999). Lipids are a form of organic matter often found in the subsurface and can include alkanes, fatty acids, esters, and alcohols. Kohl and Rice (1999) showed the non-linear sorption of some PAH's can be attributed to lipids that are naturally present in the soil which compete for sorption sites in soil organic matter. When lipids are removed from the soil by extraction, the sorption capacity of the soil is increased causing an increase in the non-linearity of isotherms but the time dependence of sorption remains unchanged. The removal of lipids opens up sorption sites, that were formerly occupied, to other organic compounds such as PAH's. Once lipids are removed from a soil, the most marked increase in PAH sorption usually occurs for that PAH which is present in the highest concentration (Kohl and Rice 1999).

Xing and Pignatello (1998) suggested that naturally occurring aromatic acids can also compete for sorption sites in the soil organic matter. Aromatic acids are prevalent in most soils because they are released from living and decomposing plants. Due to their competition with organics for sites in the soil organic matter, aromatic acids may cause organic contaminants to increase in mobility and bioavailability (Xing and Pignatello 1998).

Many models assume that sorption and desorption isotherms will produce the same results. However, a number of investigations have shown that competitive sorption and other mechanical effects may, in some instances, lead to sorption phenomena such as hysteresis and particle concentration (Fu et al. 1994; Miller and Weber, Jr. 1984; Xing and Pignatello 1998). Hysteresis occurs when a compound's affinity for soil is higher when measured by a desorption isotherm rather than a sorption isotherm (Figure 2.3). Particle concentration occurs when the sorption coefficient decreases with increasing compound concentration. Both occurrences can be a result of competitive sorption.



$C^*$  = amount of solute sorbed to soil per dry unit weight of soil (mg/kg)  
 $C$  = equilibrium concentration of the solute in the aqueous phase (mg/L)

**Figure 2.3 Freundlich sorption-desorption isotherms displaying hysteresis ( Miller and Weber, Jr. 1984)**

#### **2.4.8 Mass-Transfer Limitations & Bioavailability**

In order for a compound to be degraded in the field, several essential conditions must be present such as an appropriate microbial community possessing the ability to degrade the compound in question and favorable environmental factors like temperature, moisture, oxygen, and nutrient supply (Mueller et al. 1989). Most importantly, the pollutant in question must be bioavailable, or in a phase that is conducive to microbial use. Generally, only aqueous phase contaminants are thought to be bioavailable since a substance must be dissolved in order to be transported across the cell membrane of a microorganism (Luthy et al. 1994; Zhang et al. 1998). Experimental studies have shown that PAH's with up to 6 rings can be biodegraded when present in the aqueous phase, but degradation of the same compounds in the sorbed phase is generally much more difficult and less efficient (Luthy et al. 1994). Therefore, the rate at which a PAH can be degraded is limited by dissolution and desorption kinetics. Consequently, the time required to remediate a site to target levels is also dependent on desorption and dissolution.

Even those compounds that are generally considered to be biodegradable may not be bioavailable due to environmental factors. Data from lab and field studies has shown that

when PAH concentrations exist below a certain threshold concentration, biodegradation can become extremely slow or stop altogether (Luthy et al. 1994). This phenomenon occurs because even low molecular weight compounds with high solubilities can be trapped within pores in the soil matrix or within the micropores in a soil grain itself. If these voids are smaller than the size of microorganisms, degradation cannot be achieved without water (Brubaker and Stroo 1992; Zhang et al. 1998).

When PAH concentrations drop below the threshold level due to low rates of desorption and dissolution, the total mass of carbon in the aqueous phase can also drop below the level of carbon needed to sustain an appropriate PAH degrading microbial community (Brubaker and Stroo 1992). PAH's with 2 to 3 rings, which have solubilities with a magnitude of parts per million, can be degraded because the carbon produced by desorption and dissolution is sufficient to maintain a viable microbial population. However, high molecular weight PAH's, which have solubilities with magnitudes of parts per billion, may not produce enough carbon by desorption and dissolution alone to support a workable level of microorganisms. Overall, the general trend reported by the literature states that the rate of dissolution and diffusion will dominate biodegradation, but biodegradation will influence the remediation at PAH contaminated sites (Brubaker and Stroo 1992; Ramaswami and Luthy 1997).

#### **2.4.9 Effects of Aged Contaminants & Soil Properties**

In addition to biokinetic and mass transfer limitations, aged contaminants and soil properties such as particle size and soil organic matter can also affect desorption and dissolution. Soil organic matter often refers to humic materials in the soil produced by the alteration or degradation of plant and animal matter. Correlations have been made between PAH concentration and soil organic matter content of soil. Jones et al. (1989) found that soils rich in organic matter generally contained higher concentrations of total PAH's. In natural systems, the carbon content may vary within a soil; therefore, the fraction of organic carbon alone may not reflect the differences in soil organic matter. For a detailed estimate of the effects of organic carbon on sorption, a model employing organic carbon as well as other parameters may be more effective (Garbarini and Lion 1986).

Soil organic matter can act as a solid-phase partitioning medium for organic compounds such as PAH's. As the molecular weight of a PAH increases, the binding capacity to soil organic matter increases (Jones et al. 1989). In addition, at high PAH concentrations, soil organic matter can swell resulting in additional sorption sites; therefore, soil organic matter has a higher capacity to hold a larger quantity of PAH's at high solution concentrations (Kohl and Rice 1999). Humic substances may also lower the surface tension of water, enhancing the solubility of pollutants and enabling them to increase in concentration in the groundwater (Mackay and Gschwend 2001). In another study of the relationship between desorption and organic sediments, Huang and Weber, Jr. (1997) showed that samples containing more physically condensed and chemically reduced soil organic matter demonstrated greater sorption to soil, non-linear sorption, and distinct hysteresis.

Hydrophobic organic compounds can exist in groundwater in both the dissolved form and also a colloid-associated form. High molecular weight compounds can exist in the dissolved form due to cosolvency. Laboratory studies show that hydrophobic compounds can also attach to colloid-associated species that include floating organic materials, microorganisms, microbial exudates, and other suspended materials (Johnson and Amy 1995; Mackay and Gschwend 2001). Mackay and Gschwend (2001) assessed groundwater at a coal-tar site to determine whether colloid-associated species can increase the amount of mobile PAH's in groundwater. The results of this experiment show strong evidence that hydrophobic organic compounds can be associated with organic colloids in groundwater causing aqueous concentrations to exceed normal solubility limits. Although the less soluble PAH's were found to increase the most in mass in the aqueous phase when associated with colloids, the more hydrophobic PAH's increased in mobility when bound to colloidal material (Mackay and Gschwend 2001). Johnson and Amy (1995) showed similar results in a study of PAH's and natural organic matter in aquifer sediments. Studies have also show that PAH's have been associated with colloids at creosote-contaminated sites (Mackay and Gschwend 2001).

The size of a soil particle can also have a major influence on the rate of PAH desorption. Large soil aggregates usually have a large number of binding sites available for sorption in comparison with smaller soil particles. Therefore, PAH's may take

considerably longer to become bioavailable in the presence of large soil aggregates because of their tendency towards sorption under these conditions (Wu and Gschwend 1986). Clay soils also highly influence the fate and transport of hydrophobic organics in the aqueous environment due to their large surface area with many sorption binding sites and abundance in the subsurface. Hundal et al. (2001) showed that smectite clays could retain large amounts of the organic chemical phenanthrene.

In general, the bioavailability of a contaminant decreases as the contaminant ages. This trend occurs as a result of slow sorption of contaminants to soil organic matter or entrapment within voids (Brubaker and Stroo 1992; Cornelissen et al. 1998; Northcott and Jones 2001). In one study, the decrease in PAH availability increased with molecular weight and partitioning coefficient (Northcott and Jones 2001). The rapidly desorbing fraction of a compound is generally bioavailable for use by microorganisms. However, as time goes by in a contaminated aquifer, there is more time for a compound to diffuse into inaccessible voids in the soil matrix as well as within soil aggregates themselves making compounds less available for biodegradation. Brubaker and Stroo (1992), citing Nam (1988), suggest that aged soils with an organic carbon greater than 2% cause a decrease in phenanthrene mineralization rates. Studies such as these show that the fraction of PAH's that were previously assumed to be biodegraded, in reality, may have been trapped within voids or bound to organic matter.

### **3. STUDY AREA & SAMPLING-SITE DESCRIPTION**

#### **3.1 Introduction**

The study area and sampling-site for this research is the Oneida Tie-Yard located in north-central Tennessee. This site was formerly used to treat railroad ties with creosote. When the site was active, creosote was discharged into the soil and migrated to the groundwater through various site operations. As a result, the site is highly contaminated. In chapter 3, a brief history of the Oneida Tie-Yard site, a description of the remediation plan for the site, an overview of the uptake and rainfall data in the Oneida area, and a summary of the recent soil and groundwater contamination trends on-site will be provided.

#### **3.2 Site History**

Most of the site history outlined in this chapter was obtained from the ARCADIS Geraghty & Miller Remediation Progress Meeting Reports from 2000 and 2001. The Oneida Tie-Yard is located in the central-southern region of Scott County, Tennessee, approximately 50 miles northwest of Knoxville, Tennessee.

The site was activated by the Tennessee Railway Company in the early 1950's as a railroad cross-tie treatment facility. The tie-yard was used continuously until the end of 1960 and then intermittently from 1960 to 1966 and 1968 to 1973. On-site operations finally ceased in 1973 when Southern Railway Company purchased the Tennessee Railway Company.

Figure 3.1 shows a plan view of the Oneida Tie-Yard site layout including the estimated locations of the wood treatment processes. The site originally included an above ground storage tank (AST) to hold creosote, a pressurized wood treatment unit, and a spur track for transporting the treated railroad ties. The treatment unit was supposedly located about 100 feet north of Pine Creek. All the runoff from the plant was collected in sump pits at the property line; however, these pits are no longer discernible. A holding pond was also located on-site, east of the treatment unit, and contained surplus creosote resulting from the pressure treatment process. The holding pond is suspected as the source area for the majority of contamination at the site. All of the creosote treatment equipment was disassembled and removed from the facility when site operations ceased.

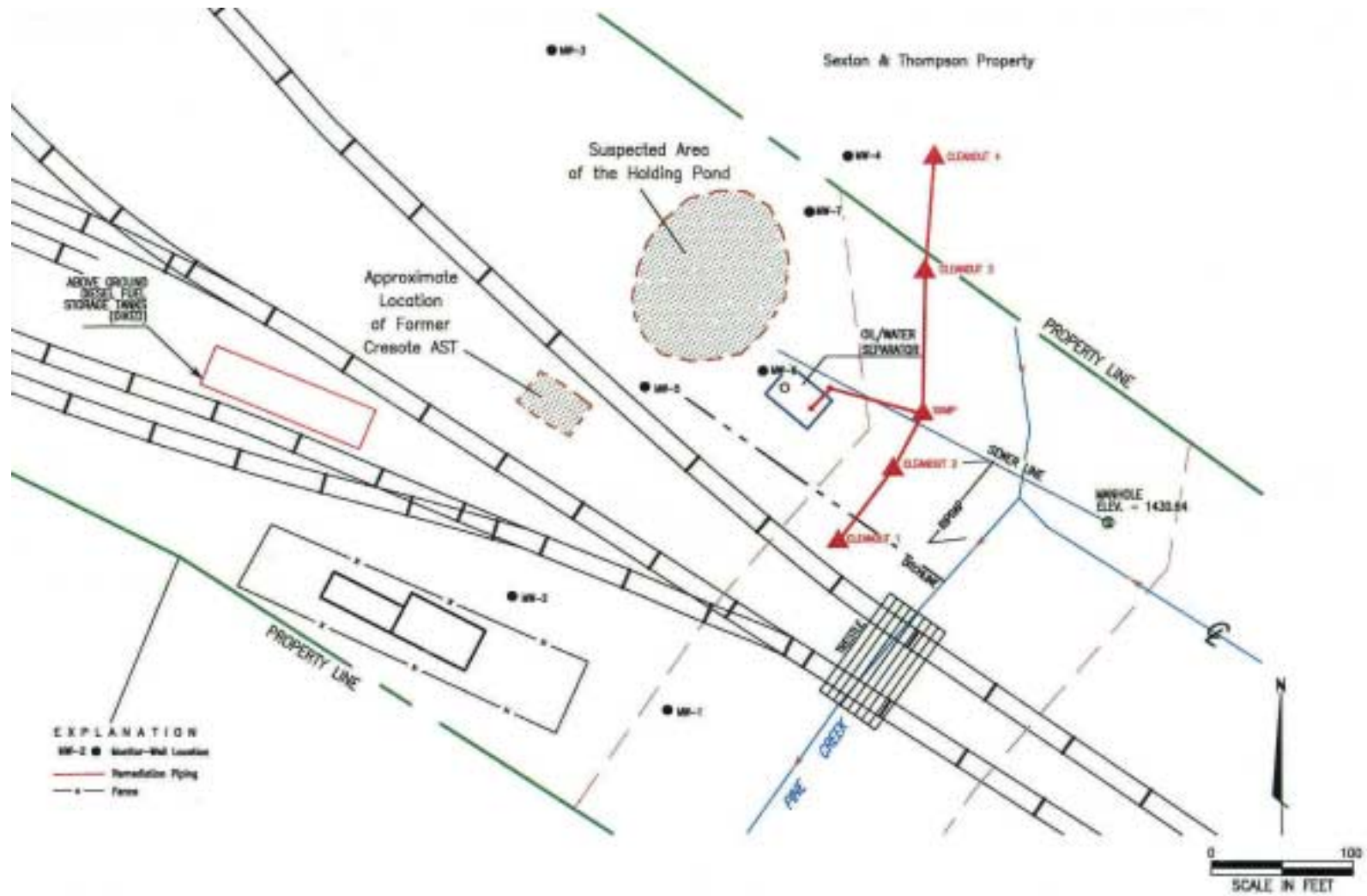


Figure 3.1 Oneida Tie-Yard site layout (ARCADIS Geraghty & Miller 2000)

The area located adjacent to the tie yard houses an active rail yard including 2 diesel fuel AST's and fueling and maintenance facilities. In addition, Pine Creek runs along the southeastern border of the site and eventually feeds into larger bodies of water.

In 1990, the United States Army Corps of Engineers was performing drainage channel work along Pine Creek, when they discovered evidence of creosote contamination near the railroad bridge that crosses over the creek. The pollution was reported to the Tennessee Department of Health and Environment (TDHE), who decided to further investigate the site conditions. The TDHE analyzed groundwater and soil samples from the treatment areas as well as surface water and sediment from Pine Creek. The results from these samples showed that there was creosote in the subsurface soil and creek sediments based on the prevalence of benzene, toluene, ethylbenzene, and xylene (BTEX) and PAH constituents.

Once it was established that contamination was present at the Oneida Tie-Yard, the TDHE required remedial action. The main goal of the initial remedial effort was to prevent any further creosote seepage into Pine Creek and to keep contamination from moving off-site. From 1991 to 1995, several different consulting firms performed soil, groundwater, and surface water sampling and analysis. In 1997, ARCADIS Geraghty & Miller, a consulting engineering firm, initiated a study to determine the appropriate method of remediation. Virginia Tech was also chosen to provide supplementary sampling and analysis and to assess the potential use of phytoremediation as a remedial technology.

### **3.3 Remediation Plan**

The initial cleanup strategy on-site was the installation of a groundwater collection trench and was conducted by Environmental Technology Incorporated (ETI). In March of 1991, ETI conducted initial abatement and preliminary site assessment (PSA) activities to determine the soil and groundwater characteristics at the site. As part of the PSA, 5 soil borings were completed and 5 monitoring wells were installed. In addition, ETI created some test pits at the southeastern end of the site. Eventually these pits were connected to form a groundwater collection trench roughly 330 feet long, 20 feet wide at the top, and 3 feet wide at the bottom. A 4 inch slotted drain tile was positioned in the trench and attached to a 24 inch vertical standpipe. The groundwater interception system

was updated in late 1997 and is still used as a method of hydraulic control to prevent creosote from traveling off-site and into Pine Creek. Groundwater from the site is collected by a submersible pump, situated in the standpipe, and sent to an on-site oil/water separator. The wastewater is then discharged to an 8 inch sanitary sewer line where it is treated at the Oneida public wastewater treatment facility. The oily free product is then separated and periodically removed.

In 1997, ARCADIS Geraghty & Miller performed additional sampling to further characterize the soil and groundwater at the tie-yard. The results of this effort showed that PAH contamination was located mainly at the water table and on top of the bedrock, which is roughly 10-12 feet below land surface. After assessing the location and nature of the contaminants, ARCADIS Geraghty & Miller proposed that an intrinsic cleanup process called phytoremediation, as well as bioremediation, be applied at the site. The TDHE approved the remedial action plan for the Oneida Tie-Yard in 1997.

ARCADIS Geraghty & Miller contracted Ecolotree to plant 1,026 hybrid poplar trees at the tie-yard in 1997 to induce phytoremediation. An additional 120 trees were planted downgradient of the original phytoremediation system in 1998. The trees were planted over roughly 2.5 acres of the site as displayed in Figure 3.2. Phytoremediation was a feasible strategy because the interceptor trench located at the southeastern end of the site served as a hydraulic control to keep contamination from moving downstream. In particular, hybrid poplar trees were chosen for this site based upon their evapotranspiration potential, growth rate, depth and distribution of roots, biomass yield and degradative enzymes produced, and their ability to bioaccumulate contaminants (Al-Yousfi et al. 2000). Poplar trees can be used to remediate contaminants through direct and indirect phytoremediation.

Contaminated soil from the excavation of the groundwater collection trench was spread over the top 2 feet of the surface of the site. A portion of the site was also covered by a layer of surplus coal from the adjacent rail yard activities. The coal layer has caused stunted growth in some trees and/or caused some trees to die because their roots cannot break through to the groundwater table. However, since they were planted many of the tree roots have been able to penetrate the groundwater table and reached the contaminated plume of creosote.



**Figure 3.2 Hybrid poplar tree layout  
(ARCADIS Geraghty & Miller 2001)**

A series of groundwater monitoring wells, as well as over 20 multi-level samplers, with ports located every foot above bedrock, were installed so that groundwater could be sampled. In addition to monitoring wells, piezometers and pressure transducers were fixed to measure the effect of the trees on groundwater flow patterns. The network of groundwater monitoring wells, multi-level samplers, piezometers, and pressure transducers allow sampling for a more accurate representation of the contaminated plume and soil and groundwater parameters.

### **3.4 Rainfall & Uptake Data**

The water table at the Oneida Tie-Yard is usually located roughly 7 feet below land surface but is highly sensitive to seasonal variability. According to seasonal data taken from the monitoring wells and multi-level samplers, ground water levels may vary from 6.5 feet below land surface to immeasurable depths. In some locations, groundwater is perched on shallow aquitards.

The general direction of groundwater flow at the Oneida Tie-Yard is from northwest to southeast toward Pine Creek. The flow direction remains constant despite the installation of the groundwater interception trench and the phytoremediation system. However, the hydraulic head and gradient have been affected by the remediation system. The average hydraulic gradient at the site is approximately 0.025 ft/ft based on groundwater contour plots of the site (Panhorst 2000). According to a Bouwer and Rice Slug-test completed in 1999, the estimated hydraulic conductivity on-site varies between

0.20 and 0.23 ft/day (Panhorst 2000). However, this approximation was determined to be low; therefore, the hydraulic conductivity was assumed an average of 10 ft/day (Panhorst 2000). The void ratio of the soil located on-site was determined, by a soil characterization test conducted by Muck (2000), to be 0.46, which corresponds to a porosity of 0.4. Darcy's law states that the linear groundwater velocity is equivalent to the hydraulic conductivity times the hydraulic gradient divided by porosity. According to Darcy's law and the aforementioned hydraulic parameters, the average linear groundwater velocity is approximately 7.5 inches/day.

The climate in Oneida, Tennessee is generally mild with typically 55 inches per year of precipitation. Water levels in the monitoring wells and multi-level samplers are very sensitive to rainfall events because the aquifer saturated thickness is fairly shallow and the water table is generally close to the land surface. In addition, spatial variations in groundwater velocity also exist. Typically, groundwater velocities increase during the summer season and decrease over the winter.

When fully grown, hybrid poplars can uptake and transpire over 50 gallons of water per tree per day which makes them useful for hydraulic control (Matso 1995). In some cases, poplar trees have even been found to transpire up to 350 gallons of water per day (Matso 1995). According to Loftis (1999), with approximately 1000 poplar trees on-site, this corresponds to an uptake rate of 4.6 gallons per tree per day. In a follow-up to this work based on transpiration data taken in 1999, Panhorst (2000) found the poplar trees at the Oneida Tie-Yard to use between 0.62 to 1.34 gallons of water per day per tree.

### **3.5 Groundwater Characteristics**

After the addition of the groundwater interception trench in 1991, additional sampling was performed, the results of which showed that no contamination was moving to off-site drinking water wells. However, PAH's were still detected in surface water and sediment samples taken from Pine Creek and also the effluent from the oil/water separator located on-site. In 1993, another site investigation was conducted and more groundwater samples were taken. The outcome of this sampling event implied that PAH's were impacting Pine Creek sediments, not only immediately adjacent to the site, but also further downstream. Off-site drinking water wells were still not affected. Samples were obtained once again in 1994 and 1995 indicating that PAH's were still present on-site.

An investigation of the soil underneath the riprap along the northern bank of Pine Creek was also conducted but creosote was only discovered seeping from one area. Since multi-level samplers were installed in 1997, groundwater samples have been analyzed by a Virginia Tech laboratory on a bi-annual basis. The selection of 10 monitored PAH's was based on groundwater analytical results over a 6 year period ending in 1997.

The plots displayed in Figure 3.3 and Figure 3.4 were created by Surfer, a contouring program, using MLS data. Each plot coincides with groundwater sampling events, conducted on-site between growing seasons, in March 1998, January 1999, December 1999, April 2000, March 2001, and March 2002. Figure 3.3 represents shallow depth-averaged data taken from multi-level sampling ports between 3 and 8 feet above bedrock, while Figure 3.4 shows deep depth-averaged data from bedrock to 2.5 feet above bedrock. The March 1998 distribution of PAH's in groundwater signifies the baseline groundwater contamination. This sampling event occurred before the first growing season of the hybrid poplars; therefore, the impacts of phytoremediation had not yet gone into effect. All sampling events after December 1999 were obtained after the third growing season when, in theory, the tree roots had fully penetrated the water table.

Overall, the plume is observed to be shrinking consistently over time in the shallow regions of the subsurface as well as in the deeper regions. A major contribution to the reduction in the northern end of the plume was the removal of a large supply of creosote in September of 1998. The concentrated creosote in this location most likely came from a waste pit used for creosote disposal. Total PAH concentrations in MLS-2 and MLS-3 were greatly reduced due to the removal of this source. The greatest reduction in PAH contamination is evident along the fringe of the plume closest to the railroad tracks. At MLS-12 along the outer portion of the plume, total PAH concentrations in the shallow ports decreased from an average of 570  $\mu\text{g/L}$  in March 1998 to 9.6  $\mu\text{g/L}$  in March 2002. In the deeper ports, total PAH concentrations at MLS-12 decreased from 1432  $\mu\text{g/L}$  in March 1998 to 14.1  $\mu\text{g/L}$  in March 2002. Figure 3.5 indicates the changes in the log of the total PAH distribution with depth over time for MLS-12.

Phytoremediation was a feasible strategy only because the groundwater interceptor trench served as a hydraulic control to keep contamination from moving into Pine Creek. Therefore, 3 multi-level samplers were located between Pine Creek and the trench to confirm the success or failure of the interception and phytoremediation system. Once the

groundwater interception trench was rehabilitated, the PAH concentrations in groundwater at MLS-9 and MLS-10 were reduced. For example, the total PAH concentration at MLS-9 located 1.27 feet above bedrock decreased from 116 to 24.23  $\mu\text{g/L}$  over a period from March 1998 to March 2002. Although PAH's have been consistently detected in MLS-10, total PAH concentrations have been limited to 45  $\mu\text{g/L}$  and below at this multi-level sampler since the inception of the groundwater trench. However, groundwater contours look as if they continue outside of the interception trench in most of the Surfer contour plots. Although concentrations at these 2 multi-level samplers are generally below the detection limit, interpolation using kriging methodology incorrectly depicts the plume as extending to MLS-9 and MLS-10. Conversely, the third multi-level sampler located beyond the interception trench, or MLS-8, has fluctuated in PAH concentration. In addition, the presence of NAPL has been occasionally detected in Pine Creek.

Much of the creosote DNAPL is still located in a pooled region right above bedrock causing deep groundwater PAH concentrations to remain high in the central portion of the plume. The most contaminated location on-site, as indicated by the darker regions in Figure 3.3 and Figure 3.4, is believed to be where the former holding pond was located. This area is situated east of the former treatment unit and close to the original location of Pine Creek. MLS-7 is located directly in the center of the most contaminated region of the plume. From March 1998 to March 2002, total PAH concentrations in the shallow ports of MLS-7 decreased from 12.7 mg/L to 2.5 mg/L, while there was no reduction in total PAH concentration in the deeper ports due to the presence of free product. Figure 3.5 indicates the changes in the log of the total PAH distribution with depth over time for MLS-7. A logarithmic scale was chosen to emphasize the difference in PAH concentration between the shallow and deeper ports at MLS-7.

Overall, remediation has progressed significantly at the Oneida Tie-Yard over the time period in which PAH concentrations have been monitored by Virginia Tech. In general, the contaminant plume has decreased in size and migrated downgradient towards Pine Creek but is interrupted by the groundwater interception trench. Creosote DNAPL has traveled downward in the soil until reaching an impermeable layer, which is for the most part bedrock. In some areas, the plume appears to follow the gradient of the confining layer rather than the hydraulic gradient.

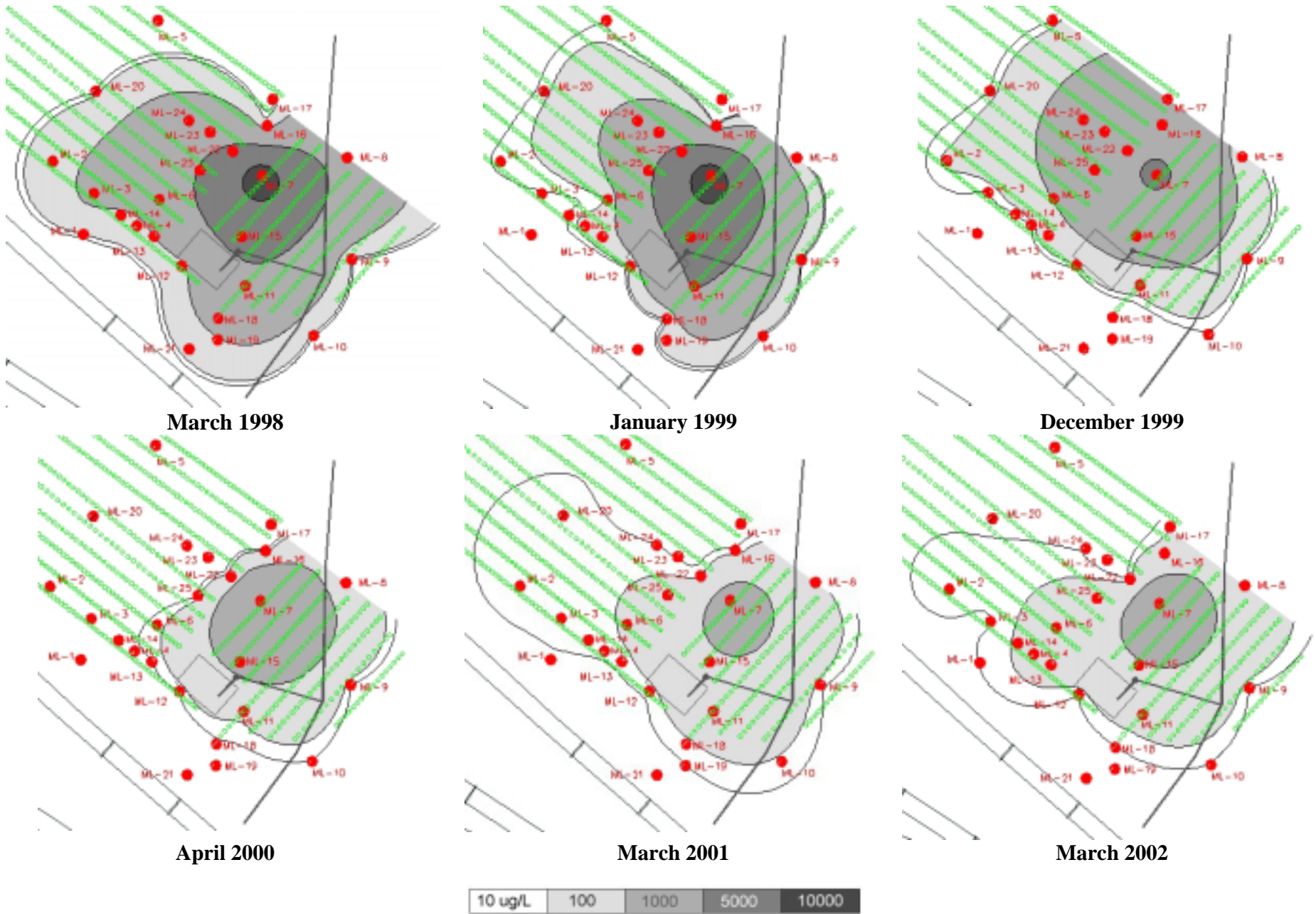


Figure 3.3 Average total PAH concentrations ( $\mu\text{g/L}$ ) in groundwater, 3 to 8 feet above bedrock

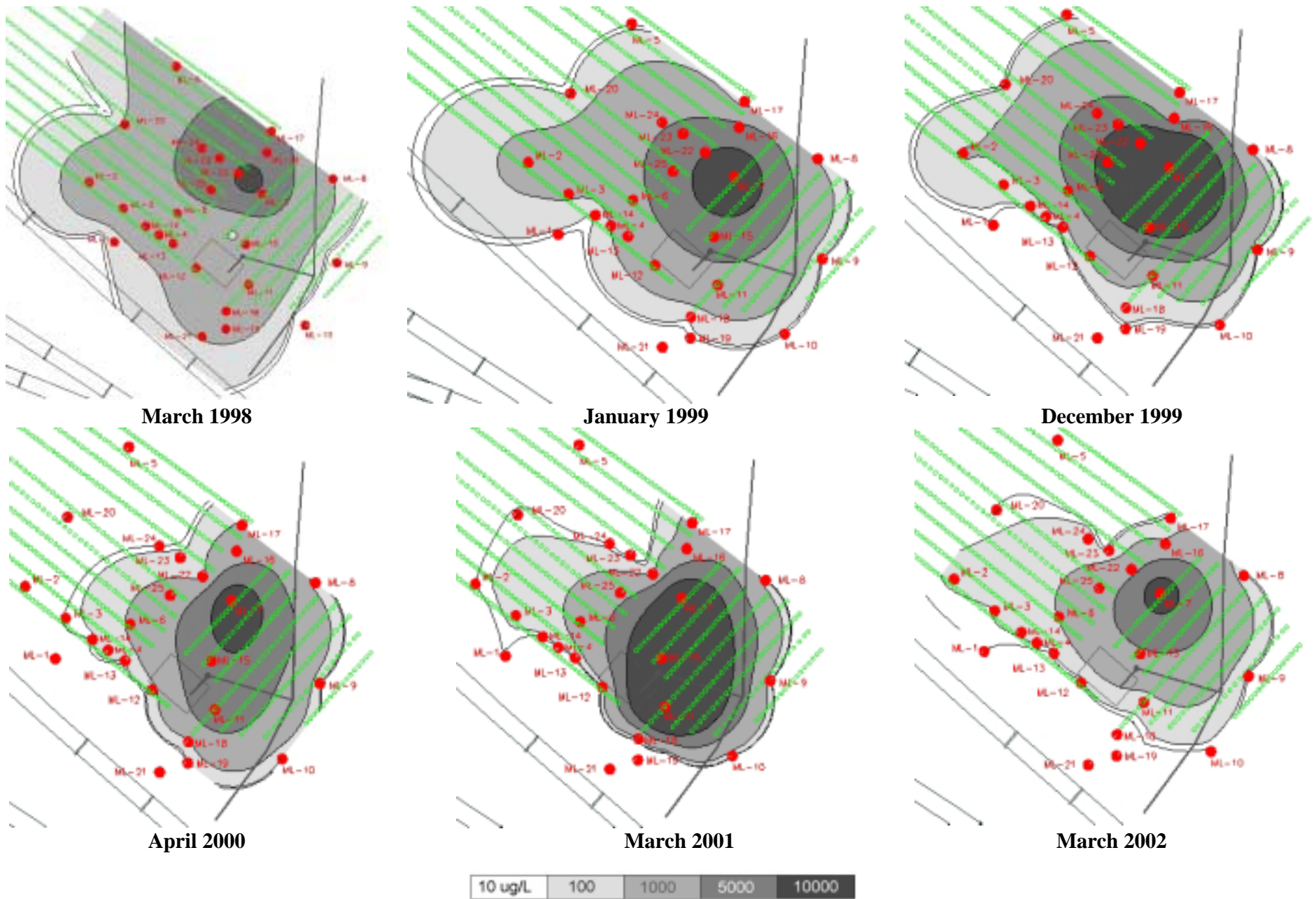
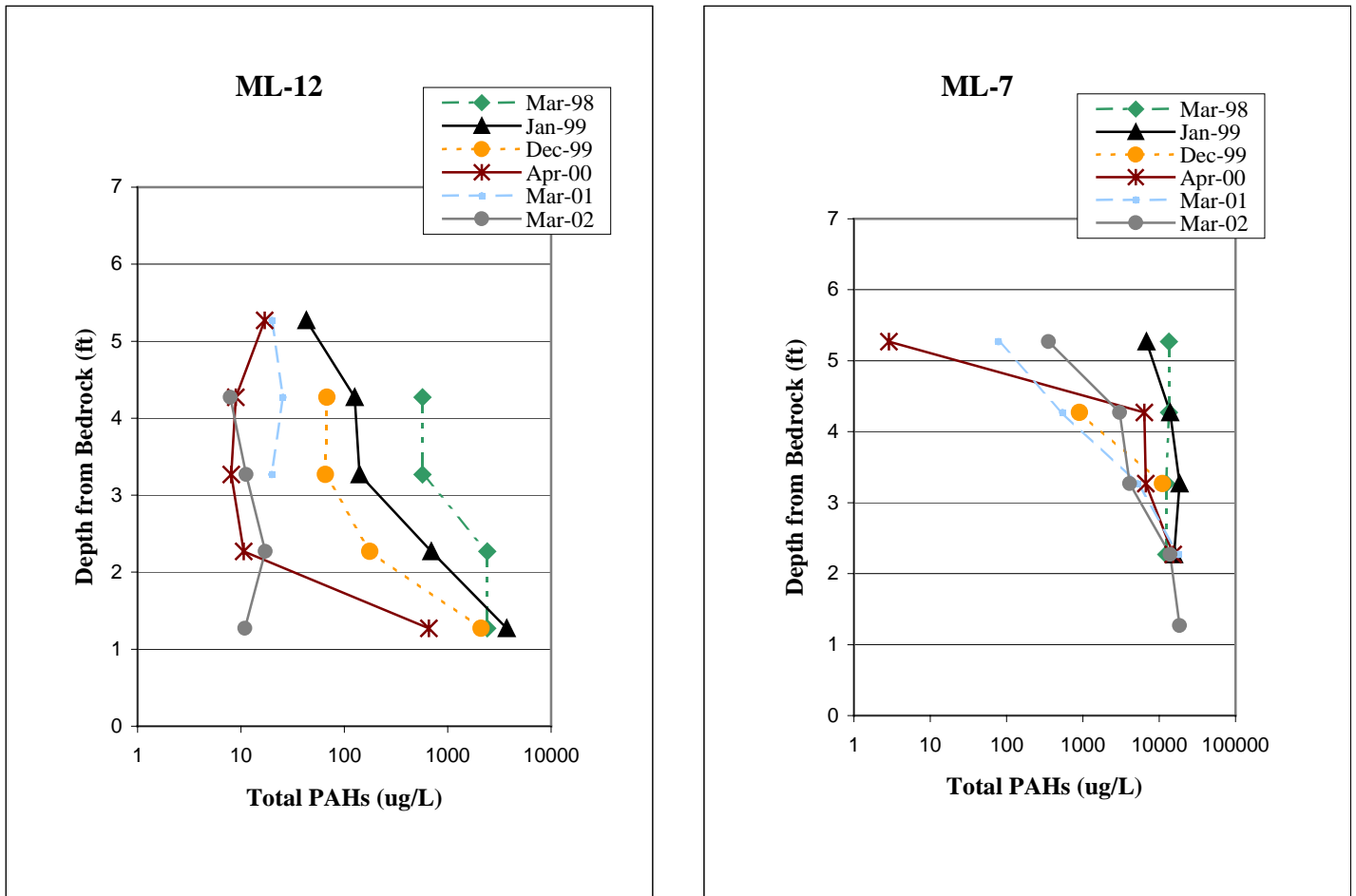


Figure 3.4 Average total PAH concentrations in groundwater, 0 to 2.5 feet above bedrock

Many of the individual multi-level samplers have shown steadily declining PAH concentrations in groundwater with time. In some areas, such as near MLS-2 and MLS-3, this decrease is due to source removal. The reduction in PAH concentration near MLS-9 and MLS-10 is due to the removal of contaminated groundwater by the interception trench. On the other hand, in the other areas of the site, PAH reduction is most likely due to a combination of phytoremediation and natural attenuation.



**Figure 3.5 PAH concentration in groundwater changes with time and depth at MLS-7 & MLS-12**

### 3.6 Soil Characteristics

The subsurface conditions at the Oneida Tie-Yard were determined during soil sampling events in 1998. Hand auger borings were taken as well as visual soil classifications of the different soil conditions on-site. The result of this investigation was an improved understanding of the extent of creosote DNAPL contamination, as illustrated in Figure 3.6. The hydrogeology on-site is characterized by a shallow unconfined aquifer consisting of 3 layers. A mixture of gravel and coal, which was placed over the site during rail yard and remediation activities, is located in the first few feet under the ground surface. The first layer of native soil, which consists of 5 to 6 feet of silty clay, is located underneath the coal and gravel mixture. A silty sand layer, which is 4 to 5 feet thick, underlies the top native soil layer and overlies bedrock. Shale bedrock is typically located 8 to 12 feet below land surface. The majority of free-product creosote is located in the silty sand layer, 6 to 8 inches above bedrock. According to a sampling investigation by Muck (2000), this layer is a non-plastic silty sand (Unified Soil Classification System - SM) and has a percentage of fines between 10 to 30%.

Soil samples have been taken with a hand auger and analyzed for PAH contamination by a Virginia Tech laboratory on an annual basis as of 1997. Soil borings (SB) are sampled along 2 transects of the site as shown in Figure 3.7. Transect 1 is located parallel to the railroad tracks on the western end of the site, while transect 2 is located in the center of the site within the interior of the NAPL plume. Subsurface conditions at transect 2 are represented in Figure 3.6. Six of the most prevalent PAH's on-site were selected for monitoring based on analytical results from a soil sampling event in 1997. High molecular weight PAH's generally have low water solubilities and tendency towards adsorption to soil and sediments. Therefore, six 3 and 4-ring compounds of high molecular weight were chosen as the focus of soil remediation at the Oneida Tie-Yard.

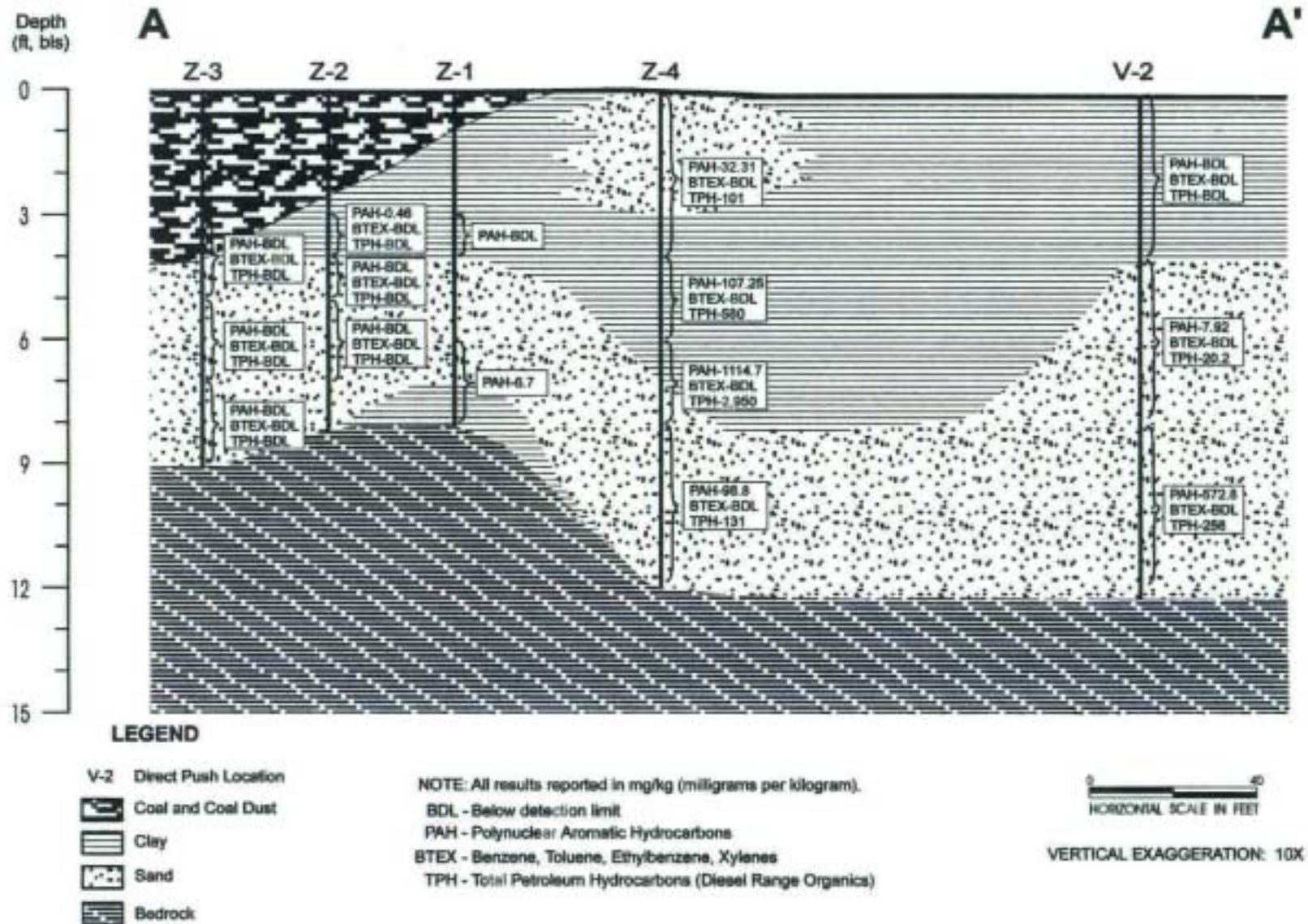


**Figure 3.6 Cross section of soil transect 2 (ARCADIS Geraghty & Miller 2000)**

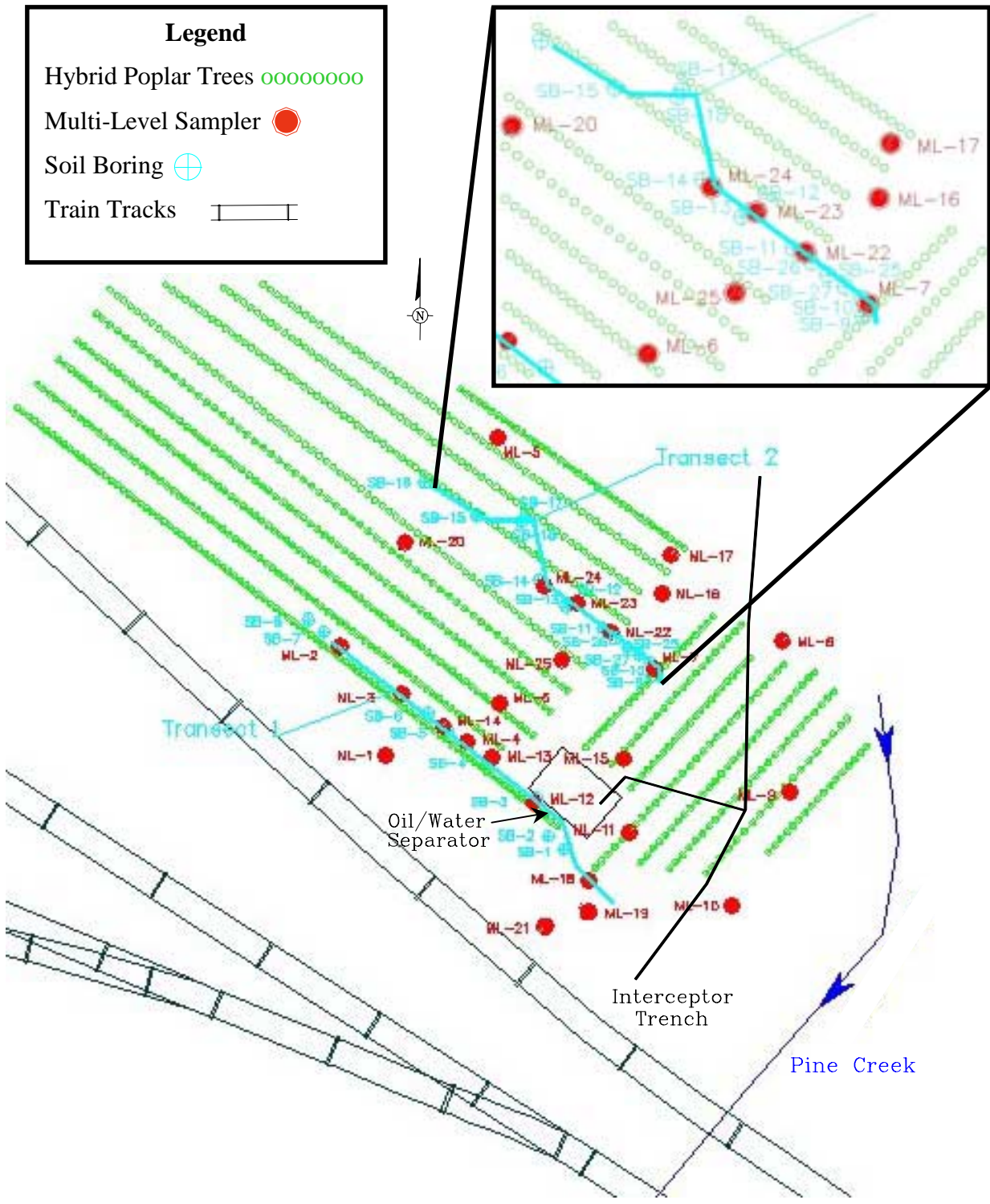


**Figure 3.7 Multi-level sampler & soil boring locations at the Oneida Tie-Yard site**

The cross-sectional plots displayed in Figure 3.8 were created using Surfer. Each plot coincides with hand auger soil sampling events conducted on-site in July 1997, June 1998, October 1999, March/April 2000, and July 2001. Samples were taken from a range of 3 to 10 feet in depth below land surface. The July 1997 distribution of PAH's in soil signifies the baseline soil contamination (time,  $t = 0$ ). This sampling event occurred before the first growing season of the hybrid poplars; therefore, the impacts of phytoremediation had not yet gone into effect.

The decrease in concentration of PAH's in soil with time is noticeable although not as marked as the reduction of PAH's evident in groundwater. At both transects, soil PAH concentrations with depth are not always consistent emphasizing the heterogeneity of the soil on-site. Human error in accurately gauging the depth of soil samples also contributes to the irregularity of PAH contaminants in the soil.

Along the fringe of the groundwater plume, at the northern end of transect 1, depth-averaged total PAH concentrations generally diminished with time. For example, depth-averaged total PAH's at a soil boring near MLS-3 decreased from 173.3 mg/kg in July 1997 to 10.85 mg/kg in July 2001. However, this reduction could be due to the removal of a large source of creosote in September of 1998. In contrast to the northern end of transect 1, total PAH concentrations remained fairly steady in the southern half of transect 1 close to the location of the oil/water separator.

The concentration of fluoranthene over time in soil along transect 2 is shown in Figure 3.8. Fluoranthene is a 4-ring compound with a fairly high molecular weight of 202 amu and a low water solubility of 0.26 mg/L. This compound was chosen as a representative example for study due to its high affinity for sorption to soil and its presence in the NAPL phase. As shown by the plot, from July of 1997 to July of 2001, the center of the fluoranthene NAPL plume appears to be moving northwest along transect 2. Free product just above bedrock may be following the geologic gradient of the confining layer rather than the hydraulic gradient. From October 1999 to July 2001, the center of the NAPL plume appears to be stabilized near SB-11. Overall, the concentration of fluoranthene close to bedrock appears to have been reduced from an average above 2500 mg/kg to between 1000 and 1500 mg/kg.

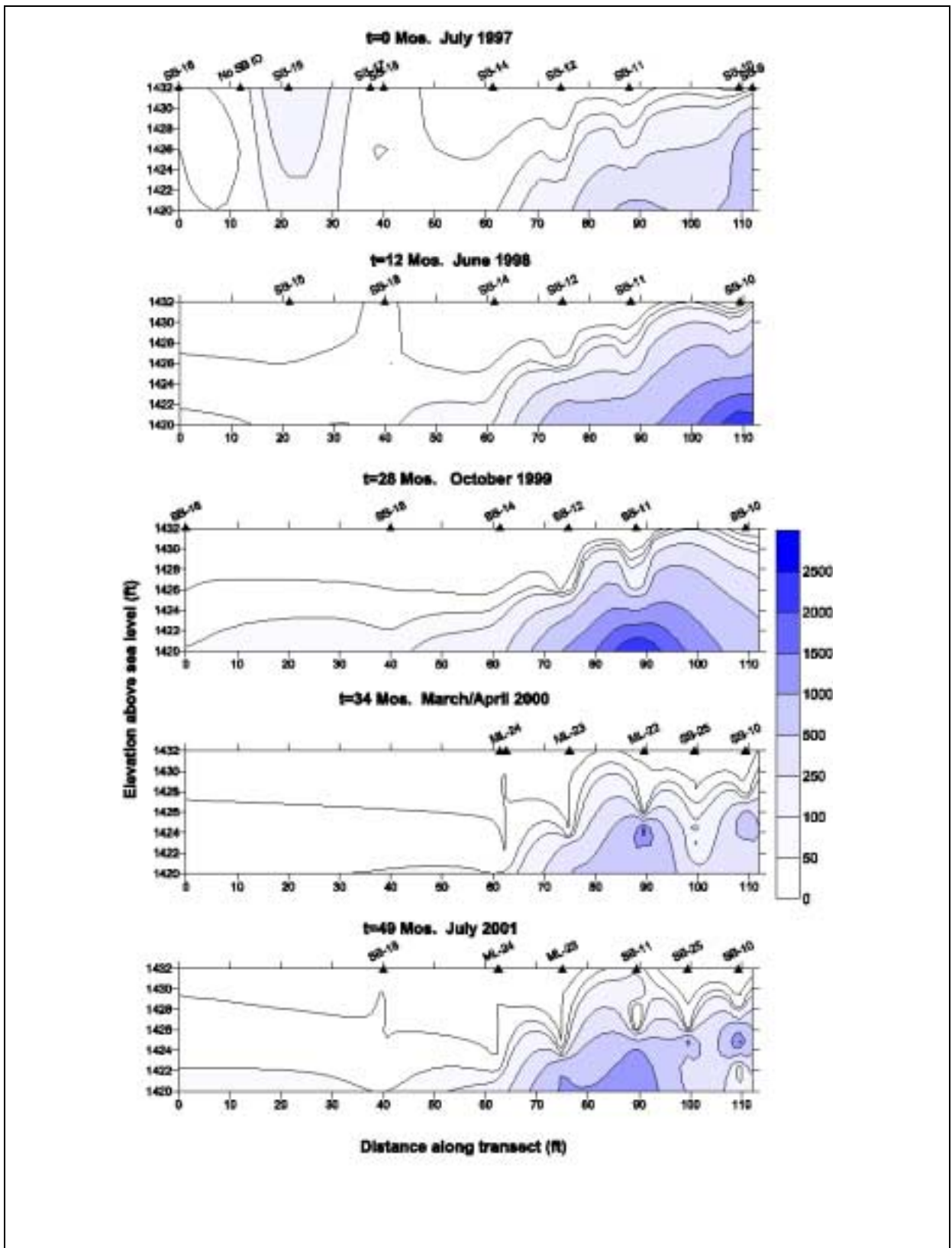
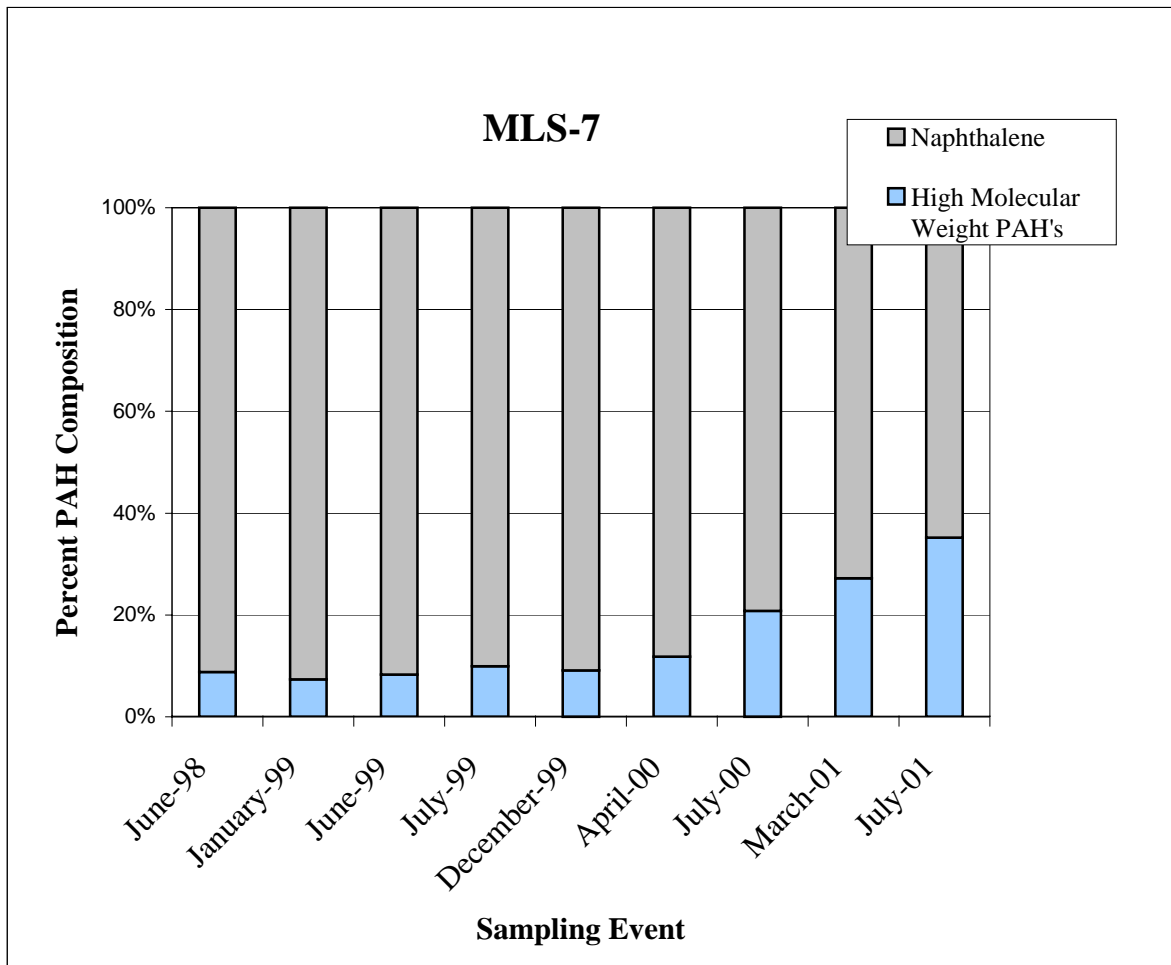


Figure 3.8 Soil concentration (mg/kg) depth profile for fluoranthene along transect 2

### **3.7 Site Desorption & Dissolution Characteristics**

The contact of clean groundwater with creosote causes desorption and dissolution of creosote constituents ultimately resulting in the generation of a PAH contaminated groundwater plume. However, because creosote is a complex matrix of contaminants, each of its components will fractionate at different rates into the air, water, or soil as a function of physical and chemical properties. While low molecular weight PAH's such as naphthalene may be directly taken up by the roots of plants and/or bioremediated, many of the 4 and 5-ring PAH's such as chrysene have a strong tendency to sorb onto subsurface particles.

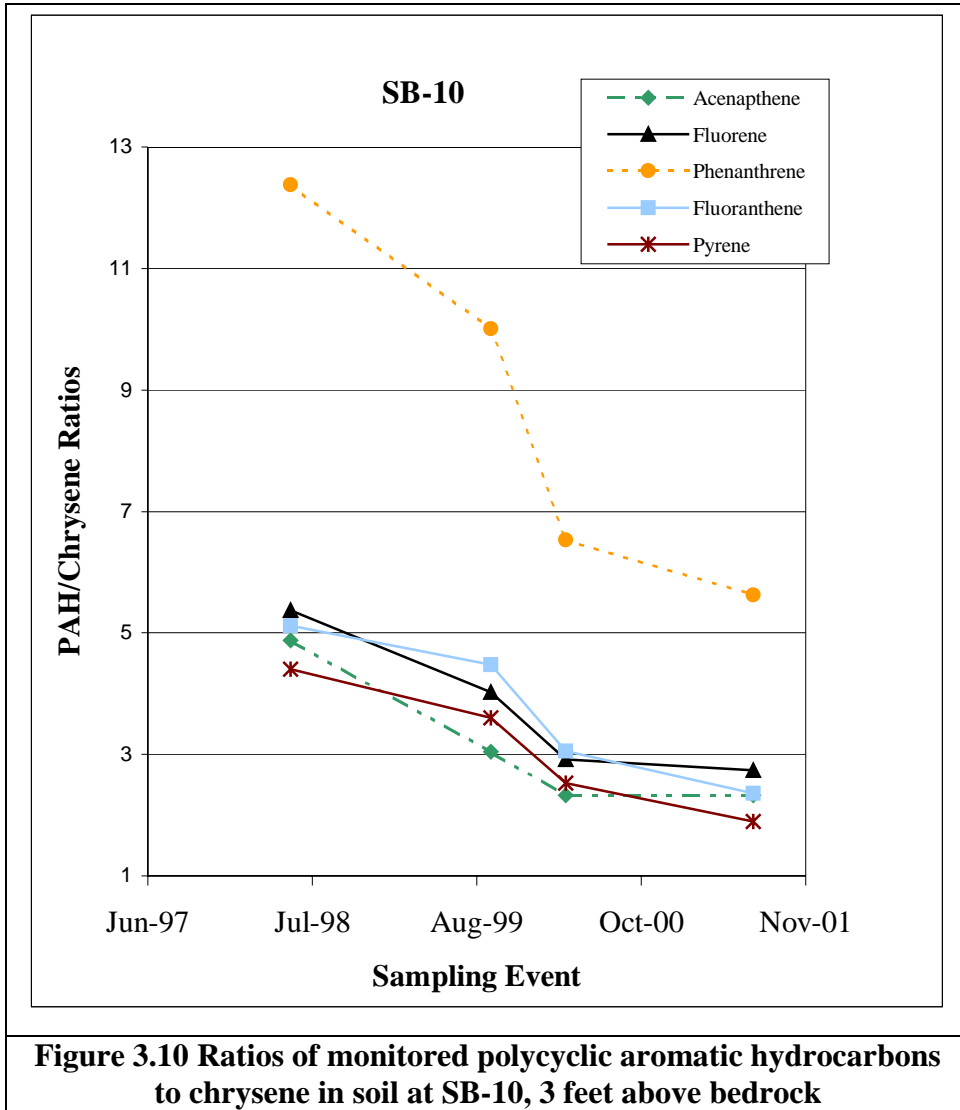
The focus study area for the research described in Chapter 4 is located in the central contaminated portion of the site between MLS-7 and MLS-24. This sampling location was chosen based on the high concentration of PAH's in groundwater at MLS-7 and the presence of free product in the lower ports. As illustrated in Figure 3.9, the percentage of naphthalene is decreasing with time at MLS-7 relative to the 4 and 5-ring PAH's indicating the change in chemical and physical composition of the contaminant at this level. As the lower molecular weight compounds dissolve and the water soluble fraction becomes enriched in low molecular mass compounds, the DNAPL becomes enriched in high molecular weight PAH's which are less susceptible to water-based technologies such as phytoremediation and bioremediation. The rate at which water-based technologies function is often controlled by the pace of desorption and dissolution. Therefore, the laboratory experiments described in this report will examine this principal rate factor limiting the performance of phytoremediation.



**Figure 3.9 Percent high molecular weight polycyclic aromatic hydrocarbons in groundwater with time at MLS-7, 3.27 feet above bedrock**

The ratios of monitored PAH's in soil at SB-10 were calculated to determine the change in creosote composition with time. SB-10 is located at the center of the NAPL plume close to MLS-7; therefore, the PAH concentrations in soil at SB-10 can be compared to PAH concentrations in groundwater at MLS 7. The ratios of 3-ring PAH's, namely acenaphthene, fluorene, and phenanthrene, are shown in Figure 3.10. For the most part, the ratios of 3-ring compounds to chrysene were reduced from approximately 5 to 2, which correspond to a 60% reduction in soluble compounds and a chrysene enrichment of 0.2 to 0.4. Conversely, phenanthrene decreased in ratio from 12 to nearly 5, which is also equivalent to a 60% reduction in soluble compounds and an enrichment of chrysene concentrations of 0.08 to 0.2. The ratios of the 4-ring compounds, fluoranthene and pyrene, are also shown in Figure 3.10. Concentrations of fluoranthene and pyrene behaved similar to those of the 3-ring compounds with a reduction in ratio from 5 to 2. The large reductions in ratio of PAH's to chrysene occurred during sampling events in late 1999, which were obtained after the third growing season once the poplar tree roots had penetrated the water table. The increased reductions at this time indicate that the trees are contributing to a reduction of the soluble PAH compounds.

Chrysene was chosen for comparison with the other PAH's because it has the lowest solubility and highest molecular weight of all of the monitored PAH's thereby making it fairly recalcitrant and prone to sorption. The soluble PAH's are removed quickly from the subsurface by means of direct uptake and biodegradation. If the most water soluble contaminants in a NAPL are removed by contact with water, the less soluble high molecular weight compounds are left in the NAPL or sorbed phase. In some circumstances, these high molecular weight compounds do not pose an appreciable risk to human health or the environment because they have limited mobility. However, in certain situations, these sorbed compounds may continue to leach contaminants after the low molecular weight compounds have been treated. For this reason, NAPL compositional changes with time, as demonstrated by this research, must be accounted for in order to estimate aqueous PAH concentrations and the ecological and public health risk.



## **4. MATERIALS & METHODS**

### **4.1 Experimental Design Approach**

In this chapter, details will be given to describe the methods of groundwater and soil sampling and analysis throughout the operation of 3 desorption and dissolution experiments conducted during the course of this research. Specific information pertaining to the analytical procedures will also be presented. Determination of soil and groundwater contamination on-site was necessary to accomplish the objectives of this research. Depth specific groundwater and soil samples were obtained from the Oneida Tie-Yard facility during sampling trips in March and July of 2001. In addition, soil and water samples were taken and analyzed periodically throughout the course of the 3 lab experiments. The target compounds in this study were: naphthalene, acenaphthylene, acenaphthene, fluorene, phenanthrene, anthracene, fluoranthene, pyrene, chrysene, and benzo(b)fluoranthene. These PAH's are prevalent in creosote and represent a range of chemical characteristics and solubilities.

Each of the 3 experiments conducted during this research were designed to characterize the desorption and dissolution properties of PAH's at the Oneida Tie-Yard. The desorption equilibrium experiment, described in Section 4.3, is a batch test to determine general isotherms for each PAH over a range of sampling locations on-site and to establish the maximum desorption capacity for 10 monitored PAH's. The desorption kinetics experiment, described in Section 4.4, is a batch test to estimate the total mass of each PAH that is irreversibly sorbed to the soil, to determine the rate of desorption of each PAH, and to develop isotherms for each PAH at specific sampling locations on-site. The dissolution kinetics experiment, described in Section 4.5, is a soil column test to estimate the rate of dissolution under field-like conditions.

### **4.2 Batch Experiment Setup**

The soil samples used in the batch experiments were collected in July 2001. The samples were collected following the field procedures listed in Section 4.6. As shown in Figure 4.1, auger holes were drilled by hand and sampled at depths of 5 to 10 feet below ground between the location of MLS-7 and MLS-24. Fluorene was chosen as a representative PAH for Figure 4.1 because it has been consistently found in background

soil samples since the first soil sampling event on-site. Once taken from the site, the soil samples were stored in Ziploc bags in the 4°C refrigerator at Virginia Tech for several months until they were removed for use in the batch experiments.

In the laboratory, samples were removed from the refrigerator and mixed thoroughly within each bag. Soil was then scooped into a correspondingly labeled aluminum soil pan using a FisherBrand™ Scoopula spatula (Fisher Scientific, Atlanta, Georgia). If there was enough sample, the soil was divided into 2 equal parts for duplicate tests. Each soil sampled filled approximately 1 soil pan volume, which is equivalent to 42 cm<sup>3</sup>, and a roughly 40 gram mass. Once the soil was measured, the sample was then placed into a clean labeled 250 mL amber Quorpak bottle with a TFE lined screw cap closure (Fisher Scientific, Atlanta, Georgia). Each bottle was filled with distilled water, representing groundwater from the site, until the water level reached the neck of the bottle. A blank, or control sample, was also prepared by filling one of the 250 mL amber bottles with distilled water only. Figure 4.2 and Figure 4.3 show the experimental setup for these batch samples. Once the samples were prepared, they were placed in a divided cardboard box and located in a darkened constant temperature (20°C) room to avoid photodegradation (Figure 4.4). Soil extractions, following the instructions outlined in Section 4.7.2, were performed prior to the setup of the first equilibrium batch experiment and after the last sampling event of the second batch trial.

### **4.3 Desorption Equilibrium Experiment**

The desorption equilibrium batch experiment was setup in twenty-four 250 mL amber jars as described in Section 4.2. Samples were agitated by hand daily and taken over an 11 week period at 3, 14, 28, and 77 days. In order to sample each jar, 40 mL of water was drawn off with a Pasteur pipette from the middle of the supernatant and placed in a 40 mL amber vial. Care was taken not to disturb the sample when opening the TFE screw cap and also when moving samples. The jars were undisturbed for 24 hours prior to sampling in order to allow settling of all solids.

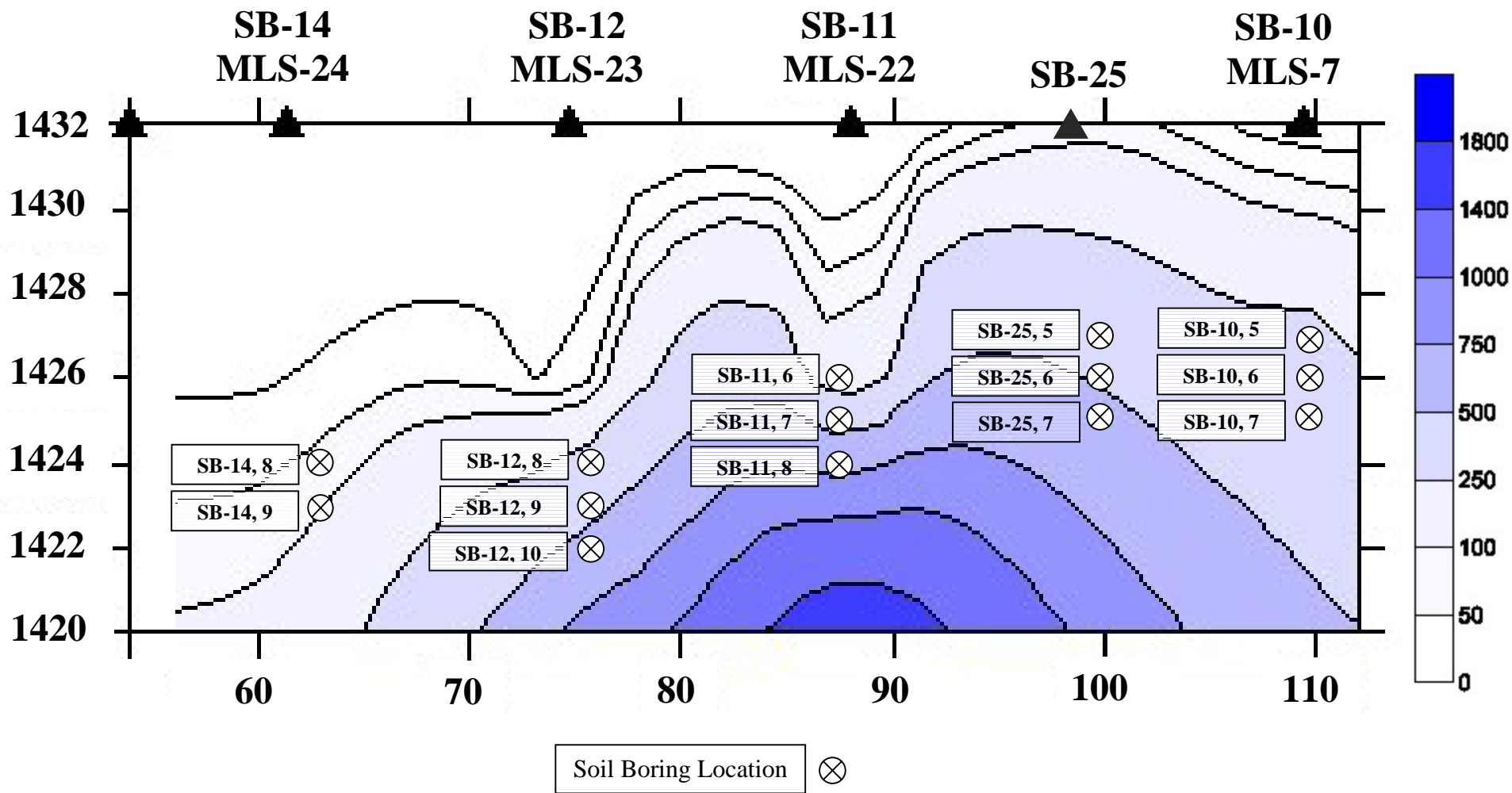


Figure 4.1 Depth profile for study area and sampling site soil boring locations (1999 fluorene soil concentrations (mg/kg) along transect 2)

In some cases, contaminated samples required dilutions. Depending upon the level of contamination, the following dilutions were used: 1:3.77, 1:18.85, and 1:37.7. After analysis with a gas chromatograph (GC), it was determined that all contaminated samples would be diluted at a 1:3.77 ratio for consistency between samples. Following sampling, the 40 mL water samples were extracted using the water extraction procedure described in Section 4.7.1. No water was added to the 250 mL amber jars to replace the sample volume that was removed.



**Figure 4.2 Schematic of batch experiment**



**Figure 4.3 Batch experiment example**



**Figure 4.4 Batch experiment storage location**

#### **4.4 Desorption Kinetics Experiment**

The desorption kinetics batch experiment used the same physical setup as the desorption equilibrium experiment, but incorporated a draw and fill method where distilled water was added after every sampling event. After a review of the results from the first equilibrium batch experiment, it was determined that by 3 days, most samples had reached their maximum equilibrium desorption capacity. Therefore, samples were agitated by hand daily and taken every 3 days over a 15 week period. However, due to time constraints, only every third sample taken from the desorption kinetics experiment was run on the GC.

For this experiment, samples were taken according to the same guidelines as listed in Section 4.3. However, in this case, after each sample was drawn out of the 250 mL amber jars and into 40 mL vials, the supernatant was carefully poured off into a waste beaker. Care was taken to ensure that an undisturbed volume of water was left containing the settled solids. Each 250 mL amber bottle was then slowly refilled with distilled water until the water level reached the neck of the bottle. The supernatant from extremely contaminated samples was disposed of according to Virginia Tech Environmental Health & Safety Services regulations. Samples were stored for 2 weeks at 4°C until the water extraction process described in Section 4.7.1 was initiated. Contaminated samples were diluted at a 1:3.77 ratio for consistency between sampling events.

#### **4.5 Dissolution Kinetics Experiment**

Soil column experiments were used to determine the rates and extent of dissolution for each monitored PAH. Each soil column was constructed using contaminated soil, overlain by medium grade sand, and filled with distilled water in a section of capped clear PVC pipe. Gravity drained water samples were taken at the soil/sand interface over 3 day, 6 day, and 12 day time periods.

Medium grade (0.053 mm – 0.46 mm) filter sand was purchased through Drillers Service, Inc. (Roanoke, Virginia) and rinsed with water to float off the fines. Once the rinse water was no longer visibly turbid, the soil was soaked in cleaning grade methanol (Virginia Tech Chemistry Storehouse, Blacksburg, Virginia) for at least 24 hours in the vent hood. At this time, the methanol was poured off and the sand was rinsed with water

until the smell of methanol was no longer evident. The sand was then left in the vent hood until it was dry.

An 8 foot section of clear Schedule 40 4 inch PVC pipe was purchased through McMaster-Carr (Atlanta, Georgia) and cut into 1 foot sections. The pipe had an outside diameter of 4.5 inches, an inner diameter of 3.998 inches, and a wall thickness of 0.237 inches. Gas valves taken from small gas standard cylinders were then attached to each PVC section at approximately 5 inches from one end. Once the burrs and shavings were removed with a file and knife, the pipes were then washed with soap and water and brushed with a clear PVC primer to ensure a good seal between the pipe and cap when bonded. Next, 4 inch Acrylonitrile-Butadiene-Styrene (ABS) caps were glued with multi-purpose PVC/ABS cement to the end of the PVC pipe farthest from the gas valve. In order to indicate the soil/sand interface, a permanent line was marked around the circumference of the PVC pipe approximately 0.5 inches below the gas valve.

The soil samples used in the soil column experiment were collected in July 2001 and February 2002. Auger holes were drilled by hand and composite samples were collected from borings near MLS-22, SB-11, and SB-25 (Figure 2.1) at approximately 8 to 9 feet below land surface. Each sample was put in a mason jar, capped, and then placed in a cooler for on-site storage. Eventually the samples were relocated to the 4°C refrigerator at Virginia Tech, where they were stored for several months before being removed and mixed together in a large bucket. Soil extractions, following the instructions outlined in Section 4.7.2, were performed prior to the setup of the soil columns and also after the last soil column sampling event.

Soil was then placed in lifts into the clear PVC column by means of a 3 inch PVC pipe placed inside the 4 inch soil column. Once the soil was added to the marked line, the 3 inch PVC pipe was removed causing the soil to settle into the soil column and the soil was then compacted. A filter, composed of 1 inch plastic tubing covered at one end with pantyhose, was attached inside the PVC column to the gas valve in order to prevent soil from clogging the valve. The columns were then filled to the top with the clean medium grade sand described above. Two blanks, or control samples, were also prepared by filling 2 of the soil columns with medium grade sand only. Distilled water was then added to the columns until the water level reached the top of the column. At this time, the columns were covered with plastic test caps fitted for 4 inch PVC piping. Figure 4.5,

Figure 4.6, and Figure 4.7 show the experimental setup for these batch samples. Once the soil columns were complete, they were stored in a cabinet located in a darkened constant temperature (20°C) room to avoid photodegradation of PAH's (Figure 4.8).



Figure 4.5 Soil column side view

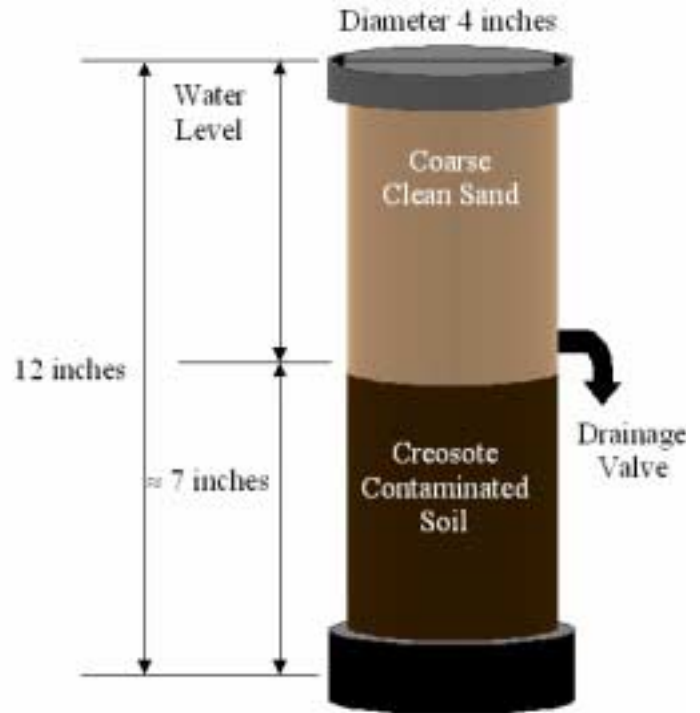


Figure 4.6 Schematic of soil column



Phase A



Phase B

Figure 4.7 Phase A & phase B soil columns

The soil columns were set up in 2 phases. Phase A consisted of 5 columns labeled as follows: 3 days A, 3 days B, 6 days A, 12 days A, and Control A (Figure 4.7). Soil for phase A was collected in July of 2001. Phase B consisted of 3 columns labeled as follows: 6 days B, 12 days B, and Control B (Figure 4.7). Soil for this phase was collected in February of 2002. Because the different phases were composed of separate soils, the results from phase A and phase B cannot be associated.

Water samples were taken from 2 columns every 3 days, 2 columns every 6 days, 2 columns every 12 days, and from the controls every 12 days. The time line for sampling activities for the dissolution kinetics experiment is outlined below in Table 4.1. Gravity drained water samples were taken at the soil/sand interface by opening the valve attached to the soil column and draining water into a series of 40 mL amber vials. Once triplicate samples were acquired for a column, the excess water was then drained into a 250 mL amber bottle for disposal (Figure 4.9). When all the soil columns for a particular sampling event had been drained until dry, their caps were removed, their valves were closed, and clean distilled water was added until the water level once again reached the top of the soil columns. Water samples were stored for 2 weeks in the 4°C refrigerator until the water extraction process described in Section 4.7.1 was initiated.



**Figure 4.8 Soil column storage location**



**Figure 4.9 Soil column drainage technique**

**Table 4.1 Dissolution kinetics sampling time line**

Sampling Event	Days	3 Days A	3 Days B	6 Days A	12 Days A	Control A	6 Days B	12 Days B	Control B
1	3	X	X						
2	6	X	X	X			X		
3	9	X	X						
4	12	X	X	X	X	X	X	X	X
5	15	X	X						
6	18	X	X	X			X		
7	21	X	X						
8	24	X	X	X	X	X	X	X	X
9	27	X	X						
10	30	X	X	X			X		
11	33	X	X						
12	36	X	X	X	X	X	X	X	X
13	39	X	X						
14	42	X	X	X			X		
15	45	X	X						
16	48	X	X	X	X	X	X	X	X
17	51	X	X						
18	54	X	X	X			X		
19	57	X	X						
20	60	X	X	X	X	X	X	X	X
21	63	X	X						
22	66	X	X	X			X		
23	69	X	X						
24	72	X	X	X	X	X	X	X	X
25	75	X	X						
26	78	X	X	X			X		
27	81	X	X						
28	84	X	X	X	X	X	X	X	X
29	87	X	X						
30	90	X	X	X					
31	93								
32	96			X	X	X			

#### **4.6 Field Procedures**

Background soil and groundwater sampling events are usually conducted at the Oneida Tie-Yard site bi-annually. Soil samples were collected, from 2 previously sampled transects, with a hand auger at depths of 3 to 10 feet below ground. Soil in the first 3 feet below the ground surface is not usually analyzed because it is above the water table and may contain a high percentage of coal. Samples are taken from the hand auger with a FisherBrand™ Scoopula spatula every foot and placed in Ziploc bags. On-site, soil samples are stored in coolers for preservation, as well as to prevent photodegradation. Once the samples are transported back to the laboratory at Virginia Tech, they are then stored in a 4°C refrigerator until they are extracted.

Groundwater samples were collected from multi-level samplers at 1 foot intervals as well. Multi-level samplers are color-coded to permit depth-specific groundwater sampling at depths ranging between approximately 0.27 and 7.27 feet above bedrock. Once the colored collection tubing has been properly purged, air-tight groundwater samples are taken in 40 mL amber vials and stored in coolers on-site. Upon arrival at Virginia Tech, the samples are then transferred to the 4°C refrigerator in the laboratory until extraction.

#### **4.7 Laboratory Procedures**

Groundwater PAH concentrations were quantified by a liquid-liquid extraction procedure developed by Fetterolf (1998). The US EPA method 625/8100 calls for a groundwater concentration method of 100:1 using a multi-step procedure (U.S. EPA 1982). However, a number of factors, including the time requirement for each sample and the cost of supplies, made the US EPA method inefficient and too costly for use on samples from the Oneida Tie-Yard. Therefore, Fetterolf (1998) came up with a comparable 1-step 30:1 extraction procedure, which is less time consuming and more economical in this case than US EPA method 625/8100. Additionally, Fetterolf's (1998) method avoids the problem of many multi-step procedures that expose light sensitive compounds like PAH's to photodegradation. Groundwater samples were outsourced to the Envirotech Mid-Atlantic laboratory for US EPA method 8100 PAH analysis in order to validate the unconventional method (Fetterolf 1998). Although the results of each

method have slight differences, the method honed by Fetterolf (1998) was reliable; therefore, it was chosen for use on samples from the Oneida Tie-Yard site.

Soil extraction procedures used for this study were developed by Fetterolf (1998) and modified by Crosswell (1999) and Brauner (2000). Before being used to analyze soil from the site, this method was validated by outsourcing duplicates to the Envirotech Mid-Atlantic laboratory that uses conventional EPA methods to do soil extractions (Fetterolf 1998). The samples that were sent out were then compared to those prepared at Virginia Tech with the modified method. According to Fetterolf (1998), the EPA method does not require destruction of the soil sample into fine particles and allows the use of sodium sulfate to reduce soil moisture. Due to these differences, the Envirotech Mid-Atlantic results had slightly lower concentrations than the unconventional methods developed by Fetterolf (1998). However, Fetterolf's (1998) methods were consistent and considered reliable enough to use at the Oneida Tie-Yard site.

#### **4.7.1 Water Extraction Procedure**

The water extraction procedure developed by Fetterolf (1998) and explained in this section presents guidelines for a 30:1 step extraction process. This method was used to quantify PAH's in groundwater samples taken directly from the Oneida Tie-Yard site and also water samples taken from each of the 3 laboratory experiments previously described.

Air-tight samples, collected in 40 mL amber vials with Teflon caps, were taken from the 4°C refrigerator and placed in a 40 mL vial rack. Additional empty 40 mL vials were then labeled with the date of extraction and the MLS port or laboratory sample that would eventually be placed in them. Using a glass pipette, 37.7 mL of water was then transferred from the original 40 mL sample to the corresponding newly labeled 40 mL vial, ensuring that no particles or colloidal materials were transmitted. In the case of extremely contaminated samples, dilutions with distilled water were necessary to stay within the proper analytical range.

After tightening the Teflon caps and cleaning the vent hood, the samples were then placed in the vent hood for all further operations with methylene chloride (MeCl). Using a 1 mL gas-tight syringe, 1.3 mL of Fisher Optima grade MeCl (Fisher Scientific, Atlanta, Georgia) was injected into each 40 mL vial by piercing the Teflon cap. Next, each vial was shaken vigorously by hand for 90 seconds and then allowed a static settling

time of 2 minutes. After settling, each vial was tilted and rotated to force smaller bubbles of MeCl to gather together into larger bubbles. Once a large enough bubble was achieved, the 40 mL vial cap was removed and a portion of the MeCl bubble was drawn up into the 1 mL gas tight syringe, ensuring that no water was transferred. The contents of the syringe were then injected into the PTFE/Silicone septa of a 1.5 mL amber GC autosampler vial labeled with a sample description and the extraction date. Each GC vial contained a target glass insert as a volume aid to make certain that the GC autosampler could reach the sample in the GC vial. After an adequate sample of MeCl was collected in the GC vial, it was recapped and then wrapped with Teflon tape to prevent volatilization. Samples were then refrigerated for a minimum of 4 hours and analyzed on the GC within a 2 week time period.

In order to ensure that the water extraction procedure was safe and efficient, some key checks and preventative maintenance were performed during each extraction period. Caution was taken not to draw up water into the syringe when removing MeCl bubbles from a water sample because water distinguishes the detector on the GC. Care was also taken to keep all solids and colloidal materials out of the water extraction vials because turbidity has been linked to increased aqueous concentrations for many hydrophobic PAH's (Mackay and Gschwend 2001).

#### **4.7.2 Soil Extraction Procedure**

The soil extraction procedure developed by Fetterolf (1998) and explained in this section presents guidelines for the extraction of PAH's from soil boring samples taken using a hand auger. This method was used to quantify PAH levels in soil samples taken directly from the Oneida Tie-Yard site for use as background site information and also for use in each of the 3 laboratory experiments previously described.

Soil samples were removed from the 4°C refrigerator and placed in labeled aluminum pans using a FisherBrand™ Scoopula spatula rinsed with MeCl. After cleaning the vent hood, soil samples were left to dry in the hood for at least 4 hours or until dry because an excess of water has been proven to decrease extraction yields (Hale 1997). However, air-drying may also cause some losses in soil for 2 to 3-ring PAH's, especially naphthalene, due to volatility. Next, each sample was removed from the hood, placed on weighing paper, and rolled with the spatula to chop the soil into fine grains. Prior to this step,

shiny black coal pieces were removed from each sample with the spatula and disposed. Coal causes positive interference with PAH's so it is necessary to remove any coal before the soil is compressed. A labeled 40 mL amber vial was then placed on the scale and the scale was tared. Soil was added to the 40 mL amber vial until a total of 5.00 grams of soil was present. The Teflon septa of the amber vial was pierced with a 0.22 gauge hypodermic needle, cleaned with MeCl, to ensure that the vials did not explode on the shaker table. The soil samples were then placed in the vent hood for the addition of 15 mL of MeCl. MeCl was added with a specially marked volumetric pipette to counteract its volatility. Each sample was agitated on the vortex machine for approximately 10 seconds at a speed of at least 1. In order to indicate the MeCl level, a permanent line was marked around the circumference of the 40 mL vial and then each vial was placed in a padded cardboard box and closed with duct tape. Samples were placed on the rotating table and agitated for 34 to 38 hours to allow adequate contact between the extracting solvent and sample. At this time, the extractions were removed and brought back to the vent hood. MeCl was added with a Pasteur pipette to bring the MeCl level back to the initial marking on the 40 mL vial. Samples were then allowed to re-equilibrate for at least 12 hours in the 4°C refrigerator.

Once the samples had a chance to re-equilibrate, they were taken out of the 4°C refrigerator and placed back in the vent hood. The 40 mL vial cap was then removed and a portion of the MeCl supernatant was drawn up into the 1 mL gas tight syringe, ensuring that no water was transferred. The contents of the syringe were then injected into the PTFE/Silicone septa of a 1.5 mL amber GC autosampler vial labeled with a sample description and the extraction date. After a sample of at least 1 to 1.5 mL of MeCl was collected in the GC vial, it was recapped and then wrapped with Teflon tape to prevent volatilization. In the case of extremely contaminated samples, dilutions in MeCl were necessary in order to avoid data extrapolation. Dilutions were completed with a 100 microliter ( $\mu\text{L}$ ) syringe. The permanent line was remarked around the circumference of each 40 mL amber vial to indicate the MeCl level after a sample was taken. Samples were then refrigerated for a minimum of 4 hours and analyzed on the GC within a 2 week time period.

## **4.8 Analytical Methods**

Because creosote is a complex matrix of contaminants, each of its components will fractionate into the air, water, or soil as a function of physical and chemical properties. Therefore, the analytical assessment of the fate and concentrations of each PAH is a complex process and must include a number of methods.

### **4.8.1 Gas Chromatography**

Both soil and water extractions were quantified by capillary gas chromatography with a Hewlett Packard 5890 gas chromatograph (Hewlett Packard, Roseville, California), which was equipped with a J&W Scientific (Fisher Scientific, Atlanta, Georgia) DB5-MS fused silica capillary column and a flame ionization detector (FID). The column had a 0.25 micron film thickness, a 0.25 mm narrow bore internal diameter, and a 30 m length. Helium was used as the carrier, or column flow gas, at a rate of approximately 1 mL/min and a pressure of 25 psi at the tank. Nitrogen was used as the auxiliary gas, or makeup flow, at a rate of approximately 20 mL/min and a pressure of 40 psi at the tank. The FID responds to compounds that produce ions when burned in a hydrogen-air flame. Therefore, breathable air and hydrogen were used to fuel the FID. Airflow was roughly 400 mL/min and 42 psi at the tank, while hydrogen flow was 30 mL/min and 18 psi at the tank.

Samples in MeCl were injected at a volume of 2 microliters using a Hewlett Packard GC/SFC Injector autosampler unit (Hewlett Packard, Roseville, California). The injector was kept at a temperature of 305°C and the FID was maintained at 310°C. Samples were analyzed in a splitless fashion. The temperature program originally devised by Fetterolf (1998) when characterizing the Oneida Tie-Yard site had to be reevaluated because of an interference problem with pyrene and another peak in the background groundwater samples from the site. Therefore, a new heating program was used to eradicate this problem and is described subsequently. The temperature program began at 80°C with a hold time of 1 minute. The temperature was then ramped at a rate of 50°C/minute for 30 minutes. At 31 minutes, the column was heated at a temperature of 10°C/minute for 9 minutes. Finally, at 47.5 minutes, a cool down program of about 8 minutes brought the

column back to a temperature of 80°C to allow adequate time for the FID to equilibrate. Total run time for 1 sample was approximately 55 minutes.

Ten PAH compounds in the soil and water samples were quantified using response factors from known external PAH standards. These standards were custom made by Supelco, Inc. (Bellefonte, PA) and most had a percent purity of approximately 99%. Chromeleon chromatography software (Dionex Corporation, Sunnyvale, California) was used to develop a standard curve for each constituent and to calculate the concentration of each constituent in every sample. Typically, a standard curve consisted of approximately 7 concentrations (0.25, 0.5, 1, 5, 10, 25, 40 mg/L). Each of the 10 monitored PAH's produces a linear standard curve up to 40 mg/L so a linear fit with offset was employed. In the case of extremely contaminated samples, dilutions were necessary in order to avoid data extrapolation. Concentrations below the detection limit of the GC were listed as having a concentration of zero in order to simplify results and facilitate comparison of samples.

#### **4.8.2 Mass Spectrometry**

In addition to gas chromatography, a gas chromatography-mass spectrometer (GC-MS) was also used to analyze a select few soil and water extractions. GC-MS is one of the most powerful analytical tools in identifying individual compounds in a complex mixture. The purpose of using the mass spectrometer was to distinguish between outside peaks interfering with naphthalene, acenaphthylene, and chrysene. An Agilent 5973 Mass Selective Detector was used with an Agilent 6890 Series GC system (Agilent Technologies, Wilmington, Delaware) containing a J&W Scientific (Fisher Scientific, Atlanta, Georgia) DB5-MS fused silica capillary column. The column had a 0.25 micron film thickness, a 0.25 mm narrow bore internal diameter, and a 30 m length. The same temperature program and gas flows used for gas chromatography with an FID were also used on the GC-MS.

#### **4.9 Statistical Analysis & Calculations**

For quality control purposes throughout all 3 experiments and on-site, a number of steps were taken to determine the statistical reproducibility and reliability of the methods employed. The soil column experiment included 2 blanks which were sampled every 12

days, while the equilibrium batch experiments incorporated 1 blank sampled every 3 days. Additionally, soil column samples were all taken in triplicate and then averaged. In the case that there was enough soil, the equilibrium batch experiments were made as duplicates. In the field, samples were taken in duplicate at some wells. All samples were extracted and run through the GC and GC-MS along with many check standards to ensure that the standard curve did not change during any one run. At least 1 check standard was analyzed along with each set of approximately 10 samples.

The following equations, modified from Fetterolf (1998), were used to calculate constituent concentrations in groundwater and soil:

$$WaterConcentration\left(\frac{\mu g}{L}, ppb\right) = Dilution \times \left[ \frac{ChromatogramConcentration\left(\frac{\mu g}{mL}\right) \times 1000 \frac{mL}{L}}{30 \times Average Recovery} \right]$$

$$SoilConcentration\left(\frac{mg}{kg}\right) = Dilution \times \left[ \frac{ChromatogramConcentration\left(\frac{\mu g}{mL}\right) \times 15mL \times 1000 \frac{g}{kg}}{1000 \frac{\mu g}{mg} \times 5g} \right]$$

MeCl was chosen as a solvent because of its good solubility properties for PAH's, low boiling point, high commercial purity, polarity, and relatively low toxicity (Greist and Caton 1983). Although 1.3 mL of MeCl is injected into each 40 mL vial during the water extraction process, only approximately 0.6 mL is recoverable due to the volatile properties of MeCl. Losses can be attributed to the high volatility of MeCl and the ability of water to solvate MeCl. With a loss of MeCl to the atmosphere and water phase from injection to extraction, the same PAH concentration can generate extraction recoveries over 100 percent. Therefore, Fetterolf (1998) calculated an average recovery value for each monitored PAH constituent to be used when determining water concentration.

In Chapter 5, the data obtained from the aforementioned laboratory experiments will be summarized and interpreted via a number of tabular and graphical techniques. The results of the desorption equilibrium experiment, the desorption kinetics experiment, and the dissolution kinetics experiment in their entirety can be found in Appendix A, Appendix B, and Appendix C, respectively.

## 5. RESULTS & DISCUSSION

### 5.1 Introduction

Cyclic desorption and dissolution kinetics experiments were conducted in which 10 PAH compounds present at the Oneida Tie-Yard site and representing a wide range of solubility values were analyzed. In the following section, results of the desorption equilibrium experiment, the desorption kinetics experiment, and the dissolution kinetics experiment are presented and discussed in detail. Experiments were performed using soil samples ranging from lightly to heavily contaminated. No additional PAH mass was added in the laboratory experiments.

### 5.2 Desorption Equilibrium Experiment Results

The results of the desorption equilibrium experiment include plots of aqueous concentration versus time for each monitored PAH at every sampling location and isotherm plots for each PAH at each sampling location. Using these plots, an estimate of the maximum desorption capacity for each of the 10 PAH's was determined and equilibrium sorption parameters were quantified.

During these experiments, aqueous concentrations were measured after PAH contaminated soil was placed in contact with clean distilled water for 3, 14, 28, and 77 days. The resulting plots of aqueous concentration versus time are grouped by soil boring position and located in Appendix A (Figures 1A – 28A). To illustrate these results, Figure 5.1 is a plot of the average aqueous concentration of fluorene in  $\mu\text{g/L}$  versus time at SB-10 six feet below land surface. Fluorene is a 3-ring compound with a molecular weight of 166 amu and a water solubility of 1.9 mg/L. This compound was chosen as an example for study because it was prevalent in background samples and has chemical and physical characteristics representative of PAH's monitored in this study. SB-10 is located in the central most contaminated portion of the site near MLS-7; therefore, the sample taken from this boring at a depth of 6 feet is highly contaminated with PAH's in the NAPL phase.

Figure 5.1 shows that between the time that the soil came into contact with the clean distilled water ( $t = 0$ ) and the first sampling event at day 3, the concentration of fluorene in water increased to approximately 375  $\mu\text{g/L}$ . From the first sampling event at day 3 to

the last sampling event at 77 days, the concentration of fluorene only increased by 100  $\mu\text{g/L}$  or approximately 25%. By day 28, the concentration reached its maximum. This behavior was observed in most samples for all PAH's. Although fluorene is not present in the aqueous phase at its solubility limit, this behavior indicates that fluorene has reached equilibrium.

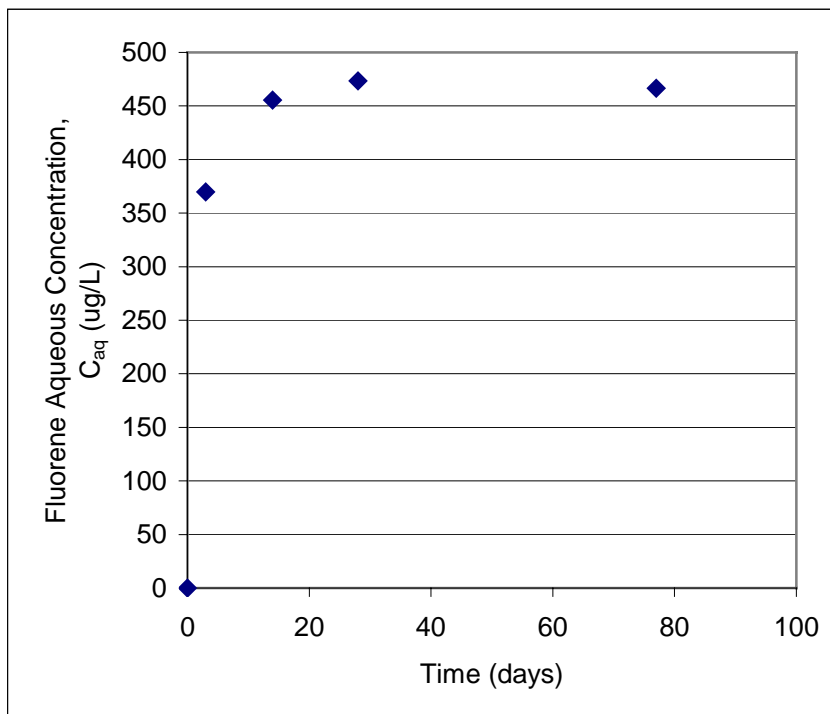


**Figure 5.1 Average fluorene aqueous concentration versus time at SB-10, 6 feet below land surface**

Samples for this experiment were taken over a period up to 77 days in order to determine the time to equilibrium between the sorbed and dissolved phases for each PAH. Between 3 and 77 days, additional desorption of PAH's was relatively insignificant. Although longer contact times than those performed in this experiment may result in some additional desorption, the majority of the PAH's were desorbed within the first 3 days. Studies at shorter time periods were not performed but it is possible that, for 2 to 3-ring compounds, significant desorption occurred even within the first few hours of soil/water contact time.

**Table 5.1 Desorption equilibrium experiment sampling event - 3 days  
groundwater PAH concentrations (µg/L or ppb)**

Sample ID	Naphthalene	Acenaphthylene	Acenaphthene	Fluorene	Phenanthrene	Anthracene	Fluoranthene	Pyrene	Chrysene	Benzo(b) fluoranthene	Total PAH's	Average 3-Ring PAH's	Average 4-Ring PAH's
SB-1, 5 ft	1.51	7.40	13.56	<b>8.58</b>	7.88	9.22	9.29	9.03	22.94	26.74	116	9	14
SB-1, 5 ft dup	1.51	7.67	14.16	<b>8.41</b>	7.48	9.10	9.27	9.06	23.40	26.84	117	9	14
SB-1, 6 ft	4869.31	127.25	601.16	355.66	388.39	149.26	76.92	61.97	91.41	102.00	6823	324	77
SB-1, 6 ft dup	5420.80	133.57	649.20	384.08	438.12	162.65	83.16	67.36	92.18	103.53	7535	354	81
SB-1, 7 ft	9239.79	154.61	720.84	454.59	584.16	208.61	123.51	98.31	105.50	115.50	11805	425	109
SB-1, 7 ft dup	8348.70	150.26	701.64	480.89	736.91	214.09	218.76	170.91	148.90	150.27	11321	457	180
SB-2, 5 ft	40.37	5.47	12.08	7.67	10.42	8.91	9.36	9.08	23.30	26.68	153	9	14
SB-2, 5 ft dup	12.46	4.93	9.22	5.54	6.47	8.58	9.03	8.87	23.38	26.71	115	7	14
SB-2, 6 ft	230.14	19.79	50.13	69.27	57.25	12.23	11.09	10.14	23.38	26.74	510	42	15
SB-2, 6 ft dup	154.01	17.97	43.71	59.58	51.16	12.12	10.86	10.02	23.14	26.73	409	37	15
SB-2, 7 ft	208.98	108.02	556.49	358.09	438.63	89.24	72.61	60.65	89.15	100.60	2082	310	74
SB-2, 7 ft dup	877.55	102.38	489.68	331.91	454.06	86.76	83.23	66.90	91.47	101.81	2686	293	81
SB-3, 6 ft	1.54	7.08	11.68	4.49	7.25	9.00	9.08	8.93	23.44	26.68	109	8	14
SB-3, 7 ft	191.27	26.62	55.78	62.05	96.41	25.11	23.86	18.79	23.65	26.79	550	53	22
SB-3, 7 ft dup	241.88	25.45	59.25	63.78	91.10	24.00	20.49	16.67	23.73	26.72	593	53	20
SB-3, 8 ft	9603.31	166.65	660.63	364.86	451.73	109.68	83.07	69.44	146.34	104.18	11760	351	100
SB-3, 8 ft dup	8962.48	147.82	598.36	334.28	418.55	103.41	78.22	65.83	145.44	102.25	10957	320	96
SB-4, 8 ft	1.59	3.93	6.68	<b>4.07</b>	5.35	8.40	8.93	0.00	23.04	26.80	89	6	11
SB-4, 9 ft	1.68	13.98	6.89	4.21	6.01	9.12	9.10	9.03	23.21	26.70	110	8	14
SB-4, 10 ft	7412.24	128.55	632.94	318.35	400.90	129.11	95.08	77.16	101.64	105.97	9402	322	91
SB-5, 8 ft	1.78	6.09	8.34	5.06	7.14	9.44	9.20	8.95	23.36	26.91	106	7	14
SB-5, 9 ft	1.66	4.60	8.23	4.84	5.72	9.79	9.20	8.98	23.53	26.97	104	7	14
SB-5, 9 ft dup	1.71	4.48	8.23	4.93	5.87	10.42	9.37	9.12	23.11	26.65	104	7	14
Blank	1.87	3.84	6.83	0.00	0.00	0.00	0.00	0.00	23.29	0.00	36	2	8

*\*denotes outlier*

In general, the 2 to 3-ring PAH's desorbed at a faster rate than the 4 to 5-ring compounds. The percent of 2 to 3-ring compounds desorbed within 3 days as compared to the maximum concentration at 77 days ranged from approximately 80% to 90%, while the percent desorbed of 4 and 5-ring compounds ranged from 60% to 70%. On average, the percent desorption after 3 days was determined to be approximately 76%. Based on these results, the desorption kinetics experiment was designed using a 3 day sampling frequency.

Table 5.1 lists the aqueous concentrations of monitored PAH's for each soil boring location after 3 days of soil/water contact time. With only a few exceptions, the percent difference between duplicate sample concentrations was consistently under 10%. Aqueous PAH concentrations for the remaining 14, 28, and 77 day sampling events are listed in Appendix A (Tables 1A – 4A). Seventy-seven day sampling values represent the maximum observed desorption concentration capacity for each PAH at each location.

The majority of PAH's present in the aqueous phase after 3 days had concentrations under or close to the respective solubility limits presented in the literature for individual PAH's. After 77 days, the aqueous concentrations of naphthalene, acenaphthylene, acenaphthene, fluorene, and phenanthrene at SB-10 twelve feet under land surface were all under the solubility limits listed in Table 2.2. However, anthracene, fluoranthene, pyrene, chrysene, and benzo(b)fluoranthene were present in aqueous concentrations exceeding the solubility limits listed in Table 2.2. The SB-10 twelve feet sample is located in a highly contaminated area so high dissolved concentrations were expected at this location. However, chrysene and benzo(b)fluoranthene were consistently present in concentrations well above previously reported levels of solubility in all soil boring locations. One explanation for this phenomenon could be the presence of mixed contaminants containing naphthalene or other organic solvents that act as cosolvents, increasing the concentration of high molecular weight compounds in the dissolved phase.

The equilibrium desorption data was organized by PAH compound and plotted as an isotherm of the sorbed concentration in mg/kg versus the duplicate averaged aqueous concentration in  $\mu\text{g/L}$  at day 3 (Appendix A Figure 29A – 30A). Sorbed concentrations, listed in Appendix A (Table 5A), were obtained from soil extractions performed prior to the setup of this experiment. The fluoranthene isotherm is shown in Figure 5.2. Fluoranthene was chosen because it was prevalent in background samples and has

chemical and physical characteristics representative of PAH's monitored in this study. The observed equilibrium relationships between soil and solution phase concentrations were described best by the non-linear Freundlich isotherm model:  $C^* = K_f \times C^N$ . For fluoranthene in Figure 5.2, the value of the Freundlich constant  $K_f$  for desorption is approximately 0.010 and the value of the Freundlich coefficient N for desorption is roughly 2.41.

The Freundlich parameter  $K_f$  is a distribution coefficient that indicates the affinity of a compound for soil. Mathematically,  $K_f$  represents the y-intercept of the best-fit line for a Freundlich isotherm. A high  $K_f$  suggests that a compound is strongly sorbed to the soil. The Freundlich parameter N is a coefficient that suggests the pattern of sorption, either linear or non-linear, that a particular compound will follow. N values close to 1 indicate linear sorption, while N values higher than 1 indicate non-linear sorption. In this case of this research, Freundlich desorption isotherms were created rather than sorption isotherms. Therefore, the results obtained from the desorption isotherms for the Freundlich constant  $K_f$  and N display behavior opposite of that which is typical for a sorption isotherm.

For each PAH, the  $K_f$  and N values obtained from isotherms for each sorbate-solute combination are listed in Table 5.2. According to the data, the Freundlich constant  $K_f$  decreases with increasing molecular weight, while the Freundlich coefficient N increases with increasing molecular weight. With the exception of naphthalene, which was calculated with limited data, all N coefficients have a value of greater than unity indicating non-linear sorption and a non-uniform sorbent, or soil. When the value of N is greater than 1, the amount of solute sorbed increases with an increase in solute concentration. Consequently, PAH's present in high sorbed concentrations may act as another partitioning phase increasing the sorbed quantity even further (Kohl and Rice 1999).

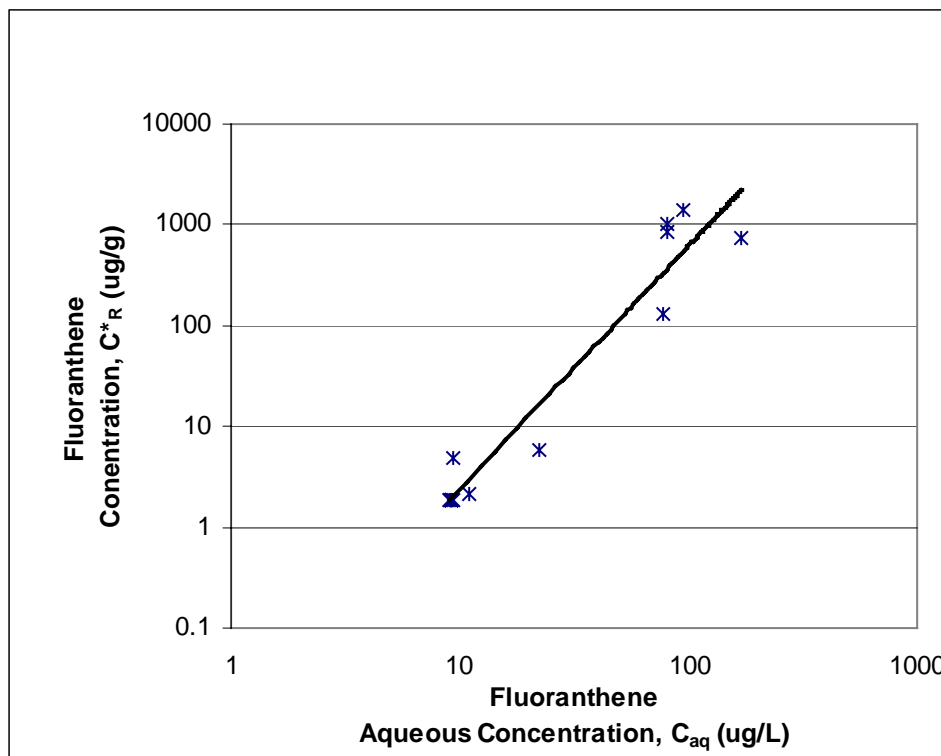


**Figure 5.2 Fluoranthene desorption Freundlich isotherm based on soil samples from all SB locations**

**Table 5.2 Summary of Freundlich desorption parameters for desorption equilibrium experiment**

PAH	Freundlich Constant, $K_f$	Freundlich Coefficient, $N$
Naphthalene	0.663	*0.68
Acenaphthylene	0.065	1.02
Acenaphthene	0.064	1.34
Fluorene	0.100	1.35
Phenanthrene	0.076	1.51
Anthracene	0.025	1.85
Fluoranthene	0.010	2.41
Pyrene	0.0076	2.54
Chrysene	0.00071	2.69
Benzo(b) fluoranthene	0.00020	2.97

*\*Calculated from limited data*

## 5.2 Desorption Kinetics Experiment Results

The results of the desorption kinetics experiment include estimates of the total mass of each PAH that is irreversibly sorbed to the soil, the total desorbable mass, and the rate of desorption of each PAH. Based on concentration versus time data, equilibrium isotherms for each PAH at specific sampling locations on-site were determined.

Aqueous PAH concentrations for all sampling events at every soil boring location for the desorption kinetics experiment are listed in Appendix B (Tables 1B – 14B). Based on the results, the following samples were chosen for kinetics and mass calculations because of the significant variation in aqueous concentration at these soil boring locations: SB-10 6 ft, SB-10 7 ft, SB-25 6 ft, SB-25 7 ft, SB-11 7ft, SB-11 8ft, SB-12 10 ft. In particular, the sampling location at SB-10 seven feet below land surface was chosen as representative of the results of this experiment. This sample was selected due to its wide range of concentrations and the presence of each monitored PAH.

The desorption kinetics experiment consisted of a successive series of equilibrium reactions and removal of the aqueous volume every 3 days. Tables 5.3 through 5.8 show the time histories of the aqueous concentrations,  $C_{aq}$ , and the calculated solids mass for SB-10 seven feet below land surface. The aqueous mass,  $\Delta M_{aq}$ , is determined by multiplying the PAH concentration in solution by the volume of exchanged distilled water. The reversibly sorbed concentration,  $C^*_R$ , is then calculated by dividing the aqueous mass by the mass of solids. Sample mass of solids calculations for each soil boring are listed in Appendix B (Table 15B). Appendix B (Tables 16B-57B) also includes aqueous concentration and solids mass data tables for the remaining soil boring locations under investigation.

The level of contamination for each sample can be estimated by the aqueous concentration ( $C_{aq}$ ) at the first 3 day sampling event as listed in (Tables 5.3 – 5.8). For the two heaviest molecular weight compounds, chrysene and benzo(b)fluoranthene, the aqueous PAH concentrations decrease to zero, with the number of fluid exchanges, indicating a 100 percent removal of the reversible PAH concentration in the aqueous phase. This occurrence may signify that the remaining solids concentration either is irreversibly sorbed or subject to a relatively slow rate of desorption after removal of the readily desorbing mass.

For 3 to 4-ring compounds, the desorbing mass is depleted by orders of magnitude within the time limits of the experiment. However, some 3 and 4-ring PAH concentrations in the aqueous phase were not depleted to zero over the course of the desorption kinetics experiment. In these cases, for the purpose of mass calculations, projections were made of the number of fluid exchanges necessary to reach a zero concentration for each PAH. Dissolved concentrations were extrapolated at 3 day intervals starting at fluid exchange number 33, after the last physical sampling event. Time and concentration estimates were based on the trend lines of concentration versus time plots for the last 6 sampling events. Extrapolated data are indicated by the shaded numbers in Tables 5.3 to 5.8 and open data points in Figures 5.3 to 5.13.

**Table 5.3 Summary of desorption kinetics experiment for naphthalene and acenaphthylene at SB-10, 7 feet below land surface**

Time (Days)	Exchanges (#)	Naphthalene			Acenaphthylene		
		Aqueous Concentration $C_{aq}$ (ug/L)	Aqueous Mass $\Delta M_{aq}$ (ug)	Reversible Sorbed Concentration $C^*_R$ (ug/g)	Aqueous Concentration $C_{aq}$ (ug/L)	Aqueous Mass $\Delta M_{aq}$ (ug)	Reversible Sorbed Concentration $C^*_R$ (ug/g)
0	0	0.00	0.00	319.65	0.00	0.00	18.40
3	1	4993.94	998.79	282.65	140.34	28.07	17.36
6	2	4451.50	890.30	249.68	131.71	26.34	16.38
9	3	5040.06	1008.01	212.35	121.68	24.34	15.48
18	6	3046.79	1828.08	144.64	111.65	66.99	13.00
27	9	2580.95	1548.57	87.29	121.80	73.08	10.30
36	12	1922.95	1153.77	44.55	112.78	67.67	7.79
45	15	1138.55	683.13	19.25	102.21	61.32	5.52
54	18	584.75	350.85	6.26	82.24	49.34	3.69
63	21	243.70	146.22	0.84	84.38	50.63	1.82
72	24	37.91	22.75	0.00	46.13	27.68	0.79
81	27	0.00	0.00	0.00	19.40	11.64	0.36
90	30	0.00	0.00	0.00	16.16	9.70	0.00
	31.8				0.00	0.00	0.00
		<b><math>\Sigma</math>Aqueous Mass</b>	<b>8630.46</b>		<b><math>\Sigma</math>Aqueous Mass</b>	<b>496.80</b>	

**Table 5.4 Summary of desorption kinetics experiment for acenaphthene and fluorene at SB-10, 7 feet below land surface**

Time (Days)	Exchanges (#)	Acenaphthene			Fluorene		
		Aqueous Concentration $C_{aq}$ (ug/L)	Aqueous Mass $\Delta M_{aq}$ (ug)	Reversible Sorbed Concentration $C^*_R$ (ug/g)	Aqueous Concentration $C_{aq}$ (ug/L)	Aqueous Mass $\Delta M_{aq}$ (ug)	Reversible Sorbed Concentration $C^*_R$ (ug/g)
0	0	0.00	0.00	132.46	0.00	0.00	64.49
3	1	696.54	139.31	127.30	327.93	65.59	62.06
6	2	674.76	134.95	122.30	290.96	58.19	59.90
9	3	649.83	129.97	117.49	337.98	67.60	57.40
18	6	633.72	380.23	103.40	318.65	191.19	50.32
27	9	704.18	422.51	87.76	352.01	211.21	42.50
36	12	718.99	431.39	71.78	359.54	215.72	34.51
45	15	697.35	418.41	56.28	328.58	197.15	27.21
54	18	558.59	335.15	43.87	275.36	165.22	21.09
63	21	754.62	452.77	27.10	356.60	213.96	13.16
72	24	568.48	341.09	14.47	281.99	169.19	6.90
81	27	394.39	236.63	5.70	194.75	116.85	2.57
90	30	256.58	153.95	0.00	115.57	69.34	0.00
	33	250.04	150.02	5.69	120.66	72.39	2.78
	36	167.68	100.61	1.96	81.18	48.71	0.98
	39	85.32	51.19	0.07	41.71	25.03	0.05
	42	2.96	1.78	0.00	2.24	1.35	0.00
	42.1	0.00	0.00	0.00			
	42.2				0.00	0.00	0.00
		<b><math>\Sigma</math>Aqueous Mass</b>	<b>3879.97</b>		<b><math>\Sigma</math>Aqueous Mass</b>	<b>1888.69</b>	

**Table 5.5 Summary of desorption kinetics experiment for phenanthrene and anthracene at SB-10, 7 feet below land surface**

Time (Days)	Exchanges (#)	Phenanthrene			Anthracene		
		Aqueous Concentration $C_{aq}$ (ug/L)	Aqueous Mass $\Delta M_{aq}$ (ug)	Reversible Sorbed Concentration $C^*_R$ (ug/g)	Aqueous Concentration $C_{aq}$ (ug/L)	Aqueous Mass $\Delta M_{aq}$ (ug)	Reversible Sorbed Concentration $C^*_R$ (ug/g)
0	0	0.00	0.00	46.15	0.00	0.00	18.30
3	1	287.72	57.54	44.02	133.36	26.67	17.31
6	2	256.60	51.32	42.12	117.05	23.41	16.45
9	3	279.18	55.84	40.05	116.79	23.36	15.58
18	6	246.12	147.67	34.58	116.53	69.92	12.99
27	9	260.81	156.49	28.79	113.42	68.05	10.47
36	12	273.84	164.31	22.70	110.53	66.32	8.01
45	15	233.90	140.34	17.50	95.65	57.39	5.89
54	18	202.82	121.69	12.99	78.30	46.98	4.15
63	21	246.75	148.05	7.51	74.68	44.81	2.49
72	24	182.66	109.59	3.45	58.38	35.03	1.19
81	27	90.43	54.26	1.44	36.99	22.20	0.37
90	30	64.93	38.96	0.00	16.61	9.97	0.00
	33	45.64	27.38	0.22	6.56	3.94	0.00
	34.3				0.00	0.00	0.00
	36	10.03	6.02	0.00			
	36.8	0.00	0.00	0.00			
		<b><math>\Sigma</math>Aqueous Mass</b>	<b>1279.46</b>		<b><math>\Sigma</math>Aqueous Mass</b>	<b>498.03</b>	

**Table 5.6 Summary of desorption kinetics experiment for fluoranthene and pyrene at SB-10, 7 feet below land surface**

Time (Days)	Exchanges (#)	Fluoranthene			Pyrene		
		Aqueous Concentration $C_{aq}$ (ug/L)	Aqueous Mass $\Delta M_{aq}$ (ug)	Reversible Sorbed Concentration $C^*_R$ (ug/g)	Aqueous Concentration $C_{aq}$ (ug/L)	Aqueous Mass $\Delta M_{aq}$ (ug)	Reversible Sorbed Concentration $C^*_R$ (ug/g)
0	0	0.00	0.00	6.89	0.00	0.00	4.71
3	1	62.28	12.46	6.43	56.31	11.26	4.29
6	2	57.68	11.54	6.01	53.45	10.69	3.90
9	3	51.75	10.35	5.62	46.14	9.23	3.55
18	6	45.81	27.49	4.60	38.84	23.30	2.69
27	9	25.52	15.31	4.04	20.01	12.01	2.25
36	12	27.98	16.79	3.42	20.44	12.26	1.79
45	15	43.67	26.20	2.45	19.59	11.75	1.36
54	18	41.39	24.83	1.53	18.74	11.25	0.94
63	21	27.37	16.42	0.92	17.90	10.74	0.54
72	24	24.15	14.49	0.38	14.51	8.70	0.22
81	27	13.22	7.93	0.09	9.89	5.94	0.00
90	30	3.93	2.36	0.00	0.00	0.00	0.00
	31.9	0.00	0.00	0.00			
		<b><math>\Sigma</math>Aqueous Mass</b>	<b>186.16</b>		<b><math>\Sigma</math>Aqueous Mass</b>	<b>127.14</b>	

**Table 5.7 Summary of desorption kinetics experiment for chrysene and benzo(b)fluoranthene at SB-10, 7 feet below land surface**

Time (Days)	Exchanges (#)	Chrysene			Benzo(b)fluoranthene		
		Aqueous Concentration $C_{aq}$ (ug/L)	Aqueous Mass $\Delta M_{aq}$ (ug)	Reversible Sorbed Concentration $C^*_R$ (ug/g)	Aqueous Concentration $C_{aq}$ (ug/L)	Aqueous Mass $\Delta M_{aq}$ (ug)	Reversible Sorbed Concentration $C^*_R$ (ug/g)
0	0	0.00	0.00	10.98	0.00	0.00	10.58
3	1	144.94	28.99	9.90	166.44	33.29	9.35
6	2	144.52	28.90	8.83	166.16	33.23	8.11
9	3	110.30	22.06	8.02	124.35	24.87	7.19
18	6	76.08	45.65	6.32	82.53	49.52	5.36
27	9	68.70	41.22	4.80	70.33	42.20	3.80
36	12	61.32	36.79	3.44	58.12	34.87	2.51
45	15	53.94	32.36	2.24	45.91	27.55	1.48
54	18	54.42	32.65	1.03	45.24	27.14	0.48
63	21	23.78	14.27	0.50	10.42	6.25	0.25
72	24	22.45	13.47	0.00	11.15	6.69	0.00
81	27	0.00	0.00	0.00	0.00	0.00	0.00
90	30	0.00	0.00	0.00	0.00	0.00	0.00
		<b><math>\Sigma</math>Aqueous Mass</b>	<b>296.36</b>		<b><math>\Sigma</math>Aqueous Mass</b>	<b>285.61</b>	

**Table 5.8 Summary of desorption kinetics experiment for total polycyclic aromatic hydrocarbons at SB-10, 7 feet below land surface**

Time (Days)	Exchanges (#)	Total PAH's		
		Aqueous Concentration $C_{aq}$ (ug/L)	Aqueous Mass $\Delta M_{aq}$ (ug)	Reversible Sorbed Concentration $C^*_R$ (ug/g)
0	0			621.12
3	1	7009.81	1401.96	569.19
6	2	6344.40	1268.88	522.20
9	3	6480.04	1296.01	474.20
18	6	4507.23	2704.34	374.04
27	9	4215.17	2529.10	280.37
36	12	3579.02	2147.41	200.83
45	15	2769.47	1661.68	139.29
54	18	1952.04	1171.22	95.91
63	21	1840.22	1104.13	55.02
72	24	1247.81	748.68	27.29
81	27	754.14	452.48	10.53
90	30	473.78	284.27	0.00
	32.6	0.00	0.00	0.00
		<b><math>\Sigma</math>Aqueous Mass</b>	<b>16770.17</b>	

PAH desorption data, shown in Figures 5.3 to 5.13, were determined from the reversible sorbed concentrations,  $C^*_R$ , calculated in Tables 5.3 to 5.8. Figures 5.3 to 5.13 show plots of the reversibly sorbed concentration of each individual PAH versus the number of fluid exchanges at SB-10 seven feet under land surface. PAH desorption data for the entire set of soil boring locations are located in Appendix B (Figure 1B – 14B).

For most compounds, a linear decay is observed at high concentrations. However, for some PAH's such as naphthalene (Figure 5.3) and the heavy compounds chrysene and benzo(b)fluoranthene (Figure 5.11 and 5.12), desorption curves followed a different trend. A linear relationship describes these desorption data over the first set of data points, while an exponential decay relationship describes the data as concentrations approach zero.

For naphthalene, an exponential desorption rate described the data after the first 3 data points. By comparing Figures 5.3 to 5.13, the initially desorbed concentrations were found to decrease with increasing molecular weight. The high molecular weight compounds chrysene and benzo(b)fluoranthene are generally sorbed tightly to the soil thus desorption into the aqueous phase results in low aqueous concentrations. Because of their low solubility, the desorption curves for chrysene and benzo(b)fluoranthene exhibit exponential behavior, rather than linear, over the entire experiment.

The presence of organic matter and suspended colloids may help explain the desorption behavior. Laboratory tests on soil from this site have shown that the typical organic matter content of soil at the Oneida Tie-Yard is typically around 1%. If a large amount of contaminants are present, the amount sorbed to soil organic matter or colloids may be relatively low. However, at low concentrations, desorption rate data may be more affected by even a small amount of sorption to soil organic matter or colloids.

Naphthalene, acting as a cosolvent, could also be affecting the sorptive properties of the 4 and 5-ring PAH compounds. Figure 5.14 and 5.15 compare the log of the aqueous concentrations of naphthalene with 3, 4, and 5-ring compounds. As shown in Figure 5.14, the presence of naphthalene enhances the concentration of the 4 and 5-ring compounds, benzo(b)fluoranthene and chrysene, in the aqueous phase. Once naphthalene is no longer present in the aqueous phase, these compounds are depleted almost immediately from the dissolved phase indicating drastic reductions in desorption. On the other hand, the 3 ring compounds in the aqueous phase are not as influenced by the presence of naphthalene, and therefore, do not decrease when naphthalene is diminished.

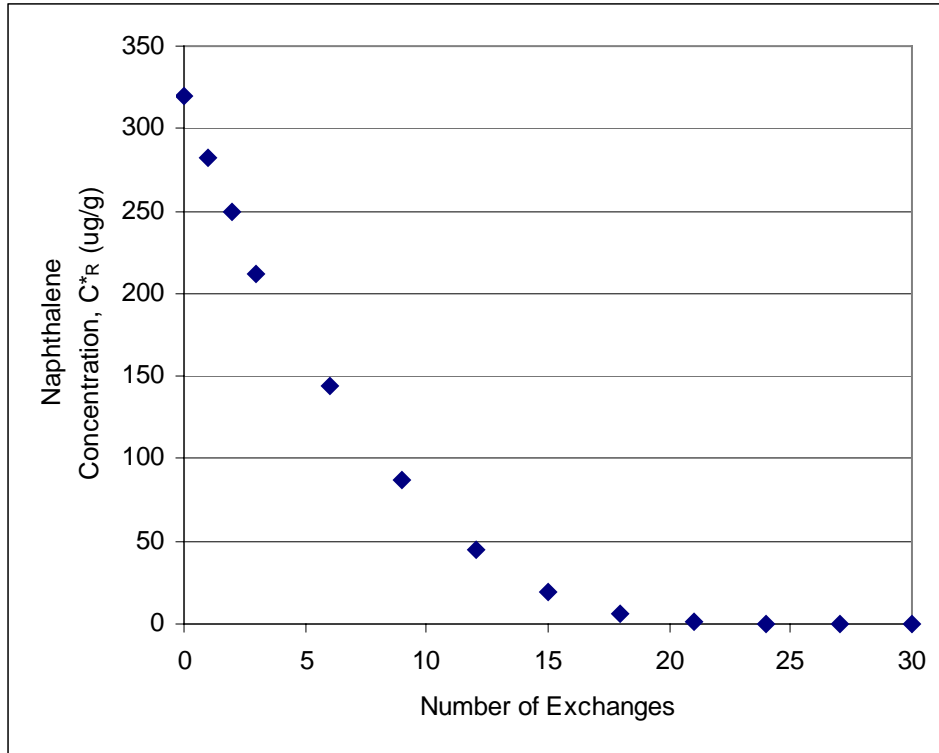


**Figure 5.3 Reversible sorbed naphthalene concentration versus the number of fluid exchanges at SB-10, 7 feet below land surface**

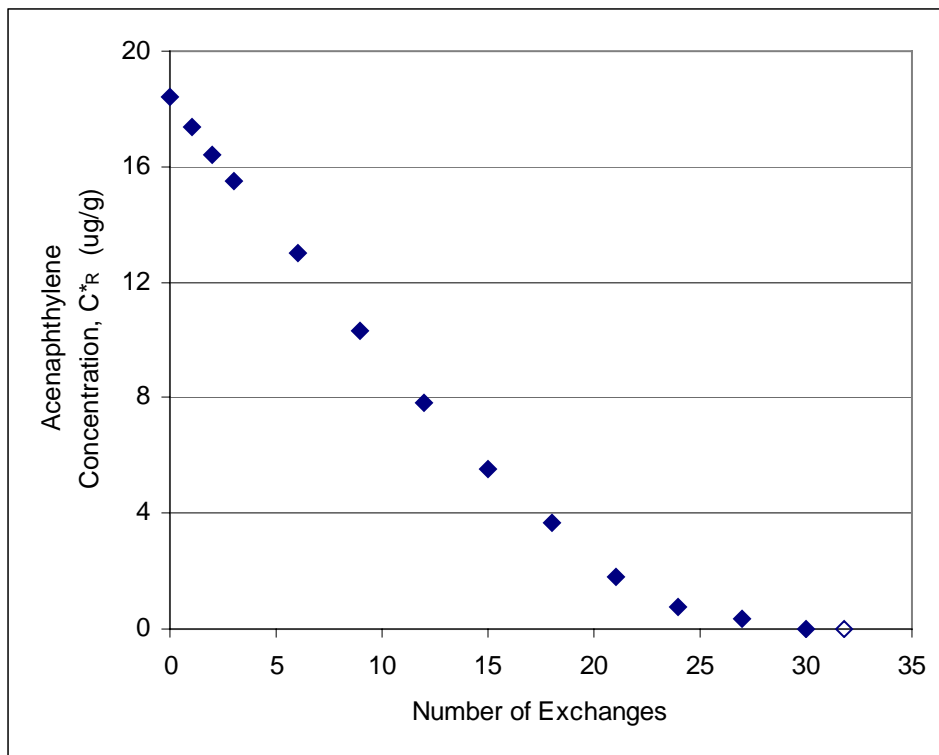


**Figure 5.4 Reversible sorbed acenaphthylene concentration versus the number of fluid exchanges at SB-10, 7 feet below land surface**

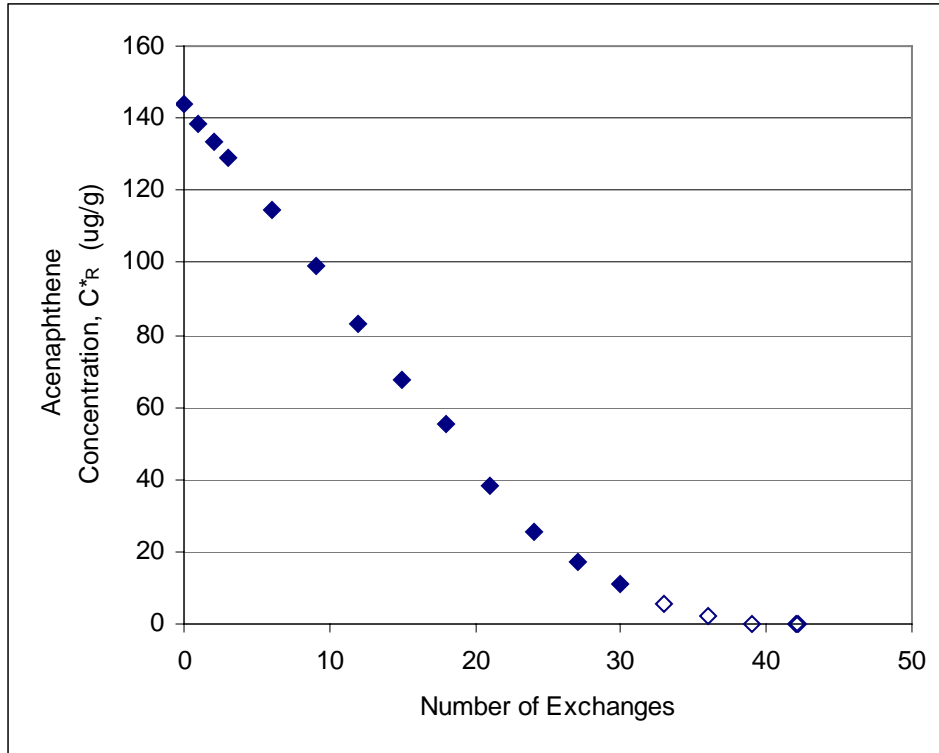


**Figure 5.5 Reversible sorbed acenaphthene concentration versus the number of fluid exchanges at SB-10, 7 feet below land surface**

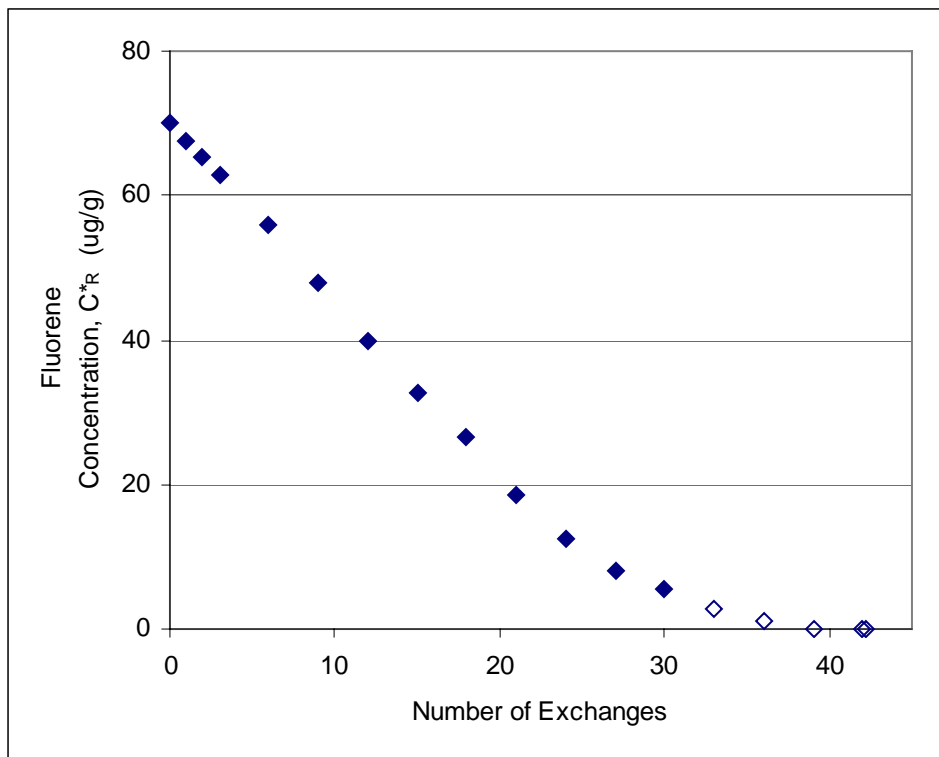


**Figure 5.6 Reversible sorbed fluorene concentration versus the number of fluid exchanges at SB-10, 7 feet below land surface**

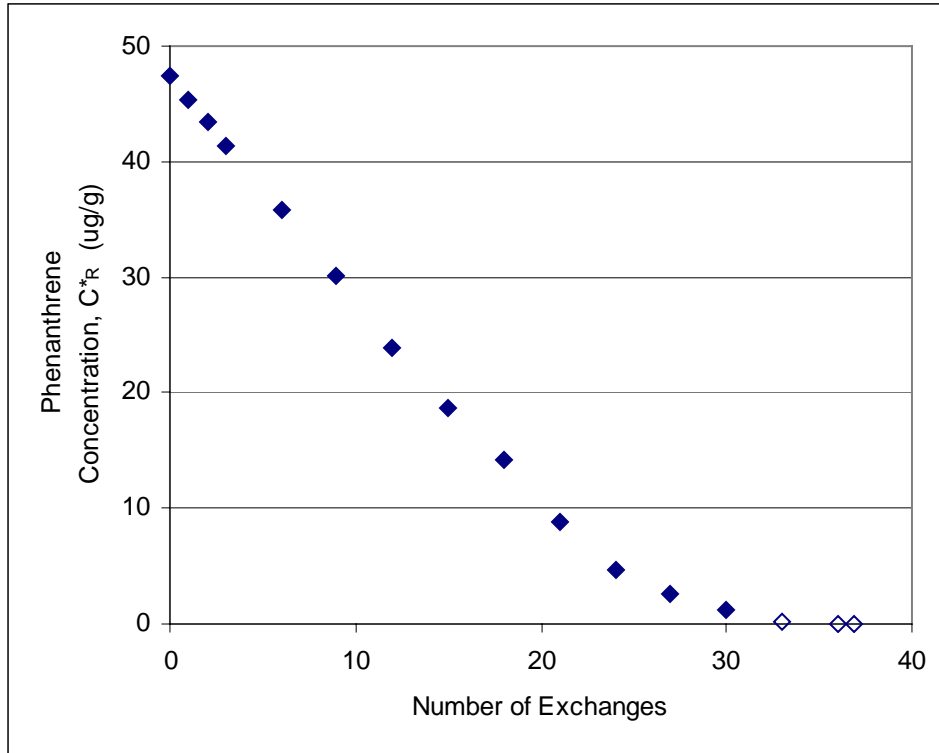


**Figure 5.7 Reversible sorbed phenanthrene concentration versus the number of fluid exchanges at SB-10, 7 feet below land surface**

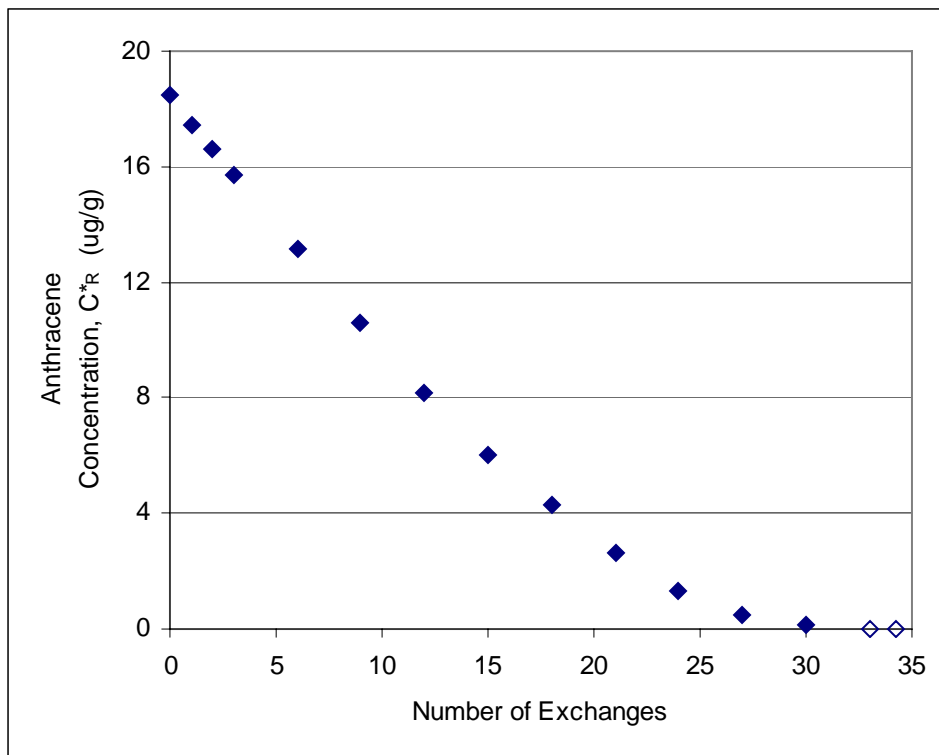


**Figure 5.8 Reversible sorbed anthracene concentration versus the number of fluid exchanges at SB-10, 7 feet below land surface**

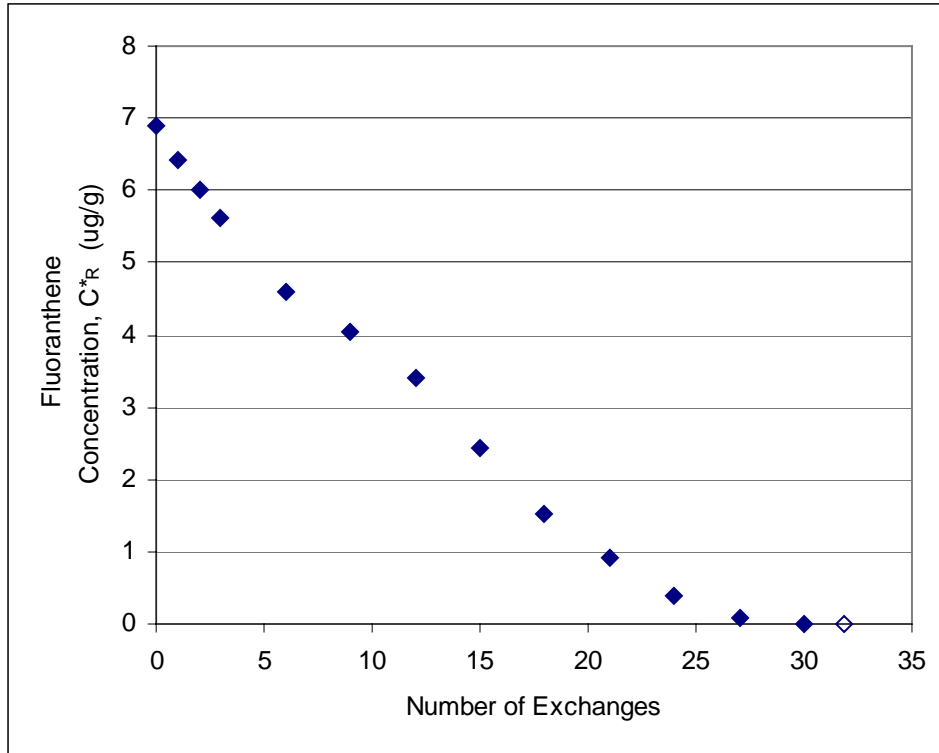


**Figure 5.9 Reversible sorbed fluoranthene concentration versus the number of fluid exchanges at SB-10, 7 feet below land surface**

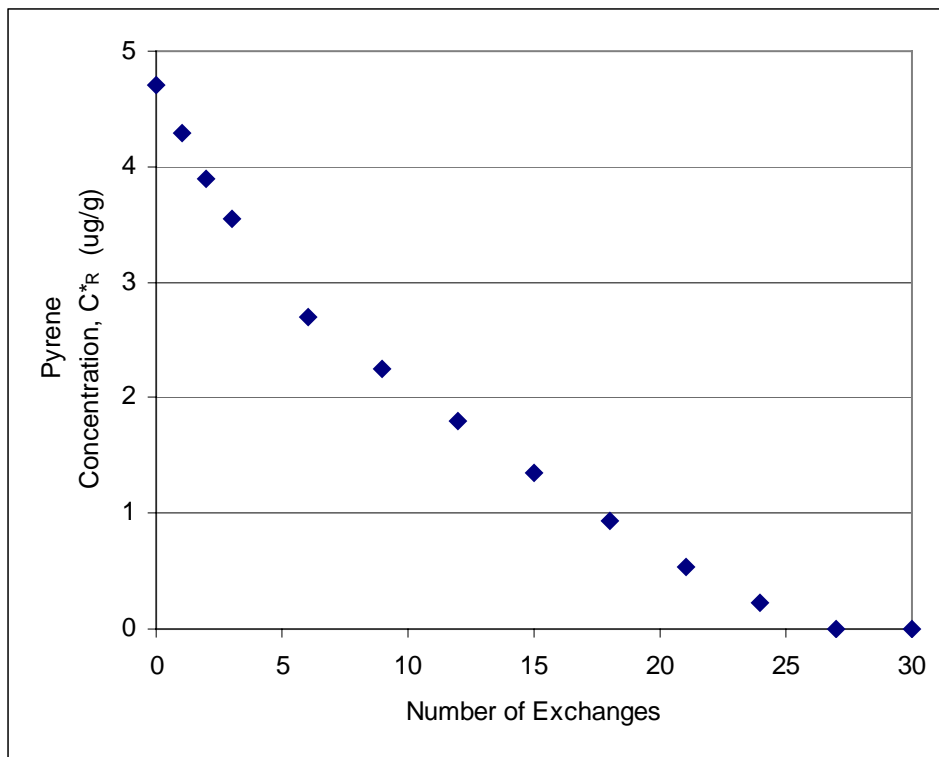


**Figure 5.10 Reversible sorbed pyrene concentration versus the number of fluid exchanges at SB-10, 7 feet below land surface**

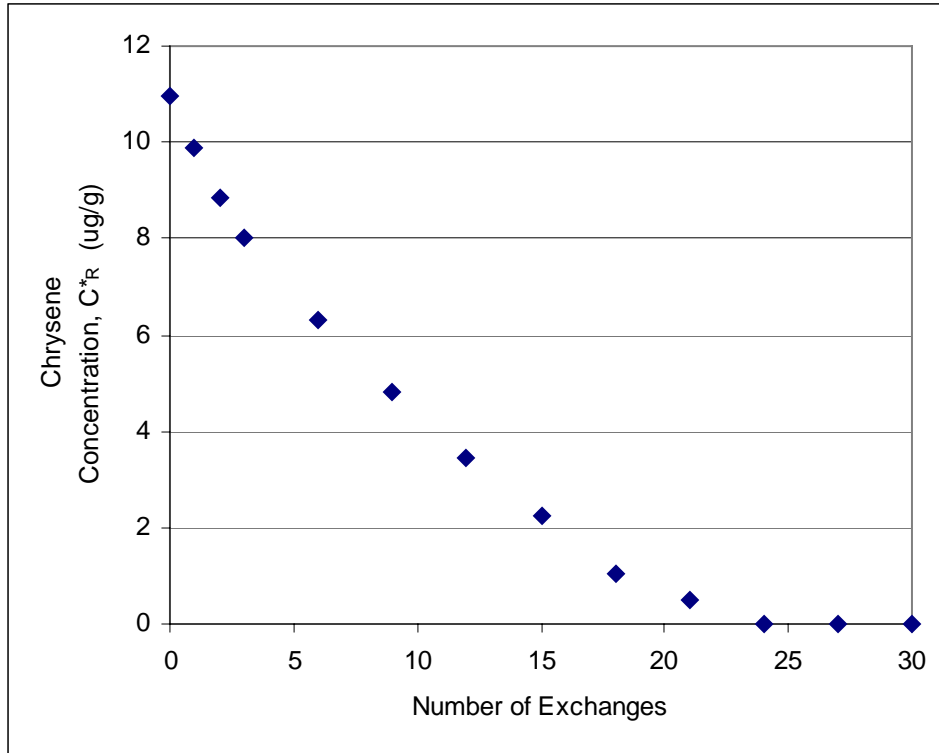


**Figure 5.11 Reversible sorbed chrysene concentration versus the number of fluid exchanges at SB-10, 7 feet below land surface**

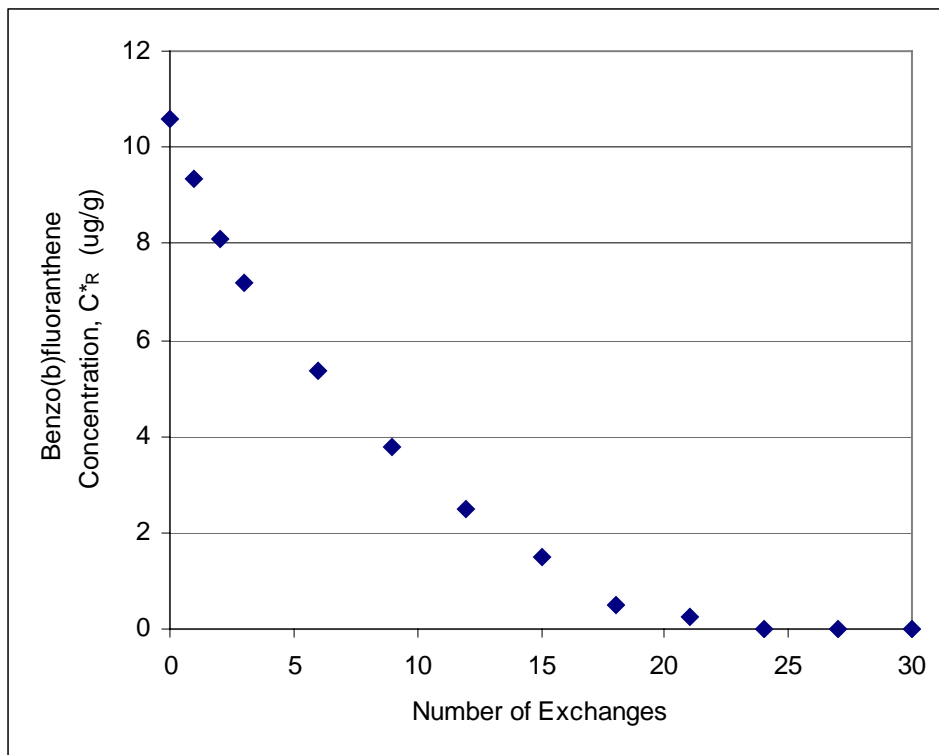


**Figure 5.12 Reversible sorbed benzo(b)fluoranthene concentration versus the number of fluid exchanges at SB-10, 7 feet below land surface**

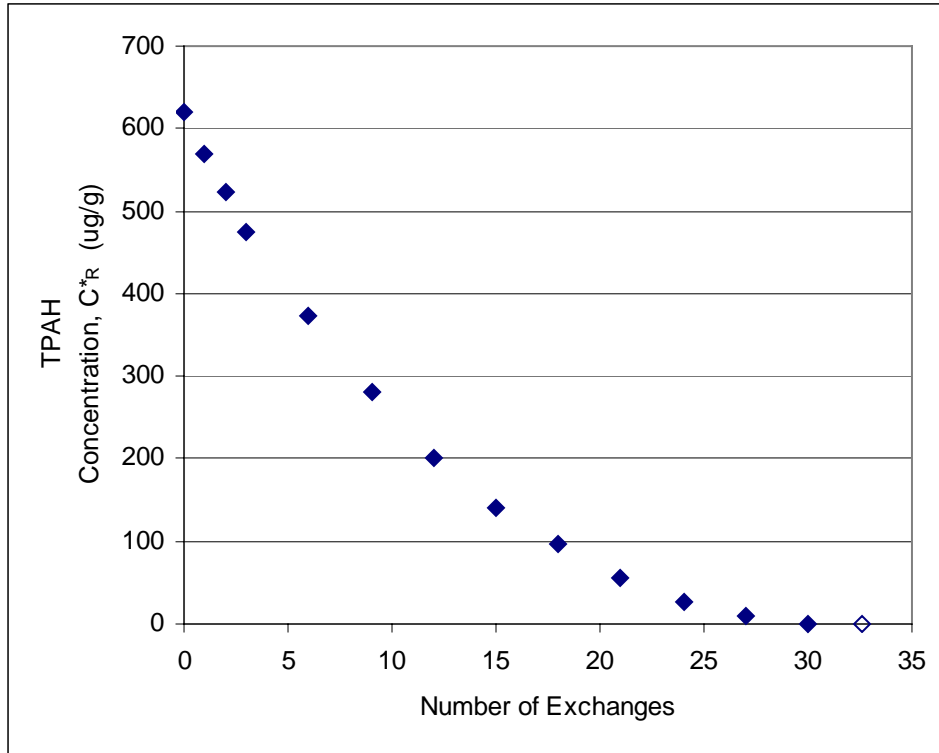


**Figure 5.13 Reversible sorbed total polycyclic aromatic hydrocarbon concentration versus the number of fluid exchanges at SB-10, 7 feet below land surface**

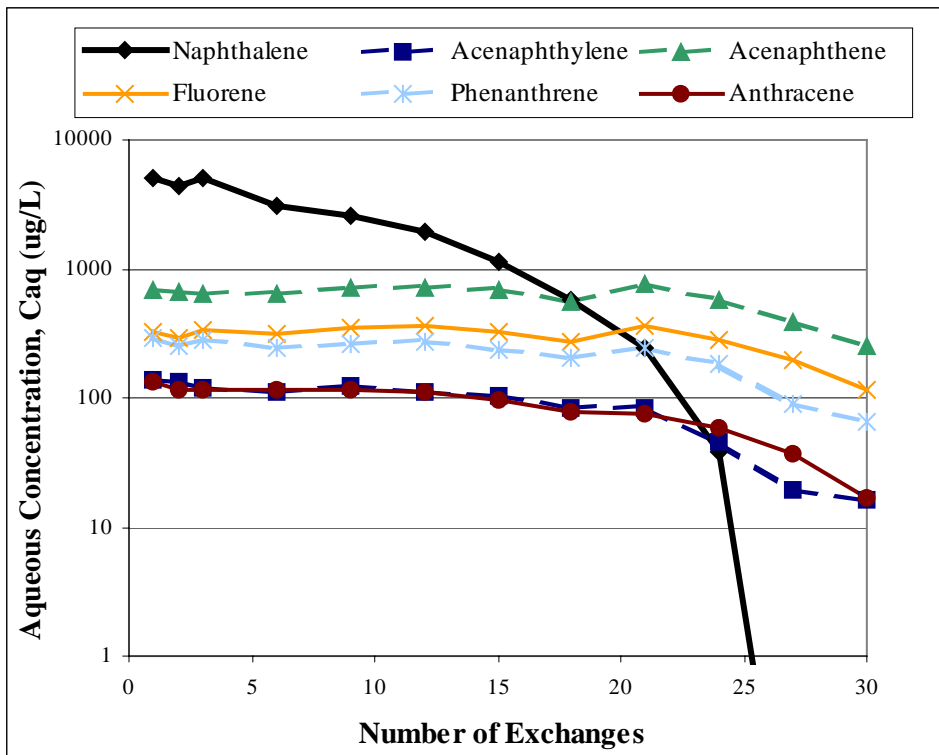


**Figure 5.14 Aqueous concentration of naphthalene and 3-ring PAH's versus the number of fluid exchanges at SB-10, 7 feet below land surface**

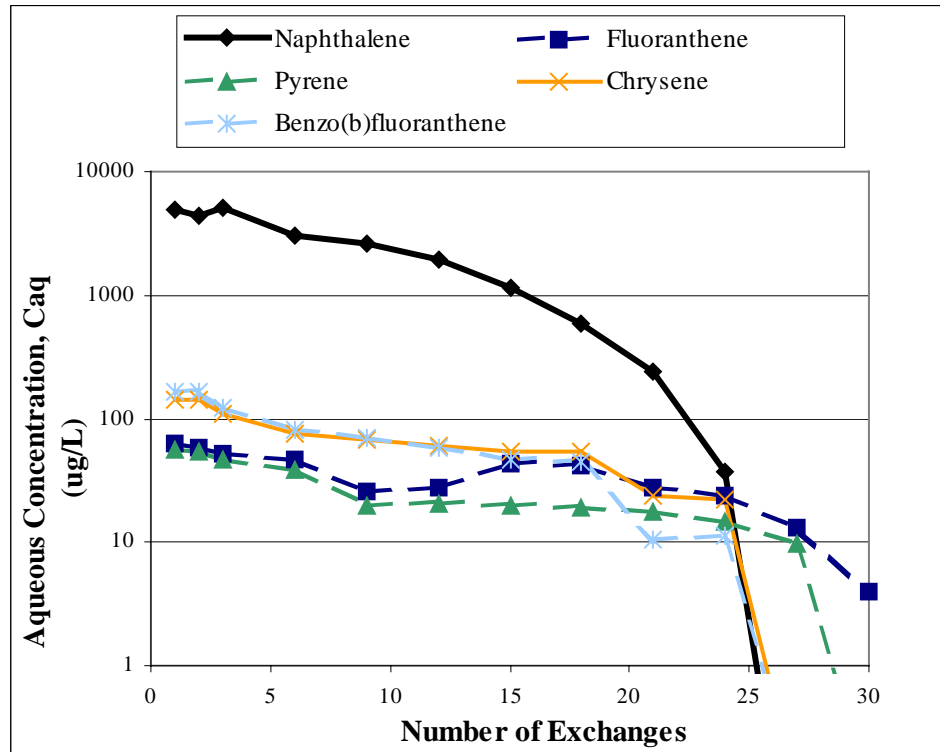


**Figure 5.15 Aqueous concentration of naphthalene and 4 to 5-ring PAH's versus the number of fluid exchanges at SB-10, 7 feet below land surface**

Desorption data were used to calculate the mass desorption rate parameter for each PAH. The data was fitted with both linear and first order rate models using regression lines. It was determined that the linear model showed a better fit for the majority of the data. Therefore, for each PAH, a desorption rate parameter was determined based on a linear trend line. However, in some cases, the last few data points did not fit a linear model so they were not accounted for in the regression. All the data points that were excluded had concentrations of 15% or less of the original sorbed PAH concentration.

Table 5.9 shows a summary of the desorption rate parameters ( $\mu\text{g/g/\#}$  exchanges) calculated for SB-10 seven feet under land surface. Appendix B (Table 58B – 64B) contains summary tables of desorption rate parameters for the remaining soil boring locations. For the majority of desorption plots, the correlation coefficient values were 0.95 or greater. The desorption data with lower correlations are noted in Appendix B (Table 58B – 64B). In general, for each sorbate, the desorption coefficient decreases as the molecular weight increases.

**Table 5.9 Summary of Freundlich and rate parameters for desorption kinetics experiment at SB-10, 7 feet below land surface**

<b>PAH</b>	<b>Desorption Rate Parameter (µg/g/# exchanges)</b>	<b>Freundlich Constant, <math>K_f</math></b>	<b>Freundlich Coefficient, <math>N</math></b>
<b>Naphthalene</b>	-25.47	3.51E-05	1.87
<b>Acenaphthylene</b>	-0.83	4.08E-04	2.11
<b>Acenaphthene</b>	-4.96	2.06E-07	3.05
<b>Fluorene</b>	-2.43	2.25E-06	2.89
<b>Phenanthrene</b>	-1.84	2.11E-05	2.52
<b>Anthracene</b>	-0.80	9.74E-05	2.45
<b>Fluoranthene</b>	-0.28	3.10E-04	2.46
<b>Pyrene</b>	-0.20	8.94E-03	1.57
<b>Chrysene</b>	-0.56	2.47E-03	1.70
<b>Benzo(b) fluoranthene</b>	-0.65	6.99E-03	1.41
<b>Total PAH's</b>	-32.00	9.09E-05	1.78

The kinetic sorption data described above were plotted as an isotherm of sorbed concentration (mg/kg) versus average aqueous concentration (µg/L). Both sorbed and aqueous concentrations used in these plots were obtained from Tables 5.3 to 5.8. The sorption data were fitted to both the Langmuir and Freundlich non-linear isotherm models but were found to correspond best to the Freundlich equation:  $C^* = K_f \times C^N$ . Figures 5.16 to 5.26 show sorption data fitted to the Freundlich equation for each PAH at SB-10 seven feet under land surface. The remaining Freundlich isotherms for all soil boring locations can be found in Appendix B (Figure 15B – 28B). While the Freundlich equation is an equilibrium, not kinetic, expression, it still can be used to explain sorption at intermediate times by considering it merely as an expression relating the sorbed concentration to the aqueous concentration at any given time.

Table 5.9 also summarizes the values obtained for the desorption Freundlich constant  $K_f$  and for the desorption Freundlich coefficient  $N$ . According to the data, the Freundlich constant  $K_f$  generally increases with increasing molecular weight. With some exceptions for the naphthalene and acenaphthylene, the Freundlich coefficient  $N$  decreases with increasing molecular weight. In general, the Freundlich parameters for the remaining soil boring locations follow a similar pattern but there are some variations depending upon the magnitude of contamination present in a particular sample.

All  $N$  values for SB-10 seven feet under land surface are greater than unity. An  $N$  value of greater than 1 indicates non-linear sorption and possibly a non-uniform sorbent, or soil. Isotherms are often non-linear in cases such as these when data exist over a wide range of concentrations. However, some  $N$  values for desorption data from locations other than SB-10 are close to 1 indicating that desorption follows a linear pattern.

The resulting trends for Freundlich parameters for the desorption kinetics experiment are not consistent with those from the desorption equilibrium experiment. According to the desorption equilibrium experiment, the Freundlich constant  $K_f$  decreases with increasing molecular weight and the coefficient  $N$  increases with increasing molecular weight. The resulting isotherms from each experiment could vary because they were prepared using separate methods and examined samples from different locations. The desorption equilibrium isotherms were organized by PAH over all sampling locations, encompassing a large variation in PAH solution concentration. On the other hand, the desorption kinetics isotherms were organized by PAH at each separate sampling location, limiting the variation in concentration to the range of concentration at that particular soil boring. In the case of the desorption equilibrium experiment, the aqueous and sorbed concentrations were determined using laboratory extraction methods. However, the desorption kinetics isotherms were determined using computed data. The sorbed phase concentration, in this case, was calculated as a reversible concentration ( $C^*_R$ ) based on the aqueous concentration measured in laboratory extraction methods.

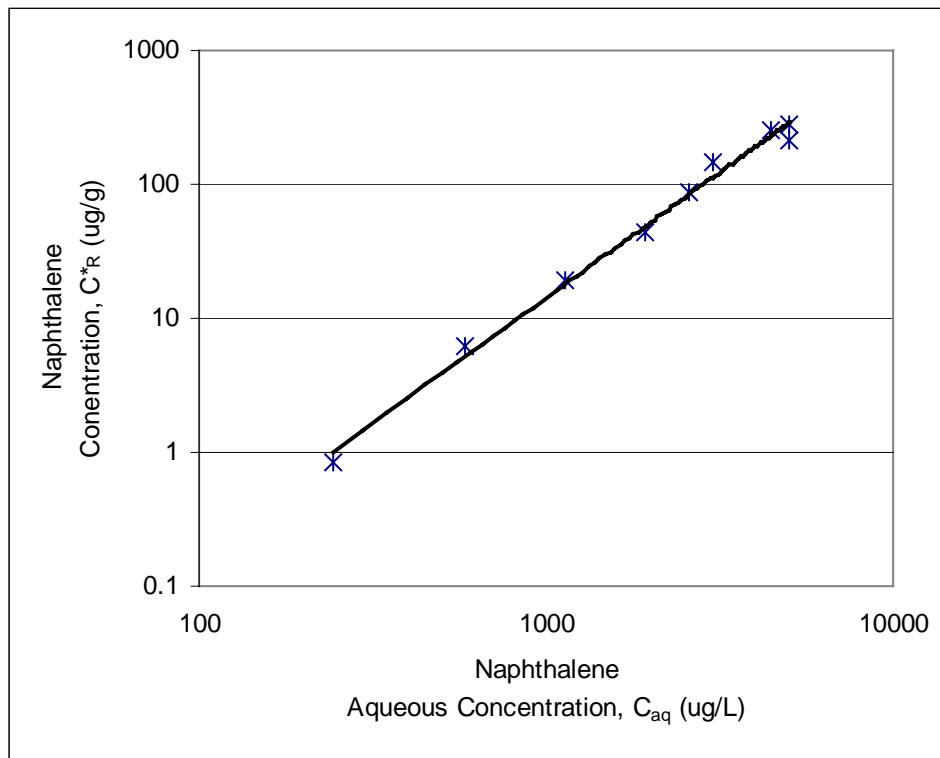


**Figure 5.16 Naphthalene Freundlich isotherm for SB-10, 7 feet below land surface**

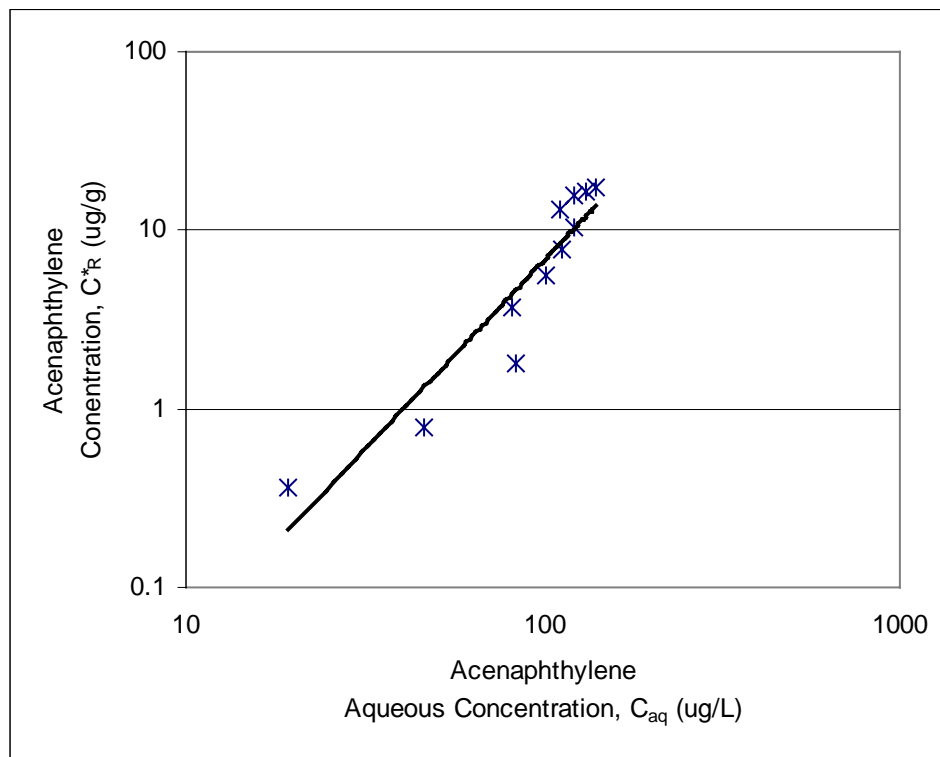


**Figure 5.17 Acenaphthylene Freundlich isotherm for SB-10, 7 feet below land surface**

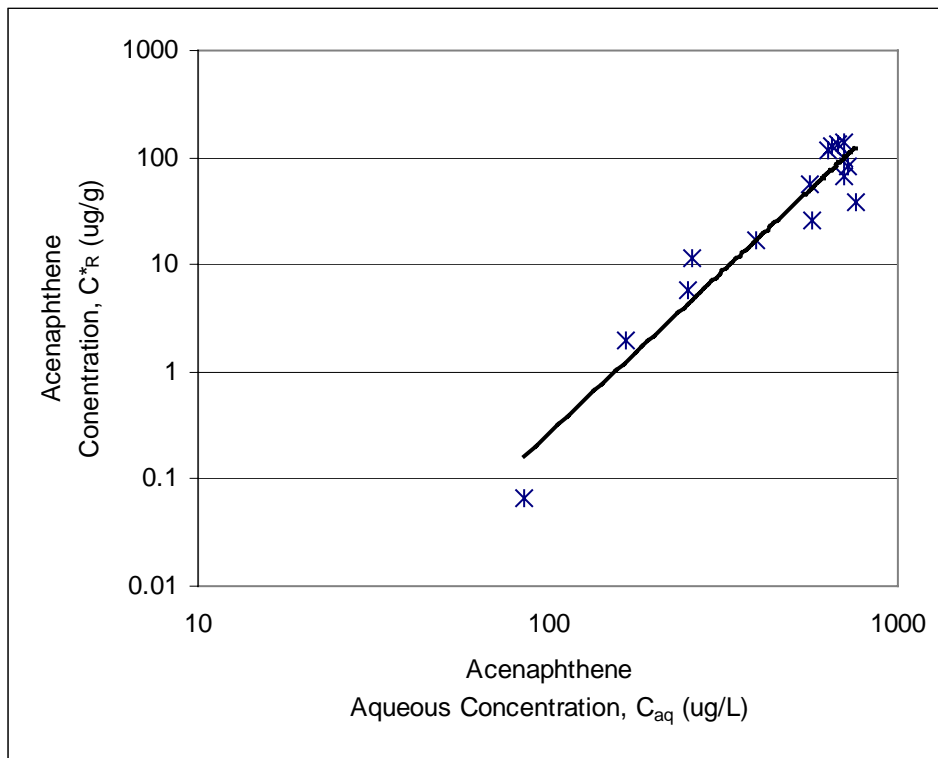


**Figure 5.18 Acenaphthene Freundlich isotherm for SB-10, 7 feet below land surface**

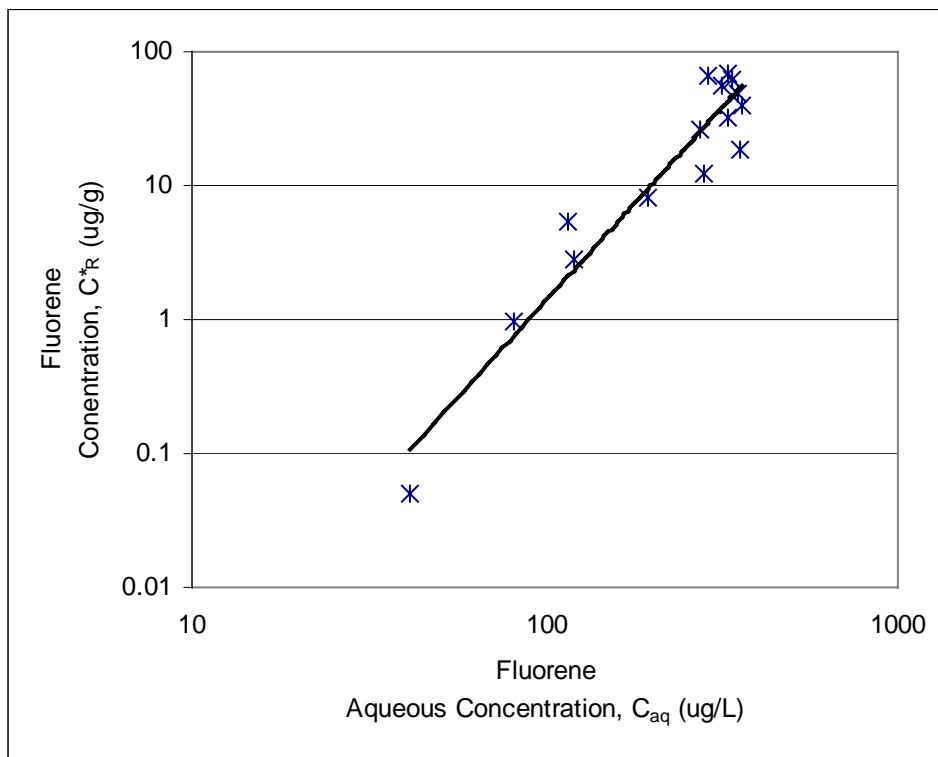


**Figure 5.19 Fluorene Freundlich isotherm for SB-10, 7 feet below land surface**

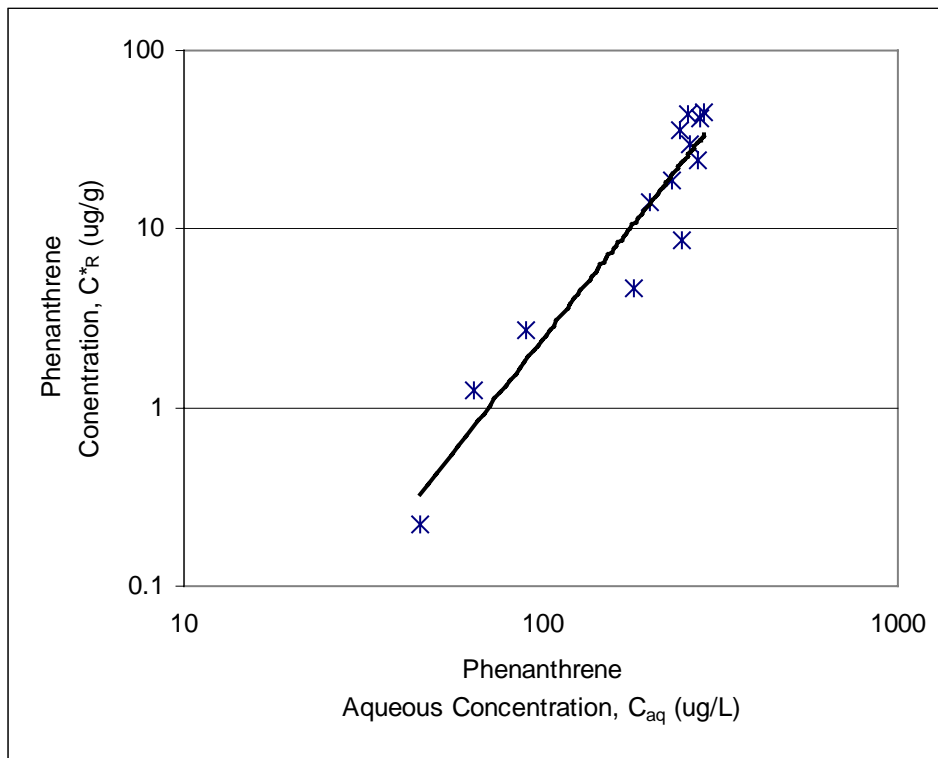


**Figure 5.20 Phenanthrene Freundlich isotherm for SB-10, 7 feet below land surface**

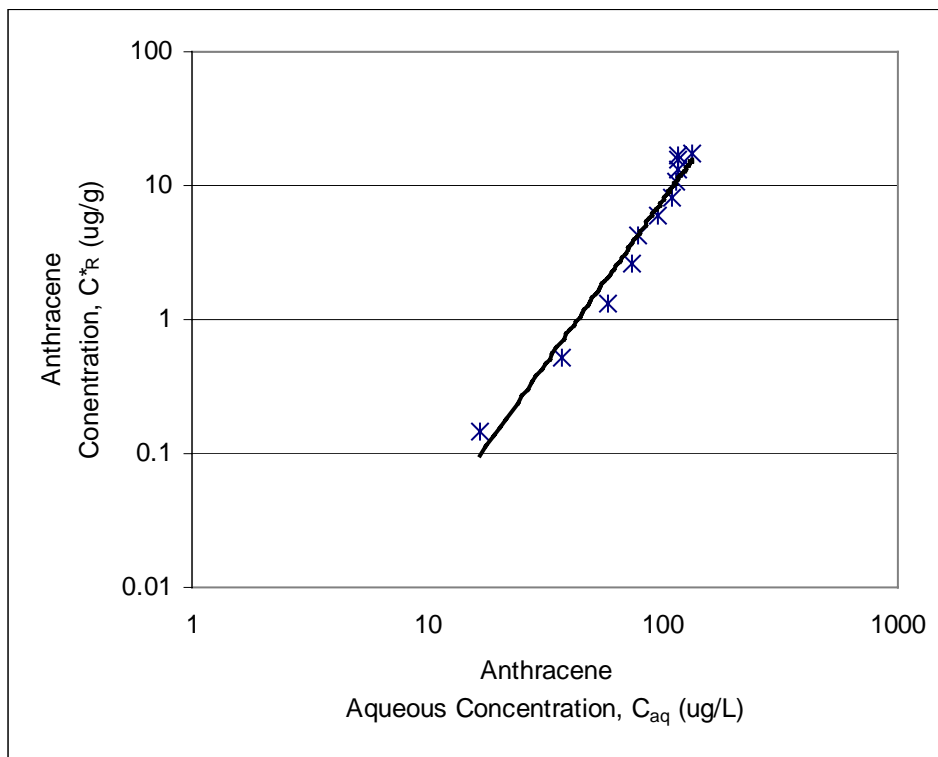


**Figure 5.21 Anthracene Freundlich isotherm for SB-10, 7 feet below land surface**

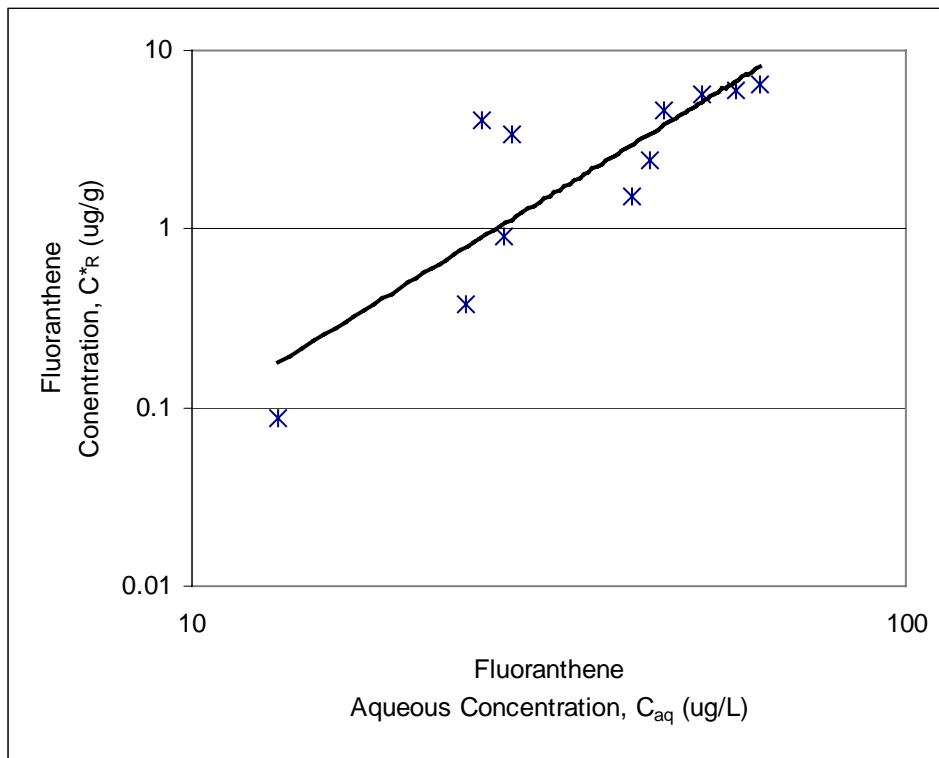


**Figure 5.22 Fluoranthene Freundlich isotherm for SB-10, 7 feet below land surface**

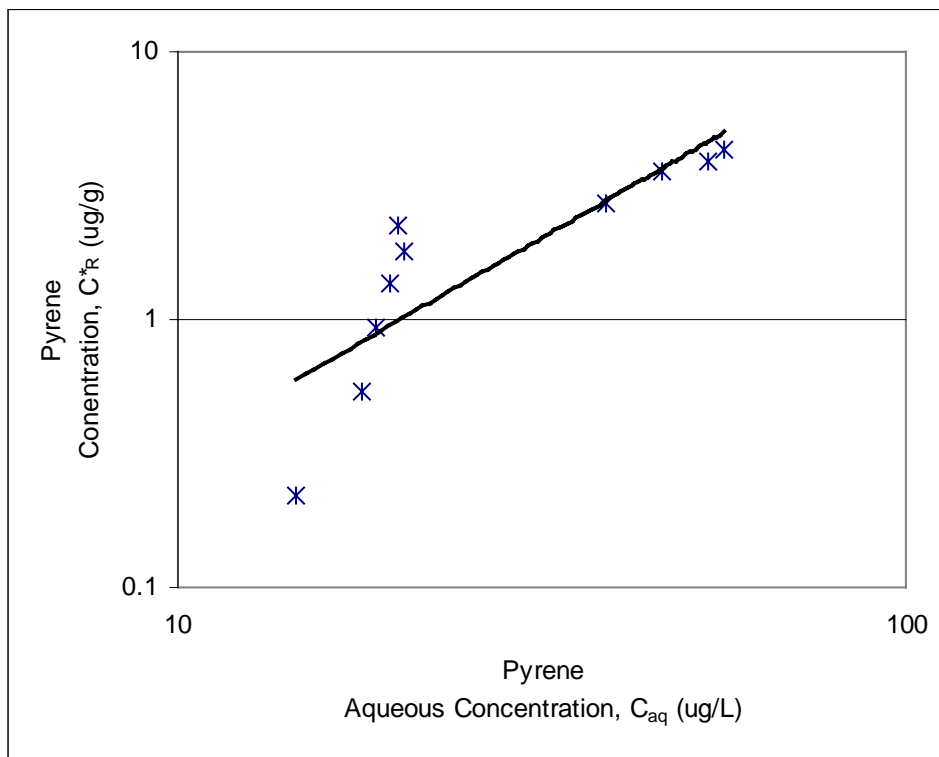


**Figure 5.23 Pyrene Freundlich isotherm for SB-10, 7 feet below land surface**

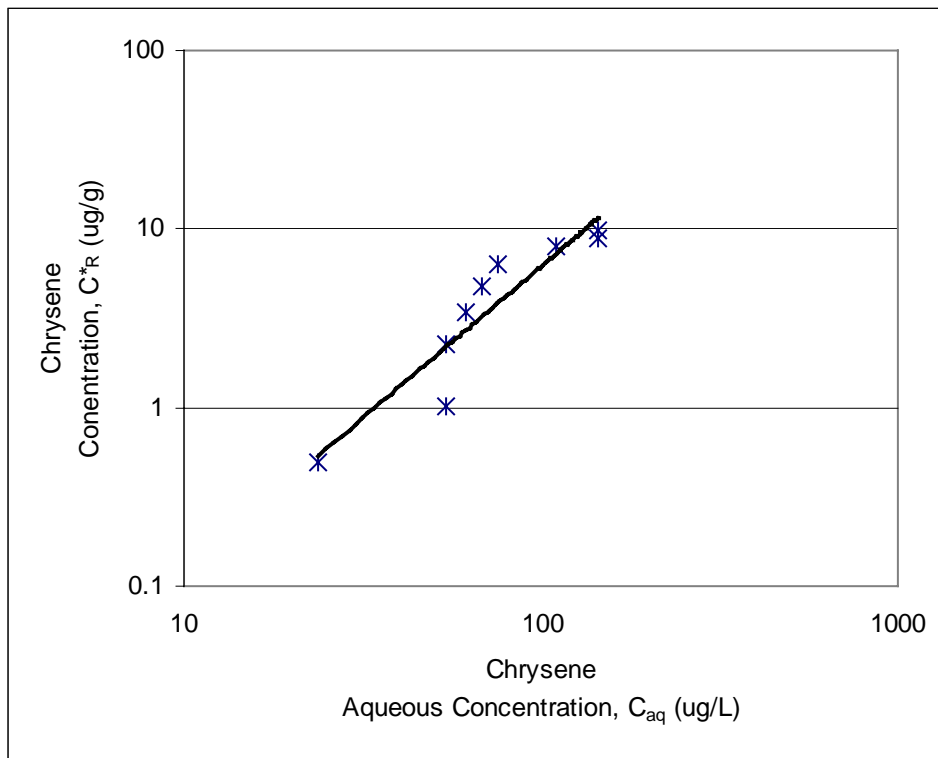


**Figure 5.24 Chrysene Freundlich isotherm for SB-10, 7 feet below land surface**

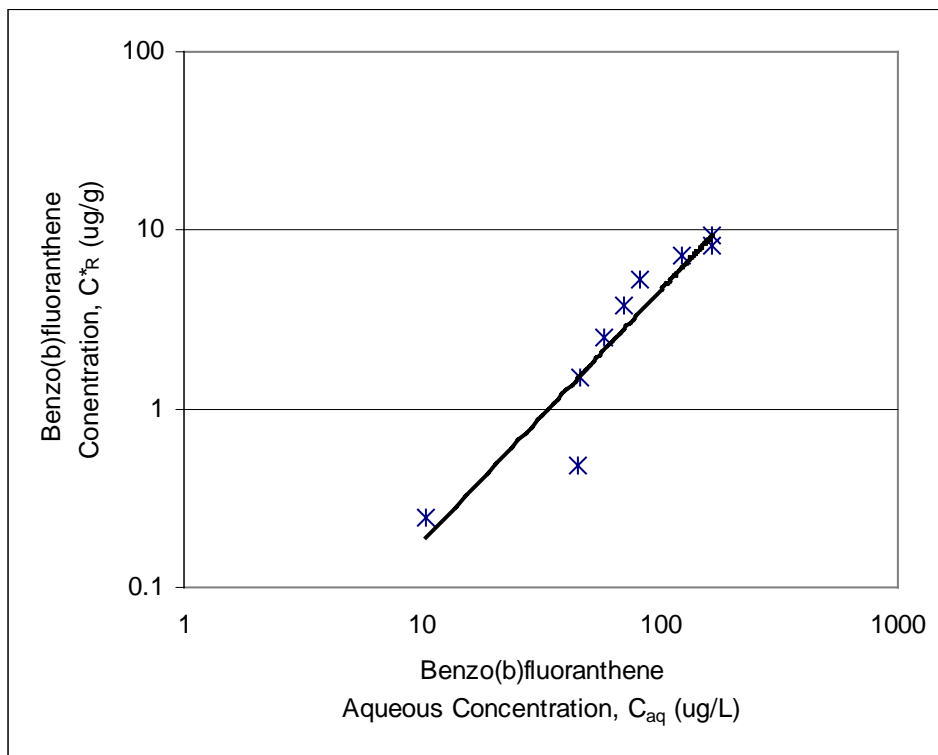


**Figure 5.25 Benzo(b)fluoranthene Freundlich isotherm for SB-10, 7 feet below land surface**

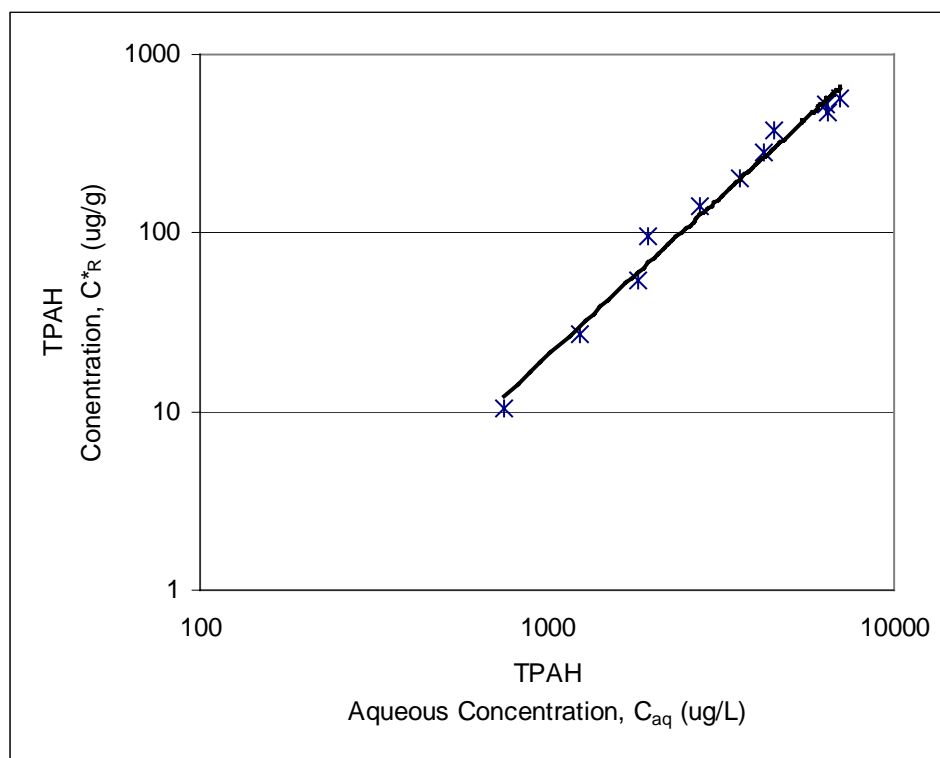


**Figure 5.26 Total polycyclic aromatic hydrocarbon Freundlich isotherm for SB-10, 7 feet below land surface**

Table 5.10 is a summary of the reversibly and irreversibly sorbed PAH concentrations at SB-10 seven feet below land surface. The initial sorbed concentration,  $C^*$ , in Table 5.10 was obtained from soil extractions performed prior to the setup of the desorption equilibrium experiment and is listed in Appendix A (Table 5A). The reversible sorbed concentration,  $C^*_R$ , in Table 5.10 represents the sum of the desorbed mass for a PAH measured during each sampling event of the desorption kinetics experiment divided by the mass of solids. This value signifies the total amount of a particular PAH that can be desorbed from the original contaminant matrix relative to the mass of solids. Assuming that the maximum amount of desorbable mass has come into solution by the end of the desorption kinetics experiment, the remaining concentration is believed to be either irreversibly sorbed or desorbing at an extremely slow rate. Therefore, the irreversible sorbed concentration,  $C^*_{IR}$ , in Table 5.10 represents the difference between the initial sorbed concentration,  $C^*$ , of a particular PAH and the corresponding reversible sorbed concentration,  $C^*_R$ . The percent removal is an estimate of the percent of the initial sorbed concentration of each PAH that can be desorbed. Percent removal is calculated by dividing the initial sorbed concentration,  $C^*$ , by the reversible sorbed concentration,  $C^*_R$ .

A summary of the reversible and irreversible soil PAH concentrations for the remaining soil boring locations under investigation is located in Appendix B (Tables 65B-71B)

**Table 5.10 Reversible and irreversible sorption as determined by desorption kinetics experiment at SB-10, 7 feet below land surface**

<b>PAH</b>	<b>*Initial Sorbed Concentration, C* (ug/g)</b>	<b>**Reversible Sorbed Concentration, C*_R (ug/g)</b>	<b>% Removal of Sorbed Concentration (C*_R/C*)</b>	<b>***Irreversible Sorbed Concentration, C*_IR (ug/g)</b>
<b>Naphthalene</b>	1103.78	319.65	28.96	784.13
<b>Acenaphthylene</b>	86.11	18.40	21.37	67.71
<b>Acenaphthene</b>	593.78	143.70	24.20	450.08
<b>Fluorene</b>	642.43	69.95	10.89	572.48
<b>Phenanthrene</b>	1584.16	47.39	2.99	1536.77
<b>Anthracene</b>	239.94	18.45	7.69	221.49
<b>Fluoranthene</b>	726.80	6.89	0.95	719.91
<b>Pyrene</b>	605.92	4.71	0.78	601.21
<b>Chrysene</b>	259.13	10.98	4.24	248.15
<b>Benzo(b) fluoranthene</b>	262.99	10.58	4.02	252.41
<b>Total PAH's</b>	6105.04	650.70	10.66	5454.35

*\*Measured by MeCl water extraction described in section 4.7.1*

*\*\* Total mass measured by Desorption Kinetics Experiment described in Tables 5.3 – 5.13*

*\*\*\*Difference between Initial Sorbed Concentration and Reversible Sorbed Concentration*

In general, the percent removal decreases with increasing molecular weight. This trend corresponds to the hydrophobicity of high molecular weight compounds. Naphthalene has the largest percent removal at SB-10 seven feet below land surface and several other soil boring locations. Because this experiment was not conducted under airtight conditions, this phenomenon is most likely a result of losses due to the volatility of naphthalene. The lowest percent removal occurs in pyrene, which has high molecular weight and tends to sorb to soil. Even though chrysene and benzo(b)fluoranthene are 4 and 5-ring compounds, they have a higher percent removal, possibly due to the effects of cosolvency. The trends revealed in Table 5.10 are similar to those found at the other soil boring locations.

Tables 5.11 to 5.13 list the desorption rate parameters and Freundlich constants for each PAH by soil boring location as determined by the desorption kinetics experiment. For the most part, the magnitude of all 3 parameters is consistent at each boring location. However, there is some difference between soil boring locations and also between the extremely contaminated samples and those that are fairly uncontaminated. For the more contaminated samples, (SB-10 7 ft, SB-11 8 ft, and SB-12 10 ft), Table 5.11 shows that the desorption rate typically decreases with increased molecular weight. For the less contaminated samples, this trend is not as obvious. In cases where there is a presence of naphthalene, the desorption rate calculated for total PAH's is usually controlled by the desorption of naphthalene. Therefore, the total PAH desorption rate may be slightly inaccurate due to losses from the volatility of naphthalene. In particular, the desorption data obtained for SB-11 seven feet under land surface did not fit well to a linear model. The correlation coefficients for most PAH desorption data at this soil boring location were well below 0.95, indicating that the data does not fit a linear trend line. This phenomenon could be correlated with low concentrations at this location and may be a result of the presence of organic matter or slow desorption.

Table 5.12 summarizes the values obtained for the desorption Freundlich constant  $K_f$  by location and Table 5.13 summarizes the values obtained for the desorption Freundlich coefficient  $N$  by location. According to the data, the Freundlich constant  $K_f$  generally increases with increasing molecular weight, while the Freundlich coefficient  $N$  decreases with increasing molecular weight. Most  $N$  values are greater than unity, indicating non-linear sorption and the presence of a non-uniform sorbent. However, some  $N$  values are close to 1 indicating that desorption follows a linear pattern.

With a few exceptions, the magnitude of  $K_f$  and  $N$  values are consistent between boring locations. However, there is some difference between extremely contaminated and uncontaminated samples for the 2 to 3-ring PAH's. The  $K_f$  and  $N$  values for the 2 to 3-ring compounds in uncontaminated soil samples (SB-25 6 ft, SB-25 7 ft, and SB-11 7 ft) generally do not follow any particular trend. For the 4 and 5-ring compounds, the magnitude of Freundlich coefficients is consistent between contaminated and uncontaminated samples. Inconsistency amongst uncontaminated samples could be a result of a limited range of aqueous PAH concentrations as compared to the more contaminated samples.

**Table 5.11 Desorption rate constants by sample location as determined by desorption kinetics experiment**

Sample Location	Naphthalene	Acenaphthylene	Acenaphthene	Fluorene	Phenanthrene	Anthracene	Fluoranthene	Pyrene	Chrysene	Benzo(b) fluoranthene	TPAH
SB-10 6 ft	-0.26	-0.57	-3.44	-1.92	-1.49	-0.54	-0.27	-0.18	-0.51	-0.59	-9.30
SB-10 7 ft	-25.47	-0.83	-4.96	-2.43	-1.84	-0.80	-0.28	-0.20	-0.56	-0.65	-32.00
SB-25 6 ft	Insufficient Data	-0.12	-0.025	-0.15	-0.15	Insufficient Data	-0.056	-0.05	-0.11	-0.14	<b>-0.40</b>
SB-25 7 ft	Insufficient Data	-0.17	-1.73	-1.02	-0.35	-0.25	-0.30	-0.16	-0.38	-0.46	-4.64
SB-11 7 ft	Insufficient Data	-0.13	Insufficient Data	Insufficient Data	Insufficient Data	Insufficient Data	<b>-0.041</b>	<b>-0.029</b>	<b>-0.030</b>	-0.18	<b>-0.28</b>
SB-11 8 ft	-27.47	-0.56	-2.68	-1.06	-1.15	-0.24	-0.14	-0.11	-0.18	-0.50	-26.19
SB-12 10 ft	-48.68	-0.67	-4.27	-1.97	<b>-2.53</b>	-0.56	-0.22	-0.18	<b>-0.22</b>	-0.71	-24.91

*\*Indicates  $r^2$  value less than 0.95*

**Table 5.12 Freundlich constant,  $K_f$ , by sample location as determined by desorption kinetics experiment**

<b>Sample Location</b>	<b>Naphthalene</b>	<b>Acenaphthylene</b>	<b>Acenaphthene</b>	<b>Fluorene</b>	<b>Phenanthrene</b>	<b>Anthracene</b>	<b>Fluoranthene</b>	<b>Pyrene</b>	<b>Chrysene</b>	<b>Benzo(b) fluoranthene</b>	<b>TPAH</b>
<b>SB-10 6 ft</b>	2.21E-02	2.53E-03	2.35E-05	1.25E-05	2.93E-05	3.42E-06	3.47E-04	2.05E-03	8.16E-04	1.31E-03	8.53E-07
<b>SB-10 7 ft</b>	3.51E-05	4.08E-04	2.06E-07	2.25E-06	2.11E-05	9.74E-05	3.10E-04	8.94E-03	2.47E-03	6.99E-03	9.09E-05
<b>SB-25 6 ft</b>	Insufficient Data	3.57E-14	4.16E-02	4.92E-02	4.90E-02	Insufficient Data	1.05E-02	1.96E-02	6.87E-03	1.25E-02	2.74E-02
<b>SB-25 7 ft</b>	Insufficient Data	6.81E-06	3.72E-04	4.37E-04	1.16E-03	2.08E-06	8.69E-05	1.96E-03	3.41E-03	3.52E-03	1.50E-04
<b>SB-11 7 ft</b>	Insufficient Data	7.79E-13	Insufficient Data	Insufficient Data	Insufficient Data	Insufficient Data	2.21E-02	1.98E-02	1.44E-01	8.50E-03	1.12E-02
<b>SB-11 8 ft</b>	6.45E-06	2.95E-05	1.54E-05	3.75E-06	3.08E-06	1.07E-04	1.19E-03	7.75E-04	4.94E-01	6.62E-03	2.33E-03
<b>SB-12 10 ft</b>	1.58E-05	1.44E-04	3.04E-06	1.77E-02	2.76E-02	4.38E-03	1.08E-03	1.24E-02	7.23E-01	5.96E-03	2.67E-02

**Table 5.13 Freundlich coefficient, N, by sample location as determined by desorption kinetics experiment**

<b>Sample Location</b>	<b>Naphthalene</b>	<b>Acenaphthylene</b>	<b>Acenaphthene</b>	<b>Fluorene</b>	<b>Phenanthrene</b>	<b>Anthracene</b>	<b>Fluoranthene</b>	<b>Pyrene</b>	<b>Chrysene</b>	<b>Benzo(b) fluoranthene</b>	<b>TPAH</b>
<b>SB-10 6 ft</b>	0.92	1.73	2.39	2.62	2.55	3.34	2.45	1.99	1.93	1.76	2.63
<b>SB-10 7 ft</b>	1.87	2.11	3.05	2.89	2.52	2.45	2.46	1.57	1.70	1.41	1.78
<b>SB-25 6 ft</b>	Insufficient Data	15.30	0.66	0.60	0.54	Insufficient Data	1.35	1.02	1.58	1.31	1.01
<b>SB-25 7 ft</b>	Insufficient Data	3.53	1.85	1.90	1.81	3.69	2.70	1.99	1.56	1.49	1.85
<b>SB-11 7 ft</b>	Insufficient Data	13.10	Insufficient Data	Insufficient Data	Insufficient Data	Insufficient Data	1.15	1.19	0.37	1.42	1.21
<b>SB-11 8 ft</b>	1.93	2.51	2.37	2.83	2.75	2.58	2.10	2.22	0.35	1.30	1.30
<b>SB-12 10 ft</b>	1.86	2.21	2.58	1.16	1.08	1.54	2.11	1.38	0.28	1.38	1.06

Table 5.14 shows the percent of reversible sorbed concentration per total PAH's by the number of rings in a PAH and the soil boring location. The values in Tables 5.14 are based on the reversible sorbed concentrations ( $C^*_R$ ) calculated in Table 5.10.

Percentages are calculated by dividing the sum of the reversible sorbed concentrations at time zero, grouped by the number of rings, by the reversible sorbed concentration for total PAH's. When added together, the sum of the 2, 3, 4 and 5-ring compounds is 100% representing the percent of total PAH's which are reversibly sorbed. Naphthalene is the lightest compound containing 2 rings, while benzo(b)fluoranthene is the heaviest compound with 5 rings. The 3-ring compounds include acenaphthylene, acenaphthene, fluorene, phenanthrene, and anthracene, while the 4-ring compounds include fluoranthene, pyrene, and chrysene. The samples in Table 5.14 can be characterized in terms of contamination by the total sorbed PAH concentration listed in mg/kg.

According to these concentrations, SB-25 6 ft and SB-11 7ft are considered fairly uncontaminated, while the other soil borings are comparatively contaminated.

As shown in Table 5.14, the percent removal of the sorbed concentration can be correlated to the number of rings in that compound. With a few exceptions for uncontaminated samples, the percent removal generally decreases with increasing molecular weight. The percent removal of naphthalene is inconsistent between soil boring locations because it was calculated based on limited data. According to the literature, as the molecular weight of a compound increases, its hydrophobicity also increases causing sorption of heavier compounds (Link 2000). Therefore, one would expect a higher degree of removal for 2 to 3-ring compounds and a lower percent removal for 4 to 5-ring compounds. With the exception of naphthalene and the uncontaminated samples, the data presented in Table 5.14 generally agree with the literature.

**Table 5.14 Reversible sorbed concentration as a percent of the total polycyclic aromatic hydrocarbons as determined by desorption kinetics experiment**

<b>Location</b>	<b>Initial Sorbed TPAH Concentration (mg/kg)</b>	<b>Naphthalene</b>	<b>3-Ring Compounds</b>	<b>4-Ring Compounds</b>	<b>Benzo(b) fluoranthene</b>	<b>TPAH</b>
<b>SB-10 6 ft</b>	6742.16	0.38	89.31	7.15	3.16	100
<b>SB-10 7 ft</b>	6105.04	49.12	45.78	3.47	1.63	100
<b>SB-25 6 ft</b>	23.66	0.00	27.40	41.59	30.88	100
<b>SB-25 7 ft</b>	907.75	0.00	71.61	21.00	7.38	100
<b>SB-11 7 ft</b>	39.60	0.00	25.51	30.87	43.78	100
<b>SB-11 8 ft</b>	6729.42	61.11	35.05	2.35	1.49	100
<b>SB-12 10 ft</b>	9223.47	41.31	52.69	3.36	2.64	100

### 5.3 Dissolution Kinetics Experiment Results

The dissolution kinetics experiment, described in Section 4.5, is a soil column test to estimate the rate of dissolution under field-like conditions. The results of the dissolution kinetics experiment are time-dependent plots of aqueous concentration versus time for each monitored PAH at every sampling location. However, the duration of the dissolution experiments proved insufficient to achieve precise estimates of the rate of dissolution for slowly released PAH's. These results demonstrate the need for conducting dissolution experiments for longer periods if complete data on the long-term dissolution of resistant compounds is to be obtained.

Much like the desorption kinetics experiment, the dissolution kinetics experiment was a successive series of equilibrium reactions and experiments measured at the time interval of fluid exchange, or sampling time. During this experiment, aqueous concentrations were taken after PAH contaminated soil, containing NAPL free product, was in contact with clean distilled water for 3 day, 6 day, and 12 day intervals. The soil columns were set up in 2 phases. Soils for phase A and B were collected in July of 2001 and February of 2002, respectively. Because the different phases were composed of separate soils, only general trends, and not specific results, from phase A and phase B can be associated.

Aqueous PAH concentrations for the all sampling events are listed in Appendix C (Tables 1C – 8C). The resulting plots of aqueous concentration versus sampling time are also located in Appendix C (Figures 1C – 12C). In addition, Appendix C (Figures 13C – 16C) compares the effects of fluid exchange time on the dissolution rate of PAH's for all soil columns with a common batch of soil (phase A or phase B). As an example, Figures 5.27 and 5.28 show plots of the triplicate averaged aqueous concentration of anthracene in  $\mu\text{g/L}$  versus time for all phase A soil columns and phase B soil columns, respectively. Anthracene is a 3-ring compound with a molecular weight of 178 amu and a water solubility of 0.05 mg/L. This compound was chosen as an example for study because it was prevalent in background samples and has chemical and physical characteristics representative of PAH's monitored in this study.

Figures 5.27 and 5.28 show an increase in aqueous concentration with time regardless of the period between fluid exchanges. However, the data demonstrate that the longer the time between fluid exchanges, the higher the aqueous concentration of a sample. This

phenomenon corresponds with the data from the desorption equilibrium experiment that shows an increase in aqueous concentration with sampling time. In general, the remaining plots in Appendix C (Figures 1C-16C) display the same increasing behavior. However, the data from the dissolution kinetics experiment does not display asymptotic behavior indicating that PAH concentrations have not reach equilibrium yet between the sorbed and dissolved states. These results illustrate the effects of the slow steady release of PAH's associated with dissolution.

The majority of PAH's present in the aqueous phase at the end of the dissolution kinetics experiment had concentrations under or close to the respective solubility limits presented in the literature for individual PAH's. With the exceptions of chrysene and benzo(b)fluoranthene, the aqueous concentration of PAH's were all under the solubility limits listed in Table 2.2. However, chrysene, and benzo(b)fluoranthene were present in aqueous concentrations exceeding the solubility limits listed in Table 2.2, possibly due to the effects of naphthalene acting as a cosolvent.

The maximum aqueous concentration values obtained for the dissolution kinetics experiment differ slightly from those resulting from the desorption equilibrium experiment. The magnitude of aqueous concentration for naphthalene is generally consistent between experiments. For the dissolution kinetics experiment, the 2 to 3-ring compounds are present in the aqueous phase at approximately half of the magnitude of those found in the desorption equilibrium experiment. As the molecular weight increases, the aqueous phase PAH concentrations for the dissolution kinetics experiment diverge even further from the maximum concentration values obtained in the desorption equilibrium experiment. Fluoranthene, pyrene, chrysene, and benzo(b)fluoranthene concentrations in solution obtained from the dissolution kinetics experiment are on average less than 20% of those values obtained from the desorption kinetics experiment. One of the reasons behind this trend may be the difference in experimental setup. The desorption equilibrium experiment was a batch test in which samples were agitated daily to promote maximum contact between water and soil. On the other hand, the dissolution kinetics experiment was conducted in soil columns that remained undisturbed throughout the length of the experiment to mimic field conditions.

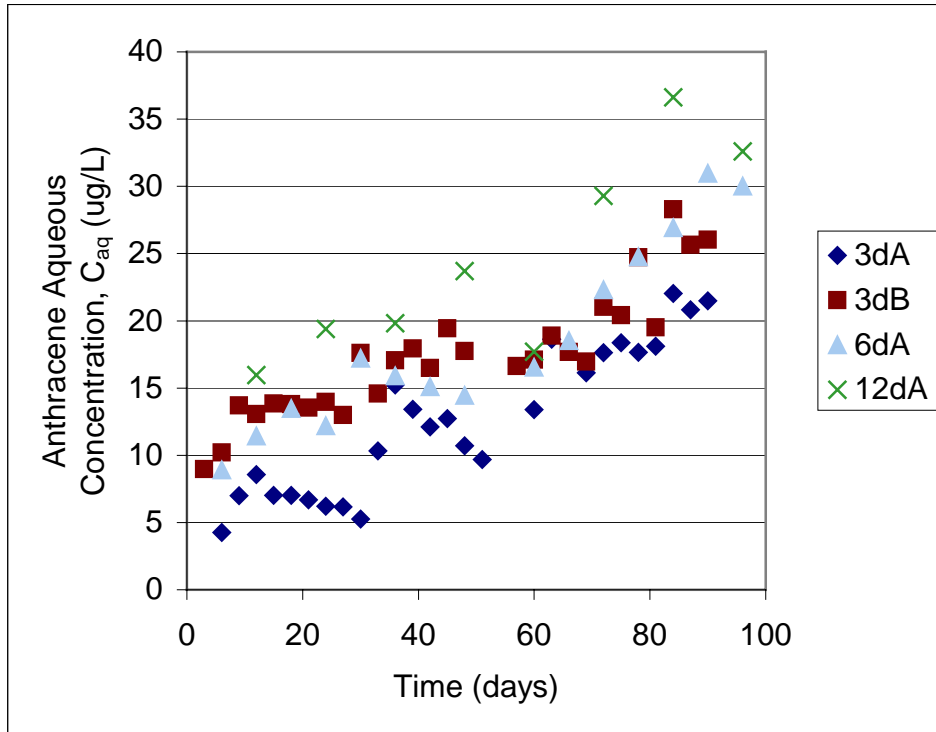


**Figure 5.27 Aqueous concentration versus sampling time for all phase A soil columns**

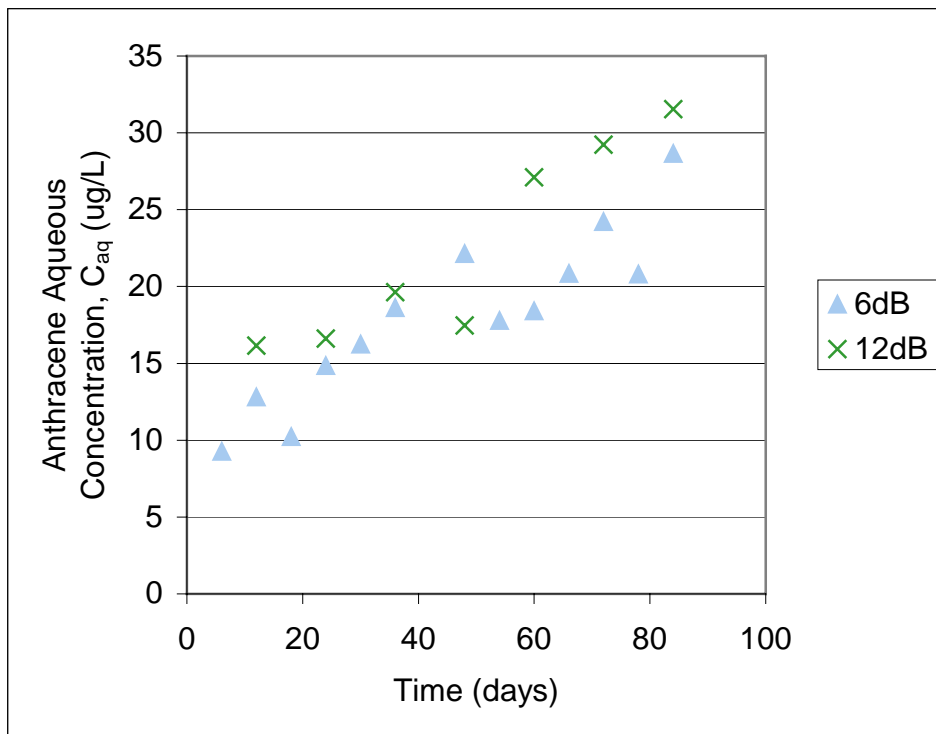


**Figure 5.28 Aqueous concentration versus sampling time for all phase B soil columns**

Although the results of the dissolution kinetics experiment point strongly toward the need for further study, they can be used to determine a rough estimate of the dissolution rates on-site. Given the previously described dissolved concentration data, the dissolution rate can be calculated based on the principles of diffusion. In the field, when a soil is contaminated with NAPL, groundwater tends not to flow directly through that soil because the voids are blocked with free product. Consequently, groundwater will flow around the edges of a NAPL where a main source of contaminant dissolution is diffusion. Therefore, if it is assumed that the mass of NAPL is constant, the dissolution rate can be calculated by multiplying the diffusive flux by the area of water/NAPL contact.

Table 5.15 shows the average dissolution rates for each PAH based on aqueous concentrations for the phase A and B soil columns sampled every 12 days. Triplicate concentrations were averaged to obtain the average aqueous concentration,  $C_{aq}$ . The aqueous mass,  $\Delta M_{aq}$ , was calculated by multiplying the average aqueous concentration by the sample volume, or 40 mL. The sample volume represents the volume of liquid that passed the NAPL/water interface. The diffusive flux,  $F_D$ , was then calculated by dividing the aqueous mass,  $\Delta M_{aq}$ , by the sampling time interval and the area of NAPL/water contact. In this case, the contact area was the inner diameter of the PVC soil column at the interface between the creosote contaminated soil and distilled water. Assuming that there were no other sources of dissolved contamination, the average dissolution rate was calculated by multiplying the area of NAPL/water contact by the diffusive flux,  $F_D$ .

Much like the results of the desorption kinetics experiment, the dissolution rates obtained from the dissolution kinetics experiment generally decrease with increasing molecular weight. Dissolution rates were calculated for concentrations based on the last sampling event of the dissolution kinetics experiment. Based on earlier results, aqueous PAH concentrations had not yet reached equilibrium between the sorbed and dissolved states; therefore, long-term dissolution rates could not be calculated.

**Table 5.15 Dissolution rates for soil columns sampled every 12 days**

**12 days A**

<b>Polycyclic Aromatic Hydrocarbon</b>	<b>Average Aqueous Concentration C<sub>aq</sub> (ug/L)</b>	<b>Aqueous Mass Δ M<sub>aq</sub> (ug)</b>	<b>Diffusive Flux F<sub>D</sub> (ug/in<sup>2</sup>/day)</b>	<b>Average Dissolution Rate ug/day</b>
Naphthalene	4011.50	160.46	1.0641	13.372
Acenaphthylene	24.16	0.97	0.0064	0.081
Acenaphthene	136.75	5.47	0.0363	0.456
Fluorene	79.28	3.17	0.0210	0.264
Phenanthrene	68.08	2.72	0.0181	0.227
Anthracene	32.61	1.30	0.0087	0.109
Fluoranthene	10.51	0.42	0.0028	0.035
Pyrene	10.85	0.43	0.0029	0.036
Chrysene	0.00	0.00	0.0000	0.000
Benzo(b)fluoranthene	13.28	0.53	0.0035	0.044

**12 days B**

<b>Polycyclic Aromatic Hydrocarbon</b>	<b>Average Aqueous Concentration C<sub>aq</sub> (ug/L)</b>	<b>Aqueous Mass Δ M<sub>aq</sub> (ug)</b>	<b>Diffusive Flux F<sub>D</sub> (ug/in<sup>2</sup>/day)</b>	<b>Average Dissolution Rate ug/day</b>
Naphthalene	5588.58	223.54	1.4824	18.629
Acenaphthylene	26.07	1.04	0.0069	0.087
Acenaphthene	162.79	6.51	0.0432	0.543
Fluorene	93.90	3.76	0.0249	0.313
Phenanthrene	84.34	3.37	0.0224	0.281
Anthracene	31.54	1.26	0.0084	0.105
Fluoranthene	11.52	0.46	0.0031	0.038
Pyrene	11.51	0.46	0.0031	0.038
Chrysene	0.00	0.00	0.0000	0.000
Benzo(b)fluoranthene	13.41	0.54	0.0036	0.045

## 6. CONCLUSIONS

Sorption/desorption kinetics is extremely important in modeling the transport of contaminants in the subsurface and predicting the partitioning of contaminants between the sorbed and aqueous phases. Although there is a considerable amount of research pertaining to the rate limiting nature of sorption, desorption and dissolution are site specific and not readily predictive. Also, there is no standard procedure for estimating the amount of desorbing mass. The results of this study can be used in modeling the transport of contaminants and to quantify desorption at the Oneida Tie-Yard site.

This work led to the following major conclusions:

- The desorption equilibrium experiment revealed that rates of equilibrium were truly not instantaneous in the systems studied. After an initially fast desorption rate, several days, and in some cases weeks, were required to attain true equilibrium. However, because approximately 76% desorbed by the first sampling event at 3 days, an equilibrium isotherm is appropriate.
- The desorption kinetics experiment revealed that there is a reversible component to the sorbed mass of PAH's that will desorb into the aqueous phase under conditions where aqueous PAH concentration decreases.
- Desorption curves based on data from the desorption kinetics experiment were found to exhibit linear behavior over large variations in aqueous concentration, but exponential behavior as concentrations approached zero.
- Freundlich sorption equilibrium isotherms for the 10 monitored PAH's on-site were generally found to have N coefficient values over 1, especially over large variations in solution phase concentration, indicating a non-uniform sorbent. Based on the desorption kinetics data, the Freundlich constant  $K_f$  generally increases with increasing molecular weight, while the Freundlich coefficient N decreases with increasing molecular weight.

- The desorption kinetics experiment revealed that the percent removal of sorbed PAH's decreases with increasing molecular weight corresponding with the hydrophobicity of high molecular weight compounds.
- Naphthalene, acting as a cosolvent, could be affecting the sorptive properties of the 4 and 5-ring PAH compounds. Once naphthalene is no longer present in the aqueous phase, benzo(b)fluoranthene and chrysene are depleted almost immediately from the dissolved phase indicating drastic reductions in desorption.
- The results of the dissolution kinetics experiment are an indication of dissolution trends under field-like conditions. The data shows an increase in aqueous concentration with the number of fluid exchanges regardless of the time between fluid exchanges. These results demonstrate the need for conducting dissolution experiments for longer periods if complete data on the long-term dissolution of resistant compounds is to be obtained.
- The dissolution rates obtained from the dissolution kinetics experiment generally decrease with increasing molecular weight.
- Remediation at the Oneida Tie-Yard site may be rate limited by the desorption and dissolution kinetics of the PAH's on-site.

Some suggestions for further research that could stem from this work are listed as follows:

- The outcome of these experiments can also be used to develop a qualitative model to describe the relationship between the rate of desorption of PAH's to the remediation time at a phytoremediation site. These results could help to assess whether phytoremediation, even if limited by desorption and dissolution, can occur fast enough so that the risk to public health and the environment is acceptably low.
- Future research could focus on a better understanding and prediction of the rates of desorption and dissolution at the Oneida Tie-Yard and also on overcoming the constraints of slow desorption for remediation purposes.

## 7. LITERATURE CITED

**Al-Yousfi, A.B., R.J. Chapin, T.A. King, and S.I. Shah.** 2000. Phytoremediation – The Natural Pump-and-Treat and Hydraulic Barrier System. *Practice Periodical of Hazardous, Toxic, and Radioactive Waste Management*. Vol. 4, No. 2, pp.73-77.

**ARCADIS Geraghty & Miller.** 2001. Remediation Progress Meeting, Norfolk Southern Railway Company. Oneida Tie-Yard Site. Oneida, Tennessee.

**ARCADIS Geraghty & Miller.** 2000. Remediation Progress Meeting, Norfolk Southern Railway Company. Oneida Tie-Yard Site. Oneida, Tennessee.

**Brauner, J. S.** 2000. Impacts of Sequential Microbial Electron Accepting Processes on Natural Attenuation of Selected Petroleum Hydrocarbons in the Subsurface Environment. Ph.D. Dissertation. Virginia Polytechnic Institute and State University. Blacksburg, Virginia.

**Brown, D.G., C.D. Knightes, and C.A. Peters.** 1999. Risk Assessment for Polycyclic Aromatic Hydrocarbon NAPL's Using Component Fractions. *Environmental Science and Technology*. Vol. 33, No. 24, pp. 4357-4363.

**Brubaker, G.R. and H.F. Stroo.** 1992. In-Situ Bioremediation of Aquifers Containing Polyaromatic Hydrocarbons. *Journal of Hazardous Materials*. Vol. 32, pp. 163-177.

**Brusseau, M.L.** 1993. Factors Influencing the Transport and Fate of Contaminants in the Subsurface. *Journal of Hazardous Materials*. Vol. 32, pp. 137-142.

**Brusseau, M.L., A.L. Wood, and P.S.C. Rao.** 1991. Influence of Organic Cosolvents on the Sorption Kinetics of Hydrophobic Organic Chemicals. *Environmental Science and Technology*. Vol. 25, pp. 903-910.

**Burken, J.G. and J. L. Schnoor.** 1998. Predictive Relationships for Uptake of Organic Contaminants by Hybrid Poplar Trees. *Environmental Science and Technology*. Vol. 32, pp. 3379-3385.

**Callahan, M.A., W.M. Slimak, N.W. Gabel, I.P. May, C.F. Fowler, J.R. Freed, P. Jennings, R.L. Durfee, F.C. Whitmore, B. Maestri, W.R. Mabey, B.R. Holt, and C. Gould.** *Water-Related Environmental Fate of 129 Priority Pollutants*, EPA 440/4-79-029a. U.S. Environmental Protection Agency. Washington, D.C, 1979.

**Carriere, P.P.E. and F.A. Mesania.** 1995. Enhanced Biodegradation of Creosote-Contaminated Soil. *Waste Management*. Vol. 15, No. 8, pp. 579-583.

- Cornelissen, G., H. Rigterink, M.M.A. Ferdinandy, and P.C.M. Van Noort.** 1998. Rapidly Desorbing Fractions of PAH's in Contaminated Sediments as a Predictor of the Extent of Bioremediation. *Environmental Science and Technology*. Vol. 32, No. 7, pp. 966-970.
- Crosswell, S.B.** 1999. Effects of Grasses on the Remediation of Creosote-Contaminated Surface Soil. M.S. Thesis. Virginia Polytechnic Institute and State University. Blacksburg, Virginia.
- Cunningham, S. D, W.R. Berti, and J.W. Huang.** 1995. Phytoremediation of Contaminated Soils. *Trends in Biotechnology*. Volume 13, pp. 393-397.
- Dzombak, D.A. and R.G. Luthy.** 1984. Estimating Adsorption of Polycyclic Aromatic Hydrocarbons on Soils. *Soil Science*. Vol. 137, pp. 292-308.
- Edwards, N.T.** 1983. Polycyclic Aromatic Hydrocarbons (PAH's) in the Terrestrial Environment – A Review. *Journal of Environmental Quality*. Vol.12, pp. 427-441.
- Elliot, M.** 2001. Polycyclic Aromatic Hydrocarbons and Redox Parameters in a Creosote-Contaminated Aquifer. M.S. Thesis. Virginia Polytechnic Institute and State University. Blacksburg, Virginia.
- Elzerman, A.W. and J.T. Coates.** *Sources and Fates of Aquatic Pollutants* (Edited by R. Hites and S.J. Eisenreich), Chapter 10. American Chemical Society. Washington, D.C., 1987.
- Fetter, C.W.** Contaminant Hydrology. *Sorption Processes*. Prentice-Hall, Inc., Upper Saddle River, New Jersey, 1993.
- Fetterolf, J.G.** 1998. Characterization of a Creosote-Contaminated Tie Yard Site and the Effects of Phytoremediation. M.S. Thesis. Virginia Polytechnic Institute and State University. Blacksburg, Virginia.
- Fu, G., A.T. Kan, and M. Tomson.** 1994. Adsorption and Desorption Hysteresis of PAH's in Surface Sediment. *Environmental Toxicology and Chemistry*. Vol. 13, No. 10, pp. 1559-1567.
- Garbarini, D.R. and L.W. Lion.** 1986. Influence of the Nature of Soil Organics on the Sorption of Toluene and Trichloroethylene. *Environmental Science and Technology*. Vol. 20, pp.1263-1269.
- Grasso, D., K. Subramaniam, J.J. Pignatello, Y. Yang, and D. Ratte.** 2001. Micellar Desorption of Polynuclear Aromatic Hydrocarbons from Contaminated Soil. *Colloids and Surfaces*. Vol. 194, pp. 65-74.

- Greist, W.H and Caton, J.E.** Extraction of PAH for Quantitative Analysis. *Handbook of Polycyclic Aromatic Hydrocarbons* (Edited by Bjorseth, A.). Marcel Dekker, Inc.: New York and Basel, 1983.
- Guevara-Escobar, A., W.R.N. Edwards, R.H. Morton, P.D. Kemp, and A.D. Mackay.** 2000. Tree Water Use and Rainfall Partitioning in a Mature Poplar-Pasture System. *Tree Physiology*. Vol. 20, pp. 97-106.
- Hale, R.C. and K.M. Aneiro.** 1997. Determination of Coal Tar and Creosote Constituents in the Aquatic Environment. *Journal of Chromatography*. Vol. 774, pp. 79-95.
- Huang W. and W.J. Weber, Jr.** 1997. A Distributed Reactivity Model for Sorption by Soils and Sediments. 10. Relationships between Desorption, Hysteresis, and the Chemical Characteristics of Organic Domains. *Environmental Science and Technology*. Vol. 31, No. 9, pp. 2562-2569.
- Johnson, W.P. and G.L. Amy.** 1995. Facilitated Transport and Enhanced Desorption of Polycyclic Aromatic Hydrocarbons by Natural Organic Matter in Aquifer Sediments. *Environmental Science and Technology*. Vol. 29, No. 3, pp. 807-817.
- Jones, K.C., J.A. Stratford, K.S. Waterhouse, and N.B. Vogt.** 1989. Organic Contaminants in Welsh Soils: Polynuclear Aromatic Hydrocarbons. *Environmental Science and Technology*. Vol. 23, pp. 540-550.
- Kan, A.T., G. Fu, M. Hunter, W. Chen, C.H. Ward, and M.B. Tomson.** 1998. Irreversible Sorption of Neutral Hydrocarbons to Sediments: Experimental Observations and Model Predictions. *Environmental Science and Technology*. Vol. 32, No. 7, pp. 892-902.
- Karickhoff, S.W.** *Contaminants and Sediments Volume II* (Edited by R.A. Baker), Chapter 11. Ann Arbor Science: Ann Arbor, Michigan, 1980.
- Kohl, S.D. and J.A. Rice.** 1999. Contribution of Lipids to the Nonlinear Sorption of Polycyclic Aromatic Hydrocarbons to Soil Organic Matter. *Organic GeoChemistry*. Vol. 30, pp. 929-936.
- Lakhwinder, S.H., M.L. Thompson, D.A. Laird, and A.M. Carmo.** 2001. Sorption of Phenanthrene by Reference Smectites. *Environmental Science and Technology*. Vol. 35, No. 17, pp. 3456-3461.
- Link, A.** 2000. Effect of Nonionic Surfactants on Dissolution of Polycyclic Aromatic Hydrocarbons from Coal Tar. *Practice Periodical of Hazardous, Toxic, and Radioactive Waste Management*. Vol. 4, No. 2, pp.78-81.

- Loftis, D.R.** 1999. Hydrogeologic Analysis and Data Collection for the Oneida Tie-Yard Site. M.S. Thesis. Virginia Polytechnic Institute and State University. Blacksburg, Virginia.
- Luthy, R.G., D.A. Dzombak, S.B. Roy, A. Ramaswani, D.V. Nakles, and B.R. Nott.** 1994. Remediating Tar-Contaminated Soils at Manufactured Gas Plant Sites. *Environmental Science and Technology*. Vol. 28, No. 2, pp. 266-276.
- Luthy, R.G., G.R. Aiken, M.L. Brusseau, S.D. Cunningham, P.M. Gschwend, J.J. Pignatello, M. Reinhard, S.J. Traina, W.J. Weber, Jr., and J.C. Westall.** 1997. Sequestration of Hydrophobic Organic Contaminants by Geosorbents. *Environmental Science and Technology*. Vol. 31, No. 12, pp. 3341-3347.
- Mackay, A.A. and P.M. Gschwend.** 2001. Enhanced Concentrations of PAH's in Groundwater at a Coal Tar Site. *Environmental Science and Technology*. Vol. 35, No. 7, pp. 1320-1328.
- Mackay, D., W.Y. Shiu, and K.C. Ma.** *Illustrated Handbook of Physical-Chemical Properties and Environmental Fate for Organic Chemicals: Vol. II.* Lewis publishers: Boca Raton, FL, 1992.
- Matso, K.** 1995. Mother Nature's Pump and Treat. *Civil Engineering*, ASCE. Vol. 65, No. 10, pp. 46-49.
- Miller, C.T. and W.J. Weber, Jr.** 1984. Modeling Organic Contaminant Partitioning in Ground Water Systems. *Ground Water*. Vol. 22, pp. 584-592.
- Mingelgrin, U. and J. Gerstle.** 1983. Reevaluation of Partitioning as a Mechanism of Nonionic Chemicals Adsorption in Soils. *Journal of Environmental Quality*. Vol. 12, pp. 1-11.
- Montgomery, J.H.** *Groundwater Chemicals Desk Reference, 3<sup>rd</sup> Edition.* Lewis Publishers: Boca Raton, Florida, 2000.
- Muck, A.J.** 2000. Creosote Migration in the Subsurface at the Oneida Tie-Yard. M.S. Research Report. Virginia Polytechnic Institute and State University. Blacksburg, Virginia.
- Mueller, J.G., P. Chapman, and P. Pritchard.** 1989. Creosote-Contaminated Sites – Their Potential for Bioremediation. *Environmental Science and Technology*. Vol. 23, pp. 97-120.
- Northcott, G.L. and K.C. Jones.** 2001. Partitioning, Extractability, and Formation of Nonextractable PAH Residues in Soils. 1. Compound Differences in Aging and Sequestration. *Environmental Science and Technology*. Vol. 35, No. 6, pp. 1103-1110.

- Panhorst, E.** 2000. Evapotranspiration Measurement and Simulation due to Poplar Trees at a Phytoremediation Site. M.S. Thesis. Virginia Polytechnic Institute and State University. Blacksburg, Virginia.
- Park, J.-H., X. Zhao, and T.C. Voice.** 2001. Biodegradation of Non-Desorbable Naphthalene in Soils. *Environmental Science and Technology*. Vol. 35, No. 13, pp. 2734-3740.
- Paterson, E., D. Mackay, and C. McFarlane.** 1994. A Model of Organic Chemical Uptake by Plants from Soil and the Atmosphere. *Environmental Science and Technology*. Vol. 28, No. 13, pp. 2259-2266.
- Peters, C. A., C. D. Knightes, and E. G. Brown.** 1999. Long-Term Composition Dynamics of PAH-Containing NAPL's and Implications for Risk Assessment. *Environmental Science and Technology*. Vol. 33, No. 24, pp. 4499.
- Pignatello, J.J, and B. Xing.** 1996. Mechanisms of Slow Sorption of Organic Chemicals to Natural Particles. *Environmental Science and Technology*. Vol. 30, pp. 1-11.
- Pignatello, J.J.** 1990. Slowly Reversible Sorption of Aliphatic Halocarbons in soils. *Environmental Toxicology and Chemistry*. Vol. 9, pp. 1117-1126.
- Poulsen, M., L. Lemon, and J.F. Barker.** 1992. Dissolution of Monaromatic Hydrocarbons into Groundwater from Gasoline-Oxygenate Mixtures. *Environmental Science and Technology*. Vol. 26, No. 12, pp. 2483-2489.
- Ramaswami, A. and R.G. Luthy.** 1997. Mass Transfer and Bioavailability of PAH Compounds in Coal Tar NAPL-Slurry Systems. 1. Model Development. *Environmental Science and Technology*. Vol. 31, No. 8, pp. 2260-2267.
- Reilley K.A., M.K. Banks, and A.P. Schwab.** 1996. Organic Chemicals in the Environment: Dissipation of Polycyclic Aromatic Hydrocarbons in the Rhizosphere. *Journal of Environmental Quality*. Vol. 25, pp. 212-219.
- Reinbold, K.A., J.J Hassett, J.C. Means, and W.L. Banwart.** *Adsorption of Energy-Related Organic Pollutant: A Literature Reviews*. EPA 600/3-79-086. U.S. EPA: Athens, GA, 1979.
- Reuther, C.** 1999. Phytoremediation Goes Commercial, but Questions Remain. *Water Quality Manager*. Vol. 32, No. 1, pp. 22-25, 45.

- Rutherford, M.P., M.R. Gray, and M.J. Dudas.** 1997. Desorption of [<sup>14</sup>C] Naphthalene from Bioremediated and Nonbioremediated Soils Contaminated with Creosote Compounds. *Environmental Science and Technology*. Vol. 31, No. 9, pp. 2515-2519.
- Salt, D.E., R.D. Smith, and I. Raskin.** 1998. Phytoremediation. *Annual Review of Plant Physiology and Plant Molecular Biology*. Vol. 49, pp. 643-648.
- Schnoor, J.L., L.A. Licht, S.C. McCutcheon, N.L. Wolfe, and L.H. Carrieria.** 1995. Phytoremediation of Organic and Nutrient Contaminants. *Environmental Science and Technology*. Vol. 29, No. 7, pp. 318A-323A.
- Travis, C.C. and E.L. Etnier.** 1981. A Survey of Sorptive Relationships for Reactive Solutes in Soil. *Journal of Environmental Quality*. Vol. 10, pp. 8-17.
- U.S. Environmental Protection Agency.** *Presumptive Remedies for Soils, Sediments, and Sludges at Wood Treater Sites*, OSWER Directive 9200.5-162. U.S. EPA: December 1995.
- U.S. Environmental Protection Agency.** *Test Method Base/Neutrals and Acid-Method 625*. U.S. EPA: Cincinnati, Ohio, 1982.
- Weber, Jr., W.J. and E.H. Smith.** 1988. Simulation and Design Models for Adsorption Processes. *Environmental Science and Technology*. Vol. 21, pp. 1040-1050.
- Weber, Jr., W.J., P.M. McGinley, and L.E. Katz.** 1991. Sorption Phenomena in Subsurface Systems: Concepts, Models and Effects on Contaminant Fate and Transport. *Water Resources*. Vol. 25, No. 5, pp. 499-528.
- Xing, B. and J.J. Pignatello.** 1996. Time-Dependent Isotherm Shape of Organic Compounds in Soil Organic Matter: Implications for Sorption Mechanism. *Environmental Toxicology and Chemistry*. Vol. 15, pp. 1282-1288.
- Xing, B. and J.J. Pignatello.** 1998. Competitive Sorption between 1,3-Dichlorobenzene or 2,4-Dichlorophenol and Natural Aromatic Acids in Soil Organic Matter. *Environmental Science and Technology*. Vol. 32, No. 5, pp. 614-619.
- Yeom, I.-T., M.M. Ghosh, C.D. Cox, and K.G. Robinson.** 1995. Micellar Solubilization of Polynuclear Aromatic Hydrocarbons in Coal Tar-Contaminated Soils. *Environmental Science and Technology*. Vol. 29, pp. 3015-3021.
- Yeom, I.-T., M.M. Ghosh, C.D. Cox, and K.-H. Ahn.** 1996. Dissolution of Polycyclic Aromatic Hydrocarbons from Weathered Contaminated Soil. *Water Science Technology*. Vol. 34, No. 7-8, pp. 335-342.
- Zhang, W., E. Bower, and W. Ball.** 1998. Bioavailability of Hydrophobic Organic Contaminants: Effects and Implications of Sorption-Related Mass Transfer on Bioremediation. *Ground Water Monitoring & Remediation*. Vol. 18, 126-138.